NOTE TO USERS

UNIVERSITÉ DE MONTRÉAL

COMPUTATIONAL BIOMECHANICS OF THE HUMAN KNEE JOINT – ROLE OF COLLAGEN FIBRILS NETWORKS

REZA SHIRAZI AGHJARI
DÉPARTEMENT DE GÉNIE MÉCANIQUE
ÉCOLE POLYTECHNIQUE DE MONTRÉAL

THÈSE PRÉSENTÉE EN VUE DE L'OBTENTION
DU DIPLÔME DE PHILOSOPHIAE DOCTOR (Ph.D.)
(GÉNIE MÉCANIQUE)
DÉCEMBRE 2008

Your file Votre référence
ISBN: 978-0-494-47725-0
Our file Notre référence
ISBN: 978-0-494-47725-0

UNIVERSITÉ DE MONTRÉAL

ÉCOLE POLYTECHNIQUE DE MONTRÉAL

Cette thèse intitulée:

COMPUTATIONAL BIOMECHANICS OF THE HUMAN KNEE JOINT – ROLE OF COLLAGEN FIBRILS NETWORKS

présentée par: SHIRAZI AGHJARI Reza

en vue de l'obtention du diplôme de: Philosophiae Doctor

a été dûment acceptée par le jury d'examen constitué de:

M. LAKIS Aouni A., Ph.D., président

M. SHIRAZI-ADL Aboulfazl, Ph.D., membre et directeur de recherche

M. BUSCHMANN Michael D., Ph.D., membre

M., RANCOURT Denis, Ph.D., membre

Dedicated to

my mom Golchin

my sisters, brother-in-law and nephew

and the memory of my dear father Ali Mohammad

Acknowledgements

I would like to express my gratitude to all those who gave me the possibility to complete this thesis.

I am deeply indebted to my supervisor Professor Shirazi-Adl whose assistance, stimulating suggestions and encouragements helped me throughout this research work and associated publications.

The financial support provided from his research grants by the Natural Sciences and Engineering Research Council of Canada and Canadian Institutes of Health Research is also gratefully acknowledged.

Earlier efforts of Dr. Leping Li in the development of a novel composite model of cartilage as well as his help and comments on the first publication in this thesis are gratefully acknowledged. The earlier efforts of M.Z. Bendjaballah, K.E. Moglo and W. Mesfar in the development of the knee model are also acknowledged.

I would also like to thank all present and former graduate students of the Applied Mechanics Section of the Department of Mechanical Engineering with whom I worked during my doctoral study at École Polytechnique de Montréal; especially Mr Abdelhak Oulmane for his touch-up on Resumé and Condensé en Français sections.

My special gratitude goes to my parents and sisters for their unconditional love and support during every step in my life through the years.

Résumé

L'arthrose est un fardeau économique important sur notre société avec une population vieillissante. Des stratégies efficaces de prévention/traitement dépendent d'une compréhension approfondie du comportement biomécanique du genou, et en particulier du cartilage, dans différentes activités physiologique quotidiennes. Des difficultés pratiques et considérations éthiques des méthodes expérimentales présentent des modèles biomécaniques comme un outil complémentaire indispensable pour l'évaluation de la biomécanique du genou. Les modèles biomécaniques existants du genou ont négligé la nature anisotropique du cartilage et du ménisque. Les réseaux de fibres de collagène, qui changent suivant la profondeur, semblent jouer un rôle crucial dans la biomécanique de ces tissus et de l'ensemble du genou.

Dans la présente étude de calcul, un modèle d'éléments finis poroélastique renforcé de fibre de cartilage a été initialement développé où un élément membrane approprié a été utilisé pour représenter des fibres horizontales de collagène. Le contenu volumique et les propriétés du matériau dépendantes de la déformation des fibres pures de collagène ont été explicitement représentés dans la formulation. Cette approche, par rapport à celles antérieures, semble être plus utile de ne pas regrouper des différentes propriétés des fibres (i.e. la fraction volumique et la courbe non-linéaire de contrainte-déformation) dans un seul paramètre de rigidité qui risque de perdre son interprétation physique et, par conséquent, son importance. Dans ce modèle composite, conformément à la structure de tissu, la matrice et le réseau de fibres de membrane ont subi différentes contraintes malgré leurs déformations identiques dans les directions des fibres. Différents cas d'études de compression non confiné et l'indentation ont été effectuées pour déterminer le rôle distinct des fibres de collagène de membrane dans la mécanique poroélastique non linéaire du cartilage articulaire. Par des ajustements de la fraction volumique et des propriétés mécaniques des collagènes, le modèle a permit la simulation

des changements dans la structure du réseau de fibres du tissu afin de modéliser des processus de dommages et des essais de réparation.

L'orientation primaire des fibres de collagène change suivant la profondeur du cartilage; elle est horizontale dans la zone superficielle, aléatoire dans la zone transitoire, et verticale dans la zone profonde. Par la suite, dans un modèle axisymétrique poroélastique de cartilage, les trois réseaux fibrillaires aux zones superficielle, transitoire et verticale ont été introduites selon la structure composite des couches du cartilage. Des éléments membrane ont été utilisés pour des fibres horizontales superficielle et verticales profondes avec des formulations et le contenu volumique appropriés. Des éléments solides avec seulement la rigidité en tension ont été utilisés pour la distribution aléatoire des fibres dans la zone transitoire. Par conséquent, à chaque itération et incrément de la solution, des éléments solides qui prennent les directions des déformations principales comme axes principaux du matériau simulent la réorientation des fibres en tension. Il a été montré que des fibres verticales profondes jouent un rôle important dans la mécanique du cartilage articulaire en augmentant la rigidité du tissu et en protégeant la matrice solide contre des grandes distorsions. Toutefois, ce rôle a disparu au fil de temps durant la période post-transitoire et à taux de chargement plus lent attendu dans les activités physiologiques telles que la marche.

Ensuite, notre modèle axisymétrique antérieur a servi d'améliorer largement le modèle 3D existant de l'ensemble du genou vers un modèle original qui a tenue compte, pour la première fois, de la nature anisotropique des cartilages fémoral et tibial en plus des ménisques. Des réseaux de fibres de collagène dans le cartilage et les ménisques du genou changent dans le contenu et la structure d'une région à l'autre rendant les tissus hautement non-linéaire et nonhomogène. Tout en résistant à la tension, ils influencent la réponse globale du joint ainsi que les déformations locales en particulier aux périodes à court terme lors des activités telles que marcher et courir. Afin d'étudier le rôle des réseaux de fibres dans la mécanique du genou et en particulier la réponse du cartilage

sous la compression, un modèle original du joint tibiofemoral a été développé qui a incorporé les réseaux fibrillaire du cartilage et du ménisque ainsi que les propriétés dépendantes de la profondeur du cartilage. La réponse du joint en position de flexion nulle sous la charge de compression allant jusqu'à 2000 N a été étudiée pour un certain nombre de conditions simulant l'absence dans le cartilage des réseaux fibrillaires verticale profonde ou superficielle ainsi que le détachement local entre le cartilage et l'os à leur jonction ou des dommages locaux aux fibres superficielles dans la zone de chargement. Il a été montré que le réseau fibrillaire verticale profonde dans le cartilage joue un rôle crucial dans le renforcement et la protection du cartilage articulaire contre les grandes déformations de tension et de cisaillement, en particulier à la jonction cartilage-os. Des fibres superficielles horizontales ont principalement protégé le tissu contre les contraintes excessives aux couches superficielles. Le détachement local du cartilage à la base a perturbé le fonctionnement normal des fibres verticales à la zone touchée causant des déformations plus élevées. Les fibres verticales, et à un degré moins fort les fibres superficielles, ont joué des rôles dominants dans la réponse mécanique du cartilage sous compression transitoire.

Ce modèle détaillé du genou a été aussi utilisé pour étudier seulement ou simultanément l'effet de la reconstruction du LCA et la méniscectomie partielle unilatérale sous les charges tiroir de 200 N et une compression de 1500 N, agissant seuls ou combinés. Le grand raffinement dans le ménisque nous a permis, à la fois, de considérer son ultrastructure détaillée de fibres de collagène avec divers arrangements aux surfaces extérieures et à l'intérieur de ces surfaces et de simuler correctement la méniscectomie partielle à la région postérieure du ménisque en enlevant les éléments à cette région. La précharge de compression a augmenté encore plus les forces/déformations du LCA sous le chargement tiroir. La méniscectomie partielle et les perturbations dans les propriétés du matériau et la pré-déformation du LCA, seules ou ensembles, a changé de façon substantielle le transfert de la force via les surfaces couvertes et non couvertes du cartilage, ainsi que la distribution de la pression du contact

sur le cartilage. La méniscectomie partielle a entièrement déchargé la zone du cartilage en dessous de la région résectée, qui aurait autrement articulé avec le ménisque. La méniscectomie partielle simultanée avec un LCA relâché a diminué encore plus la charge transférée par le ménisque touché générant deux régions de déchargement distinctes sur le cartilage en dessous. Ces changements antérieurs devraient augmenter encore plus en présence de plus grandes charges extérieures, plus grandes résections de ménisque, une déchirure complète du LCA et des dommages aux réseaux fibrillaire de cartilage.

Les modèles originaux de cartilage et de genou développés dans la présente étude ont incorporé les réseaux détaillés anisotrope et nonhomogène des fibres de collagène. Les prédictions ont été en bon accord avec les mesures expérimentales. Le rôle du réseau des fibres verticales profondes de collagène, et à un degré moins fort, des fibres horizontales superficielles et aléatoires transitoires dans la protection de la matrice solide contre des déformations excessives et l'augmentation de la rigidité de tissu ont été démontrées. Toute modalité de traitement qui tente de réparer ou de régénérer des défauts du cartilage incluant des greffes osteochondraux partielle ou en pleine épaisseur devrait tenir compte du rôle crucial des réseaux de fibres de collagène et de l'environnement mécanique exigeant du tissu. Des changements dans des paramètres de reconstruction du LCA tels que la pré-déformation et les propriétés du matériau ainsi que la méniscectomie partielle ont considérablement changé la distribution de la charge dans le genou. Des considérations adéquates du nouvel environnement mécanique du joint sont d'une importance cruciale pour une meilleure évaluation de la probabilité de succès dans divers essais de traitement.

Abstract

Osteoarthritis is a significant economic burden on our society with ageing population. Effective preventive/treatment strategies depend on a thorough understanding of knee joint, and in particular cartilage, biomechanical behaviour in various physiological daily activities. Practical difficulties and ethical considerations in experimental methods present biomechanical models as an indispensable complemetary tool for assessment of the knee joint biomechanics. Existing biomechanical models of the knee have neglected anisotropic nature of cartilage and meniscus. The collagen fibrils networks, which change along the depth, appear to play a crucial role in biomechanics of these tissues and, hence, the entire joint.

In the present computational study, a poroelastic fibril-reinforced finite element model of cartilage was initially developed in which an appropriate membrane element was used to represent horizontal collagen fibrils. Volume fraction contents and the strain-dependent material properties for the pure collagen fibrils were explicitly accounted in the formulation. This approach, as compared to earlier ones, is more meaningful in not lumping various fibril properties (i.e. volume fraction and nonlinear stress-strain curve) into one stiffness term which risks losing its physical interpretation and significance. In this composite model, in accordance with tissue structure, the matrix and fibrils membrane network experienced dissimilar stresses despite identical strains in the fibre directions. Different unconfined compression and indentation case studies were performed to determine the distinct role of membrane collagen fibrils in nonlinear poroelastic mechanics of articular cartilage. By individual adjustments of the collagen volume fraction and collagen mechanical properties, the model allowed for the alterations in the fibrils network structure of the tissue that can simulate damage processes and repair attempts.

The primary orientation of collagen fibrils alters along the cartilage depth; being horizontal in the superficial zone, random in the transitional zone, and vertical in the deep zone. In a subsequent axisymmetric poroelastic model of cartilage, the three fibrillar networks at superficial, transitional and vertical zones based on the layerwise composite structure of cartilage were introduced. Membrane elements were used for horizontal superficial and vertical deep fibrils with appropriate formulation and volume content. Brick elements were used for transitional zone to consider random distribution of fibrils in this region. Therefore, at each increment of load and iteration of solution, continuum elements that take the principal strain directions as the material principal axes simulate reorientation of fibrils with tension-only stiffness. Under both relaxation and creep indentation loading conditions, it was shown that deep vertical fibrils play an important role in mechanics of articular cartilage by increasing the stiffness of the tissue and protecting the solid matrix against large distortions. This role, however, disappeared both with time in post-transient period and at loading rates slower than those expected in physiological activities such as walking.

Our foregoing axisymmetric model studies subsequently served as a foundation to extensively improve an existing 3-D model of the entire knee joint towards a novel one that considered, for the first time, the anisotropic nature of tibial and femoral cartilage layers in addition to menisci. Collagen fibrils networks in cartilage and menisci of knee joints change in content and structure from a region to another yielding highly nonlinear and nonhomogeneous tissues. While resisting tension, they influence global joint response as well as local strains particularly at short-term periods in activities such as walking and running. To investigate the role of fibrils networks in knee joint mechanics and in particular cartilage response in compression, a novel model of the tibiofemoral joint was developed that incorporated the cartilage and meniscus fibrils networks as well as depth-dependent properties in cartilage. The joint response at full extension under up to 2000 N compression was investigated for a number of conditions simulating the absence in cartilage of deep vertical or superficial fibrils networks as well

as localised split of cartilage at subchondral junction or localised damages to superficial fibrils at loaded areas. It was shown that deep vertical fibrils network in cartilage plays a crucial role in stiffening and protecting articular cartilage from large tensile and shear strains, in particular at the subchondral junction. Superficial horizontal fibrils protected the tissue mainly from excessive stresses at superficial layers. Local cartilage split at base disrupted the normal function of vertical fibrils at the affected areas resulting in higher strains. Vertical fibrils, and to a lesser extent superficial fibrils, played dominant mechanical roles in cartilage response under transient compression.

This detailed model of the knee joint was also used to investigate the effect of isolated or concurrent ACL reconstruction and unilateral partial meniscectomy under 200 N drawer and 1500 N compression loads acting alone or combined. The extensive refinement in the meniscus allowed us both to consider its detailed ultrastructure of collagen fibrils with different arrangements at exterior surfaces and in the bulk regions and to properly simulate partial meniscectomy at the inner region of meniscus close to its posterior horn. Compressive preload further increased ACL strains/forces in drawer loading. Partial meniscectomy and perturbations in ACL prestrain and material properties, alone or together, substantially altered the load transfer via covered and uncovered areas of cartilage as well as contact pressure distribution on cartilage. Partial meniscectomy completely unloaded the cartilage area underneath the resected region which would otherwise articulate with the meniscus. Concurrent partial mensicectomy and slacker ACL further diminished the load via affected meniscus causing two distinct unloaded regions on the cartilage underneath it. Foregoing alterations are expected to further increase in presence of greater external forces, larger meniscal resections, complete ACL rupture and damages to cartilage fibril networks.

Novel models of cartilage and entire knee joint developed in the current study incorporated the detailed anisotropic and nonhomogeneous collagen fibrils networks. The predictions on joint kinematics, liagemnt forces and contact areas/pressures were in

good agreement with reported experimental measurements. Role of deep vertical collagen fibrils, and to a lesser extent, horizontal superficial and random transitional fibrils networks in protecting the solid matrix from deleterious strains and in augmenting tissue stiffness were demonstrated. Any treatment modality attempting to repair or regenerate cartilage defects involving partial or full thickness osteochondral grafts should account for the crucial role of collagen fibrils networks and the demanding mechanical environment of the tissue. Alterations following ACL reconstruction attempts simulated by changes in prestrain and material properties as well as partial meniscectomy significantly changed the load distribution in the knee joint. Adequate considerations of the new mechanical environment of the joint are crucial for an improved assessment of the likelihood of success in various treatment attempts.

Condensé en Français

Introduction

Il est estimé que plus de 13.9% des adultes âgés de 25 ans et plus et 33.6% des personnes de 65 ans en Amérique du Nord (Lawrence et al., 2008) souffrent d'arthrose (OA) qui reste une invalidité nécessitant un traitement le long de leurs vies. Souvent, les signes cliniques et radiographiques apparaissent lorsqu'une dégénérescence irréversible des changements est déjà présente rendant la prévention et le traitement des tâches un défi de taille. La douleur et la perte de mobilité/dextérité associée à l'arthrose du genou peut être dangereuse à la qualité de vie (Davis et al., 1991), y compris la fatigue, l'insomnie, la baisse des revenus, les soins hospitaliers, la chirurgie, les effets secondaires de médicaments, et l'instabilité de la famille (Health Canada). En effet, la deuxième plus fréquente des maladies chroniques (après les maladies cardiovasculaires), l'OA a bel et bien un plus grand impact économique parce que l'effet de l'OA dure plus lentement. Du point de vue économique, le coût annuel de l'OA dépasse 3.4 milliards de dollars (Health Canada) et 13.2 milliards de dollars par an (Buckwalter & Mankin, 1998) au Canada et aux États-unis, respectivement, et le genou est associée ainsi à une grande partie de cette charge financière. L'OA du genou est de 1 sur 5 des principales causes d'incapacité (Guccione et al., 1994) et occupe un rang élevé dans la vie ajustées des années de l'incapacité (Michaud et al., 2006). Dans une décennie, près d'un million de Canadiens adultes vont être touchés, et d'ici à 2026, 5 millions de Canadiens seront touchés. Aux États-unis l'OA devrait doubler à 41.1 millions en 2030 (Reuters, 2003).

Les troubles du genou compte également les ménisques et les ligaments. Ceux qui souffrent des blessures des ligament et/ou des ménisques du genou ont une augmentation significative du risque de produire, à long-terme, les maladies chroniques telles que l'OA (Indelicato & Bittar, 1985; McNicholas et al., 2000; Noyes et al., 1980; Roos et al., 1998). La déchirure des ligaments du genou, surtout le ligament croisé antérieur (LCA), se produit parfois pendant des activités sportives. On estime à 200,000

blessures liées au LCA chaque année seulement aux États-Unis, avec environ 95,000 déchirure du LCA (C. H. Brown, Jr. & Carson, 1999; Miyasaka et al., 1991). Environ 100,000 reconstructions du LCA sont effectuées chaque année, avec des coûts des soins de santé totalisant près d'un milliard de dollars. Environ 50% des patients ont des blessures du LCA et de ménisque en même temps. En raison des effets négatifs significatifs de la méniscectomie totale sur la distribution des charges (McNicholas et al., 2000) et le développement de l'OA (Roos et al., 1998), des meniscectomies partiels sont effectuées avec la résection de la déchirure des tissus. Les blessures simultanées du LCA et de ménisque sont traitées par la reconstruction du LCA et méniscectomie partielle. L'occurrence de l'OA à moyen et à long terme a persistée malgré la reconstruction du LCA (van der Hart et al., 2008) et la méniscectomie partielle (Hill et al., 2005; Neuman et al., 2008; Rangger et al., 1995; von Porat et al., 2004). Outre la réadaptation non-chirurgical des troubles du genou, les traitements invasifs varient de la dissection partielle des tissus endommagés et la réparation biologique des défauts du cartilage et finalement au remplacement total des ligaments, ménisques et joint (c'est-à-dire, arthroplastie). Par conséquent, il est d'une grande importance d'étudier la biomécanique du joint afin d'obtenir une meilleure compréhension des fonctions des cartilages, des ligaments et des ménisques et leurs interactions dans l'ensemble du genou dans des conditions normales et perturbées.

Le cartilage est un matériau poreux rempli d'eau avec une perméabilité très basse. Le cartilage articulaire est constitué principalement de collagène (de type II), de proteoglycans et de l'eau. La composition et la structure du cartilage articulaire changent suivant la profondeur. Dans le cartilage, à la zone superficielle, des fibres sont horizontalement parallèle à la surface articulaire (Kaab, Gwynn et al., 1998; Minns & Steven, 1977) alors qu'ils deviennent aléatoire dans la zone transitoire (Broom & Marra, 1986) et finalement tournent perpendiculairement à la zone profonde (Benninghoff, 1925; Kaab, Gwynn et al., 1998; Lane & Weiss, 1975; Minns & Steven, 1977) pour attacher fermement le tissu avec l'os (Broom & Poole, 1982; Minns & Steven, 1977;

Redler et al., 1975). Le module d'élasticité d'équilibre de la matrice solide non-fibré augmente également suivant la profondeur (Schinagl et al., 1997).

Cette non-homogénéité de profondeur et le changement d'orientation des fibres collagène ont des effets importants sur les propriétés du matériau, ce qui rende le tissus hautement non-linéaires, non-homogène et anisotrope (C. Y. Huang et al., 2005). La présence de l'eau dans les pores de la matrice (proteoglycans) qui contribue au comportement viscoélastique des tissus mène à des effets de relaxation de contrainte et de fluage. Dans la relaxation de contrainte, le cartilage soulage la contrainte sous une déformation constante quand l'eau sort du tissu. D'autre part, le fluage est la tendance du tissu à se déformer sous une charge constante, un phénomène qui peut se produire par exemple au cours d'une position debout à long-terme.

Tout au long de la vie d'un adulte, le cartilage articulaire des joints tel que le genou subit un niveau élevé de contrainte biomécanique (Hodge et al., 1986). Pour de nombreux individus et dans la plupart des emplacements anatomiques, le cartilage est en mesure de maintenir ses propriétés normales avec peu de changements pour des décennies. Mais le traumatisme et, chez certains individus, l'âge causes des dommages locaux au cartilage. En présence des blessures même mineures, le cartilage a une mauvaise capacité intrinsèque de réparation (Buckwalter & Mankin, 1998). Malgré de nombreuses enquêtes sur l'OA, l'étiologie de cette maladie est encore non claire en raison de la très complexe structure du cartilage, ainsi que ses interactions avec l'os.

Le ménisque a une forme semi-lunaire fibro-cartilagineuse de tissu avec ses bouts attachés au condyle du tibia et mène à une distribution plus uniforme de la charge à l'articulation tibiofémorale. Il est composé principalement d'un réseau dense de fibres de collagène (de type I) et des proteoglycans et de l'eau. Semblable au cartilage, la présence de l'eau coincée dans les pores de la matrice (proteoglycans) donne lieu à des tissus avec des propriétés viscoélastiques (relaxation de contrainte et fluage). Alors que

les fibres de collagène en haut, en bas ainsi que les surfaces périphériques n'ont pas d'orientation préférée, ils sont néanmoins orientées vers la circonférence entre ces surfaces (Aspden et al., 1985; Petersen & Tillmann, 1998). Il a été démontré que la non-homogénéité et l'anisotropie structurelles du ménisque dominent le comportement de la résistance en traction des tissus (Fithian et al., 1990; Proctor et al., 1989).

Entre autres, quatre grands ligaments (LCA, LCP, LCM et LCL), contrôle le mouvement relatif du joint tibiofémoral. Selon les conditions de chargement, un ou plusieurs de ces ligaments agissent en tant que restrictions principales pour la stabilité de l'articulation. Les ligaments, avec leurs fibres collagéniques parallèles aux tissus, sont semblables à des cordes de connexion fémur-tibia. Ce dispositif rend la stabilité et la résistance au tissu. À une grande déformation, l'ondulation des fibres diminue ou disparaît et la rigidité augmente de manière significative. Pour cette raison, deux régions distinctes de la courbe contrainte-déformation des ligaments sont observées, une région non linéaire faiblement chargé et une région linéaire hautement chargé avec une plus grande rigidité (Chandrashekar et al., 2008).

Initialement, le cartilage a été simulé comme matériau élastique (Hayes et al., 1972), visco-élastique (Parsons & Black, 1977) et poroélastique composé d'un milieux poreux homogène isotrope rempli d'un fluide (Buschmann & Grodzinsky, 1995; Frank & Grodzinsky, 1987; Mow et al., 1980). Par la suite, un modèle renforcés de fibres du cartilage articulaire a été développé où les fibres de collagène ont été simulées distinctement de la matrice isotrope (L. P. Li et al., 2000; L. P. Li et al., 1999; Soulhat et al., 1999).

Au début des modèles théoriques ont simulé l'articulation du genou seulement pour les surfaces fémorales et tibiales, tout en négligeant les ménisques (Blankevoort et al., 1991; Crowninshield et al., 1976; Grood & Hefzy, 1982; Wismans et al., 1980). Les plus récent modèles théoriques ont utilisé des techniques d'imagerie pour obtenir des

renseignements plus précis sur la géométrie de surface et ont inclus les ménisques afin d'étudier la biomécanique du joint tibiofémoral dans son état sain et perturbés (Bendjaballah et al., 1995; Donahue et al., 2002; Pena et al., 2005). Toutefois, des modèles théoriques du genou n'ont pas réussi à incorporer la structure composite de ces tissus.

Initialement, l'objectif global de cette étude était d'améliorer les modèles existant du cartilage renforcés de fibres, et ensuite incorporer la structure détaillée non-homogène du cartilage articulaire et des ménisques dans notre modèle existant du genou humain (Bendjaballah et al., 1995; Mesfar & Shirazi-Adl, 2006b) développant ainsi un modèle original du joint tibiofémoral. La réponse tibiofémorale sous une force de compression, une force de tiroir et de leur combinaison a été étudiée. Par la suite, le rôle mécanique des réseaux de fibres collagène dans les couches du cartilage de fémur et tibia ainsi que l'effet de la reconstruction du LCA et la méniscectomie partielle sous des charges tiroir et compression ont été étudiés.

Méthode

Initialement, un modèle éléments finis poroélastique renforcés de fibres du cartilage a été développé où un élément de membrane approprié a été utilisé pour représenter des fibres horizontale de collagène. Le contenu volumique en collagène et des propriétés du matériau qui dépendent de la déformation des fibres de collagène pures ont été explicitement représentés dans la formulation. Des fibres de collagène dans le plan de membranes sont supposées être distribuées de façon homogène dans toutes les directions. Cependant, malgré cette distribution une réponse dépendant de la direction domine en raison de la dépendance de déformation dans les propriétés du matériau des fibres et l'anisotropie dans le champ de déformation. À chaque étape de chargement, des directions principales de déformation dans le plan de membranes ont été prises comme axes principaux du matériau. Ensuite, les contraintes dans ces directions principales ont été évaluées selon l'ensemble des déformations principales et la courbe de contrainte-

déformation des fibres. Des déformations principales égales produiraient une matrice de rigidité pour un matériau isotrope alors que les déformations principales non-positives produisent un composant diagonale de valeur zéro (ou proches de zéro) dans les matrices correspondante de rigidité et de contrainte.

La formulation de ces éléments de membrane avec des propriétés du matériau non-linéaires a été introduite dans le code de calcul ABAQUS via la sous-routine *UMAT*. Les résultats ont été validés en comparant des prédictions pour différentes relations constitutives existantes. Dans le maillage d'éléments finis, l'épaisseur de l'ensemble d'élément de membrane pour chaque élément de matrice solide a été initialement calculée selon la fraction volumique de fibre collagène de cette direction.

Ensuite et afin d'étudier le rôle des fibres verticales dans la mécanique du cartilage, un modèle cylindrique de rayon R=17 mm et de hauteur H=2.5 mm a été considérée, ce qui représente environ le cartilage au plateau médial du tibia basé sur notre modèle détaillé du genou humain (Bendjaballah et al., 1995). Le pénétrateur est supposé rigide et imperméable avec un profil identique à celui du condyle médial du fémur dans le plan sagittal. Le cartilage a été modélisé comme une matrice solide poreuse isotrope rempli d'eau et renforcée de réseaux de fibres. La matrice poreuse a été représentée par des éléments axisymétriques avec les champs de pression et de déplacement linéaires, tandis que les réseaux fibrillaires ont été simulés, soit par des éléments membrane ou solide. Dans la zone superficielle, les fibres de collagène ont été distribués d'une façon isotrope dans le plan des éléments membrane (Shirazi & Shirazi-Adl, 2005). Les contraintes dans chacune des directions circonférentielle et radiales ont été évaluées en utilisant la courbe non-linéaire contrainte-déformation de collagène de type II basé sur des travaux antérieurs. Dans la zone transitoire avec des fibres d'orientation aléatoire dominante, des éléments solides qui prennent les directions principales de déformation comme axes principaux du matériau ont représenté des fibres de collagène. Dans la zone profonde, des fibres verticales ont été représentées avec des

éléments membranes verticaux similaires aux fibres horizontales superficielles sauf qu'ils n'ont offert aucune résistance dans la direction circonférentielle. Des contraintes en tension peuvent, par conséquent, être générées dans ces fibres verticales seulement dans leur direction, qui est initialement verticale. La formulation de ces réseaux fibrillaire a été introduite dans le code commercial d'éléments finis ABAQUS. L'épaisseur des éléments membranes dans les zones superficielles et profondes a été évaluée en fonction de la fraction volumique des fibres dans ces zones. Les fractions volumiques dans les zones transitoire et profonde ont été, par la suite, estimées selon les mesures reportées.

Afin d'étudier le rôle mécanique des réseaux fibrillaires des cartilages articulaires du fémur et tibia de l'ensemble du genou, le maillage d'un modèle 3-D existant validé du genou humain (Bendjaballah et al., 1995) a été modifié par un grand raffinement des régions du cartilage articulaire et des ménisques. Ces améliorations ont permis l'incorporation des réseaux fibrillaires à différentes régions ainsi que la variation des propriétés du matériau du cartilage dépendant de la profondeur. Les ligaments du joint, c'est-à-dire les ligaments croisée antérieur/postérieur (LCA/LCP) et les ligaments collatéral médial/latéral (LCM/LCL) ont été inclus avec des propriétés du matériau non-linéaires et des pré-déformation initiales (Mesfar & Shirazi-Adl, 2006a, 2006b).

La matrice non-fibrillaire du cartilage a été modélisée par un élément solide incompressible isotrope hyperélastique avec des propriétés dépendant de la profondeur alors que les réseaux de fibres ont été simulés, soit par des éléments membrane ou solide avec architecture et formulation similaire à ceux du modèle axisymétrique du cartilage (Shirazi & Shirazi-Adl, 2008b). Dans les surfaces extérieures des ménisques, les fibres de collagène ont été uniformément distribuées dans le plan des éléments de membrane. Dans la région intérieure de chaque ménisque entre les surfaces périphériques, les fibres de collagène dominantes dans la direction circonférentielle ont été représentées par des éléments membranes avec axes locaux principaux du matériau définis dans les directions orthogonales radiale et circonférentielle. La réponse passive du genou a été, par la suite,

étudiée en position de flexion nulle sous des charges de compression allant jusqu'à 2000 N et le rôle des fibres de collagène à différentes zones a été évalué. Afin d'examiner les rôles des fibres verticales profondes et horizontales superficielles, des analyses ont été effectuées où le contenu de la fraction volumique de l'une de ces réseaux fibrillaires dans les deux cartilages du fémur et tibia a été réduit à néant. De plus, afin d'évaluer le rôle de détachement du cartilage de l'os, une région a la jonction entre le cartilage du tibia et l'os a été détaché qui résulte du glissement libre (séparation avec non pénétration) à l'interface cartilage-os. Finalement, l'effet de perturbation des fibres de collagène superficielles sur la réponse du joint a été étudié en enlevant le réseau des fibres de collagène superficiel dans le plateau latéral.

Ensuite, ce modèle détaillé du genou a été utilisé afin d'étudier la réponse passive tibiofémorale en position de flexion nulle sous une charge tiroir postérieur fémoral allant jusqu'à 200 N, agissant seule ou en présence de 1500 N pré-charge de compression. Les effets probables des changements dans les propriétés du matériau/pré-déformation dans le LCA sur la réponse ont été étudiés. Pour ce faire, les propriétés du matériau du LCA ont été remplacée par celles du tendon patellaire (Butler et al., 1986) ou la pré-déformation dans les deux faisceaux antéromédiaux et postérolatéraux du LCA ont été changées par +4% ou -4% dans les déformations, i.e. des valeurs initiales de 1% et 8% respectivement, soient changées à 5% et 12% (cas plus tendu) ou -3% et 4% (cas relâché). De plus, pour évaluer le rôle de méniscectomie partielle sur la réponse du joint, une partie interne des régions postérieures-centrales du ménisque latéral d'une part ou médiale d'autre part a été résecté. Les perturbations simultanées du LCA et de la méniscectomie latérale ont été également étudiées.

Résultats

La réponse transitoire dans le modèle axisymétrique du cartilage a été significativement rigidifiée quand la fraction volumique des fibres horizontales augmente tandis que la charge d'équilibre reste à peu près la même indépendamment de

ces variations (dans la fraction volumique). Les réponses de la rigidité normalisée transitoire et post transitoire et de la pression ont été influencées de manière significative par les changements de taille des spécimens. L'effet est beaucoup plus marqué lors de la période transitoire que la crête transitoire.

Les fibres verticales ont considérablement augmenté la rigidité transitoire du cartilage dans le modèle de relaxation de contrainte, un effet qui a complètement disparu à l'équilibre. Malgré l'augmentation considérable des forces de réaction axiale/radiale et de pression, la déformation maximale principale dans la matrice solide et la déformation maximale de tension dans la direction des fibres verticales ont nettement chuté quand des fractions volumiques plus élevé des fibres verticales ont été considérées. Le champ de déformation du tissu a aussi été substantiellement changé en présence des fibres verticales. Le changement dans la fraction volumique des réseaux fibrillaire superficiel et transitoire a causé beaucoup moins d'effets sur les prédictions au temps transitoire dans le modèle de relaxation. Ce rôle considérable des fibres verticales sur la mécanique transitoire du cartilage a été très sensible au taux de déformation dans le modèle de relaxation. Pour toutes les raisons pratiques, les réponses et observations transitoires dans les modèles du fluage et de la relaxation sont équivalentes. Dans le fluage, à mesure que le temps avançait, les couches superficielles sous charge ont été compressés de plus en plus et la forme de chevron de la déformation des fibres verticales près de la région au bord du chargement est devenu de plus en plus évidente.

Dans l'étude du genou entier, l'enlèvement du réseau des fibres verticales a augmenté la flexibilité du joint. Le détachement locale entre le cartilage du tibia et de l'os a aussi allégé la réponse, mais à un degré moins fort. Par contre, l'absence locale et totale des fibres superficielles horizontales n'a pas influencé la réponse. Pour le modèle sain de référence à 2000 N, la pression du contact a atteint le maximum de 4.32 MPa sur la partie non couverte du plateau latéral du cartilage tibial où la pression a aussi atteint son maximum de 4.97 MPa aux éléments superficiels. Sous la région de chargement, des

fibres de collagène verticales profondes dans les deux cartilages fémoral et tibial ont montré le minimum de déformation alors que les fibres superficielles ont été le plus tendues. Des fibres verticales ont subi des plus grandes déformations loin de la région sous chargement.

La déformation principale en tension dans la matrice du cartilage a augmenté de la surface articulaire vers la jonction cartilage-os dans les deux cartilages fémoral et tibial. Sous une charge de compression de 1800 N, la déformation principale en tension dans la matrice solide du cartilage a considérablement augmenté partout lorsque les fibres verticales ont été entièrement enlevées. De même, la déformation maximale en tension dans la direction verticale des fibres a substantiellement augmenté. La déformation maximale en tension à la jonction entre cartilage-os a également augmenté, mais à un degré moins fort, lorsque l'attachement entre cartilage et l'os a été perturbé localement. L'absence locale ou totale des fibres superficielles a eu beaucoup moins d'effet sur ces déformations de matrice. Ils ont, toutefois, augmenté la déformation en tension dans les surfaces articulaires du cartilage. L'enlèvement des fibres verticales a aussi augmenté la déformation dans les fibres superficielles. La déformation maximale en tension dans la matrice du ménisque, contrairement à la matrice du cartilage, a seulement changé d'une façon négligeable (<1.3%) lorsqu'on compare le cas sain de référence avec d'autres cas étudiés.

La translation primaire fémorale a démontré un comportement non linéaire de rigidification sous un tiroir fémorale postérieure seul qui s'est transformée en un comportement linéaire et beaucoup plus rigide en présence de compression. L'augmentation de pré-déformation du LCA en plus de 4% déformation ou le remplacement par un matériau plus rigide a augmenté la charge dans le LCA sous les deux charges simples et combinées. Par contre, la diminution de pré-déformation du LCA de 4% déformation ou l'enlèvement des fibres verticales profondes dans le cartilage a considérablement diminué la charge dans le LCA de 31% et 38% sous charge

combinée, respectivement. Ces dernières chutes sont beaucoup moins sous seulement tiroir et en particulier dans le cas sans des fibres verticales; le rôle des fibres verticales a été plus marqué en présence de compression axiale. La méniscectomie médiale ou latérale a influencé la charge dans le LCA seulement d'une façon négligeable (<3%) sous tiroir seul ou combiné avec la compression.

La méniscectomie partielle a changé la forme de distribution de charge sur les plateaux du tibia et condyles du fémur en transférant la compression appliquée du ménisque (région couverte) vers le cartilage aux régions non couverte, en particulier du côté de la résection. Après la méniscectomie et contrairement au cas sain, aucun contact n'a été détecté sous la zone de la résection méniscale tandis que la crête de contrainte du contact a augmenté de ~5%. Des propriétés du matériau plus rigide ou une plus grande déformation initiale dans le LCA a augmenté la charge totale et la portion transférée à travers la surface non couverte du cartilage. Au contraire, un LCA relâché a diminué la force de contact sur les deux surfaces couverte et non couverte du plateau latéral et a déchargé une zone de la région antéro-centrale du ménisque latéral.

Les changements de la pré-déformation du LCA ont changé encore plus l'état de la distribution de contrainte après la méniscectomie. Un LCA relâché dans le joint avec une méniscectomie partielle latérale a réduit la force sur les deux surfaces couverte et non couverte du plateau latéral et a causé une deuxième zone de déchargement latéral en dessous de la région antéro-centrale du ménisque, loin de la zone de résection. Au contraire, un LCA plus tendu a augmenté la force transférée par la surface de contact non couverte du contact cartilage-cartilage sur les deux plateaux.

Discussion et Conclusion

Le modèle composite renforcé de fibre du cartilage articulaire a décrit avec succès la réponse temporelle caractéristiques du cartilage articulaire observée expérimentalement dans les tests avec les configurations confiné ou non confiné (L. P.

Li et al., 2000; L. P. Li et al., 1999; Shirazi & Shirazi-Adl, 2005; Soulhat et al., 1999). Dans ce modèle, la matrice (c.à.d. proteoglycans) et le réseau fibrillaire (c.à.d. collagène) ont subi des contraintes non similaires malgré des déformations identiques dans les directions des fibres. Les réseaux fibrillaires, sous tension, confinent et appliquent de la compression sur la matrice et influencent donc le champ de contrainte dans l'ensemble de tissu par rapport à celui des modèles orthotropes homogènes. La prédiction de la contrainte en tension dans les réseaux fibrillaires et de la compression dans la matrice semble souhaitable dans l'emploi de chaque composant résistant aux contraintes pour lesquels il est le mieux structuré.

Dans nos études antérieures de modélisation du cartilage articulaire, les réseaux fibrillaires dans la direction radiale ont été représentés par des éléments ressort uniaxiaux avec des propriétés non linéaires en tension et non résistantes en compression. Cependant, ces études n'ont pas explicitement tenu compte des propriétés physiques importantes du tissu, tels que la fraction volumique et les courbes non linéaires de déformation-contrainte des réseaux fibrillaires à différents endroits et directions. En outre, les fibres radiales ont été modifiées pour tenir compte également des fibres circonférentielles en utilisant des énergies de déformation équivalentes dans un disque sous un état uniforme de contrainte. Par contre, dans cette étude les éléments membrane sont utilisés pour représenter directement des réseaux fibrillaires dans les deux modèles axisymétrique et 3D. En plus, la formulation d'élément membrane tiens explicitement compte des propriétés des fibres de collagène du tissu, telles que la fraction volumique et la courbe contrainte-déformation. Cette approche semble être plus utile de ne pas regrouper des différentes propriétés des fibres dans une matrice de rigidité qui risque de perdre son interprétation physique et, par conséquent, son importance.

Dans le modèle axisymétrique du cartilage avec une représentation détaillée de réseau des fibres de collagène, le réseau fibrillaire verticale a considérablement augmenté la rigidité transitoire du cartilage; le ratio transitoire à équilibre de charge

(c'est-à-dire, dynamique à statique) a augmenté d'environ trois (de ~18 à 51) lorsque la fraction volumique des fibres verticale a augmenté de 0% à 9%. Ce ratio pour le cas où on néglige des fibres verticales se trouve dans la gamme la plus élevé de celle rapporté dans les essais de compression confiné sous des mêmes ordres de grandeur et de taux de déformation (L. P. Li et al., 2003). Les fibres verticales ont également protégé la matrice solide d'un excès de déformation et, par conséquent, les dommages et la rupture; la déformation principale maximale transitoire a diminué de 51.3% à 22.8% en présence de 9% du contenu de fibres verticales et ça, malgré une augmentation de près de trois fois la charge appliqué.

Les déformations principales maximales et en cisaillement maximum dans la matrice solide ont eu lieu en effet à la jonction osteochondral dans la zone profonde où les détachements horizontaux ont été observé. La prédiction des fibres tressées près du centre et pas loin de la zone du chargement est corroborée par des études expérimentales (Broom & Poole, 1982; Glaser & Putz, 2002). Les résultats des études paramétriques ont démontré que, pour presque le même changement relatif, le réseau de fibres verticales a eu plus d'influence sur la mécanique du cartilage que celles des réseaux fibrillaire superficiel et transitoire. Par exemple, la force de réaction a changé autant que 60 N lorsque la fraction volumique des fibres superficielles a augmenté de 5%, alors qu'elle a changé de plus que 110 N lorsque les fibres verticales ont été changées de 3% seulement.

Dans le modèle original 3-D du genou, des prédictions ont confirmé l'hypothèse selon laquelle les réseaux des fibres verticales profondes et horizontales superficielles (à un degré beaucoup moins fort) renforcent le tissu du cartilage tout en le protégeant contre les déformations excessives et les distorsions sous des charges de compressions physiologiques aux périodes transitoires. Donc, des perturbations dans ces réseaux (en particulier dans les fibres verticales) mettraient le tissu à un risque de blessure

traumatique et de dégénérescence plus élevé. Les perturbations simulées dans le cartilage ont eu beaucoup moins d'effets sur les ménisques.

L'aire totale du contact du tibia, la moyenne et la crête de la contrainte du contact et la déflection axiale sous compression prédit dans cette étude ont été en général en accord avec les mesures. Le cartilage articulaire a subi une plus grandes distorsions de la surface articulaire vers les couches profondes où les détachements horizontaux se produisent dans les activités quotidiennes (Meachim & Bentley, 1978) et sous des charges d'impact (Atkinson & Haut, 1995; Vener et al., 1992). Les plus grandes déformations à la jonction cartilage-os sont probablement dues au gradient de rigidité existant entre le cartilage et l'os (Radin & Rose, 1986). Malgré un léger (~10%) effet d'assouplissement sur la réponse globale du déplacement axial, l'enlèvement des fibres verticales profondes a considérablement augmenté les déformations maximales en tension/cisaillement du cartilage surtout à la jonction cartilage-os où de grandes déformations en tensions ont déjà existé. Par conséquent, le présent modèle d'étude éclaire le rôle principal du réseau des fibres verticales à renforcer le cartilage articulaire en le protégeant contre les déformations excessives en tensions et les distorsions. Contrairement aux crêtes de déformations de compression, les déformations maximales en cisaillement et en tension aux couches plus profondes du cartilage et aux fibres verticales se produisent loin de la zone de chargement.

L'effet des différents dommages locaux dans le cartilage tibial à la zone de chargement (~2 cm^2 en plateau latéral) ont aussi été examinées; le tissu a été soit détaché au niveau de la jonction cartilage-os ou affaibli à la surface en éliminant les fibres superficielles. Ce type de détachement à la base n'est pas sensé de simuler les défaillances sous-chondrales où le compromis associés dans l'os sous-jacent, n'est pas simulés dans le présent modèle, augmenteraient encore plus les distorsions dans le cartilage articulaire qui est en dessus. Le détachement de base a démontré des effets beaucoup plus importants dans l'augmentation de la déformation maximale en tension

dans la matrice du cartilage du plateau touché. Toute modalité de traitement qui tente de réparer ou de régénérer des défauts du cartilage incluant des greffes osteochondral partielle ou en pleine épaisseur devrait tenir compte du rôle crucial des réseaux de fibres de collagène et de l'environnement mécanique exigeant du tissu.

Sous des charges tiroirs allant jusqu'à 200 N, la moyenne du relâchement antérieur du tibia reporté en position de flexion nulle (Markolf et al., 1981; Rudy et al., 2000) est en concordance avec nos prédictions. La translation postérieure du fémur par rapport au tibia sous la compression est due à la pente postérieure du tibia (Torzilli et al., 1994) et est en accord avec l'observation du déplacement antérieur du tibia par rapport au fémur (Markolf et al., 1981; Torzilli et al., 1994). La valeur relative et la variation de la translation primaire du fémur sous la charge tiroir avec la charge de compression sont également en accord avec les mesures (Hsieh & Walker, 1976; G. Li et al., 1998; Markolf et al., 1981; Torzilli et al., 1994).

La force calculé dans le LCA est également en bonne accord avec les valeurs mesurées et reporté sous une charge tiroir de ~100 N en position de flexion nulle (Markolf et al., 1995; Takai et al., 1993). Une précharge de compression augmente la force du LCA sous la charge tiroir de ~1.6 fois, en accord avec 150% dans les mesures (Markolf et al., 1995), à plus de deux fois de la charge tiroir appliquée. La prédiction de l'augmentation considérable dans la force du LCA en présence de la précharge de compression corrobore des découvertes antérieures (Fleming et al., 2001; G. Li et al., 1998; Torzilli et al., 1994), mais est en contredit avec d'autres suggérant l'idée que la précharge de compression protège le LCA de dommages sous des charge tiroir (Markolf et al., 1990). Donc nos prédictions préconisent des stratégies et des formations de réhabilitation qui évitent les grandes précharges de compression à/près de position de flexion nulle sur le genou sous des charges tiroir.

Les perturbations dans les pré-déformations/propriétés du matériau du LCA attendues suivant la reconstruction influencent la redistribution des force de contact sur les surfaces couvertes et non couvertes. Le remplacement d'un LCA déchiré par une greffe de tendon patellaire avec rigidité plus élevé semble avoir un effet mécanique similaire sur la réponse du genou que l'augmentation de ~4% en pré-déformation du LCA, une découverte en accord avec nos études antérieures du genou sous des activations des quadriceps (Mesfar & Shirazi-Adl, 2006a). Au contraire, une diminution de 4% dans la pré-déformation du LCA semble en quelque sorte simuler un cas de dommage partiel du LCA. Dans ce cas, avec un LCA relâché, la forme de pression du contact sur le plateau latéral démontre une région déchargée du cartilage en dessous du ménisque. Ce phénomène de déchargement aurait probablement augmenté si une déchirure complète avait été simulée dans cette étude. Ces changements de redistribution de la charge du genou (c.à.d., les forces et pression du contact) à la suite de la reconstruction ou la déchirure du LCA pourraient donc contribuer au développement de l'arthrose (van der Hart et al., 2008).

Alors que des charges considérées dans cette étude de méniscectomie partielle n'influencent notablement pas les forces du LCA, cependant il change considérablement la distribution de la pression du contact sur le cartilage articulaire. La méniscectomie partielle transfert la compression appliquée du ménisque résecté vers le cartilage adjacent tandis qu'elle décharge entièrement les zones couvertes de cartilages fémoral/tibial qui auraient autrement articuler avec le ménisque. En outre, la pression maximale sur la zone non couverte du cartilage adjacent augmente de ~5%. Quand la méniscectomie partielle latérale est combinée avec une augmentation de 4% en pré-déformation du LCA (un LCA plus tendu), la charge/pression du contact augmente encore plus sur le cartilage adjacent aux zones non couvertes. Par contre, une diminution simultanée de 4% du LCA (un LCA relâché) diminue la charge via le ménisque latéral à son minimum par rapport à tous les cas examinés dans cette étude et crée une zone de déchargement supplémentaire sur le cartilage couvert par le ménisque latéral. L'absence

du LCA dans les joints déficients, qui n'est pas simulés dans cette étude, aurait influencé encore plus les changements mentionnés antérieurement dans la façon de distribution de la pression en dehors du cas sain de référence. Ces changements de contraintes du contact sur le cartilage du genou, qui devraient accentuer encore plus sous des charges plus grande que celles qui sont prises en compte dans cette étude, affecte défavorablement la fonction et la santé du cartilage causant probablement et à long terme l'OA (Rangger et al., 1995; van der Hart et al., 2008).

Table of Contents

List of Tables

List of Figures

List of Abbreviations

ACL	Anterior Cruciate Ligament
LCL	Lateral Cruciate Ligament
MCL	Medial Collateral Ligament
PCL	Posterior Cruciate Ligament
OA	Osteoarthritis
VF	Volume Fraction

Chapter one

Introduction and Literature Review

1.1 Overview

It is estimated that more than 13.9% of adults aged 25 and older and 33.6% of those 65+ in North America (Lawrence et al., 2008) suffer from Osteoarthritis (OA) which remains a life-long disability requiring treatment. The knee is the most common weight-bearing joint affected (Oliveria et al., 1995; Slemenda et al., 1998). Often clinical and radiographic signs appear when irreversible degenerative changes are already present making prevention and treatment a daunting tasks. The pain and loss of mobility/dexterity associated with knee OA can be detrimental to overall quality of life (Davis et al., 1991) in many ways including fatigue, sleeplessness, reduced income, hospitalization, surgery, side effects from medication, and family instability (Health Canada). While the second most prevalent chronic disease (after cardiovascular disease), OA has a far greater economic impact because OA is slowly crippling. From an economic perspective, the annual cost of OA exceeds $3.4 billion (Health Canada) and $13.2 billion per year (Buckwalter & Mankin, 1998) in Canada and the U.S.A., respectively, and the knee is associated with a large proportion of this financial burden. OA of the knee is 1 of 5 leading causes of disability among non-institutionalized adults (Guccione et al., 1994) and ranks high in disability adjusted life years and years lived with disability (Michaud et al., 2006). Within a decade, nearly 1 million more Canadian adults are expected to have OA, and by 2026, 5 million Canadians will be affected. In the U.S.A. OA is expected to double to 41.1 million by 2030 (Reuters, 2003).

Disorders of the knee joint often involve menisci and ligaments as well. Those suffering from knee ligament and/or meniscus injuries have a significantly increased risk of generating a long-term, chronic disease such as OA (Indelicato & Bittar, 1985;

McNicholas et al., 2000; Noyes et al., 1980; Roos et al., 1998). Rupture of knee ligaments, mostly anterior cruciate ligament (ACL), sometimes occurs during sports activities. An estimated 200,000 ACL-related injuries occur annually in the U.S. alone, with approximately 95,000 ACL ruptures (C. H. Brown, Jr. & Carson, 1999; Miyasaka et al., 1991). Approximately 100,000 ACL reconstructions are performed each year, with health care costs totaling nearly one billion dollars. Approximately 50% of patients with ACL injuries also have meniscal tears. Due to the dramatic adverse effect of total meniscectomy on load distribution (McNicholas et al., 2000) and development of joint osteoarthritis (Roos et al., 1998), partial meniscectomies are performed with the resection of the torn tissues. Concurrent ACL and meniscus ruptures are treated by ACL reconstruction and partial meniscectomy. Incidence of osteoarthritis in mid- and long-term outcome studies of ACL reconstruction (van der Hart et al., 2008) and partial meniscectomy (Hill et al., 2005; Neuman et al., 2008; Rangger et al., 1995; von Porat et al., 2004) has nevertheless persisted. Apart from non-surgical rehabilitation of joint disorders, invasive treatments vary from partial dissection of damaged tissues and biologic repair of chondral and cartilage defects to finally total replacement of ligaments, menisci and joint (i.e., arthroplasty).

Therefore, it is of great importance to investigate joint biomechanics to get a better understanding of the functions of cartilage, meniscus and ligaments and their interactions in the entire knee joint in normal intact and perturbed conditions.

1.2 Functional Anatomy

Knee joint consists of a number of soft tissues with different functions for which they are best structured. Cartilage covers bony ends of proximal tibial and distal femoral bone as well as inner surface of patella to cushion their contacts. The major mechanical function of articular cartilage is to facilitate, without much resistance, the articulation of joints while undergoing different loading and movements. Menisci, on the other hand, increase conformity between tibial and femoral surfaces resulting in more uniform

distribution of stress and greater load bearing. Ligaments constrain and limit the relative motion of femur and tibia and so provide stability to the knee joint by connecting the bones while enabling the wide ranges of motion required by the knee during daily activities. The functional anatomy and structure of these soft tissues are briefly outlined.

1.2.1 Joint and Loading

A knee joint (Fig. 1) consists of three bones: the femur, the tibia and the patella. The two major articulations within the knee are the tibiofemoral and patellofemoral joints. In activities of daily living, different dynamic and static loadings applied to the knee joint are transferred via the cartilage, meniscus and ligaments. The knee joint can rotate by as much as ~135° from hyperextension to hyperflexion depending on the activities. In normal walking, for example, the knee joint flexes from full extension to ~30° flexion and bears in compression 3 to 4 times body weight. This load can even increase to higher values in activities like running, stair ascending/descending and jumping. In addition to axial compression, anterior-posterior force, varus-valgus moment and internal-external torque are also supported by the knee joint.

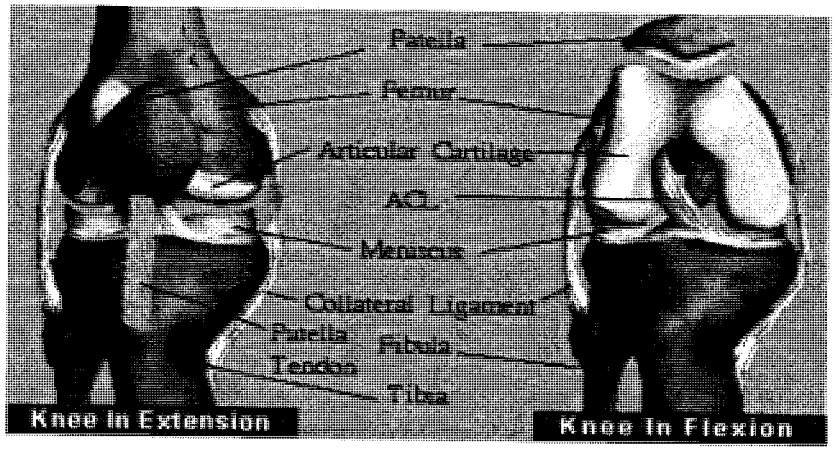

Figure 1. 1 Right knee at full extension (left) and deep flexion (right)
http://www.arthroscopy.com/sp05001.htm

1.2.2 Cartilage

Cartilage is a porous material filled with water with a very low permeability (Fig. 1.2). Articular cartilage is made mainly of collagen (mainly type II), proteoglycans and water, with relative amounts of, respectively, 50-73% (dry weight), 15-30% (dry weight) and 58-78% (Akizuki et al., 1986; Broom & Marra, 1986; Clarke, 1974; Kempson et al., 1973; Maroudas, 1968; Mow et al., 1991; Muir, 1983; Roth & Mow, 1980; Setton et al., 1998). The composition and structure of articular cartilage change with depth from the joint surface (Clarke, 1974; Kaab, Gwynn et al., 1998; Lane & Weiss, 1975; Lipshitz et al., 1976; Muir et al., 1970; Ratcliffe et al., 1984). In cartilage (Fig 1.2), at the superficial zone, fibrils are horizontally oriented parallel to the articular surface (Kaab, Gwynn et al., 1998; Minns & Steven, 1977) whereas they become rather random in the transitional zone (Broom & Marra, 1986) and finally turn perpendicular in the deep zone (Benninghoff, 1925; Kaab, Gwynn et al., 1998; Lane & Weiss, 1975; Minns & Steven, 1977) to anchor the tissue firmly to the subchondral bone (Broom & Poole, 1982; Minns & Steven, 1977; Redler et al., 1975). The equilibrium modulus of nonfibrillar solid matrix also increases along the depth from articular surface to subchondral junction (Schinagl et al., 1997).

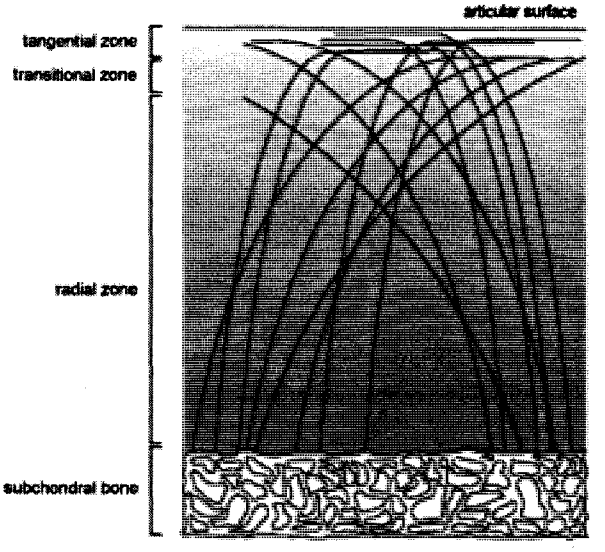

Figure 1. 2 A schema of collagen fibrils orientation in cartilage along the depth
http://luotain.uku.fi/bbc/research_fields/mri/cartilage.jpg

This layered inhomogeneity along the depth and change in orientation of the collagen fibrils have significant effects on material properties, resulting in a highly nonlinear, nonhomogeneous and anisotropic tissue (C. Y. Huang et al., 2005). The presence of water in the pores of solid matrix (proteoglycans) contributes to the tissue viscoelastic behavior leading to stress-relaxation and creep effects. In Stress-relaxation condition, cartilage relieves stress under constant strain as the water exudes from the tissue. Creep, on the other hand, is the tendency of the tissue to deform under permanent load, a phenomenon that can occur for example during a long-term standing position.

Throughout adult life, the articular cartilage of diarthrodial joints such as the knee (Fig 1.3) experiences a high level of biomechanical stress (Hodge et al., 1986). In many individuals and in most anatomic sites, cartilage is able to maintain its normal properties with little change over decades. However trauma and, in some individuals, age causes local damages to cartilage. In presence of even minor injuries, adult cartilage as a tissue has a poor intrinsic capacity for repair (Buckwalter & Mankin, 1998). Despite numerous investigations in osteoarthritis, the etiology of this disease is still unclear due to the very complex structure of cartilage as well as its interactions with subchondral bone.

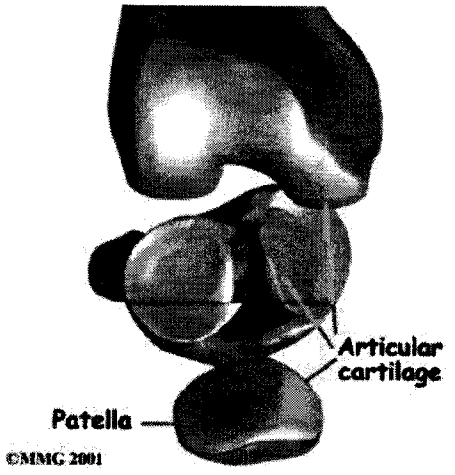

Figure 1. 3 Articular cartilage of femoral, tibial and patellar bones.
www.zmescience.com

1.2.3 Meniscus

Meniscus is a semi-lunar shaped fibrocartilaginous tissue with its horns attached to the condylar surface of the tibia (Figure 1.4) and yields a more uniform distribution of load at the tibiofemoral articulation. It is composed mainly of a dense network of collagen fibers (mainly type I) and proteoglycans and water. Similar to cartilage, presence of water trapped in pores of solid matrix (proteoglycans) gives rise to the tissue viscoelastic properties (stress-relaxation and creep). While the collagen fibrils at top, bottom and peripheral exterior surfaces show no major preferred orientation, they are nevertheless circumferentially oriented in the bulk of the tissue in between these surfaces (Aspden et al., 1985; Petersen & Tillmann, 1998). In addition, radial tie fibres are present that increase the tensile resistance of the meniscus (Skaggs et al., 1994). The structural inhomogeneity and anisotropy of meniscus have also been shown to dominate the tensile behaviour of the tissue (Fithian et al., 1990; Proctor et al., 1989).

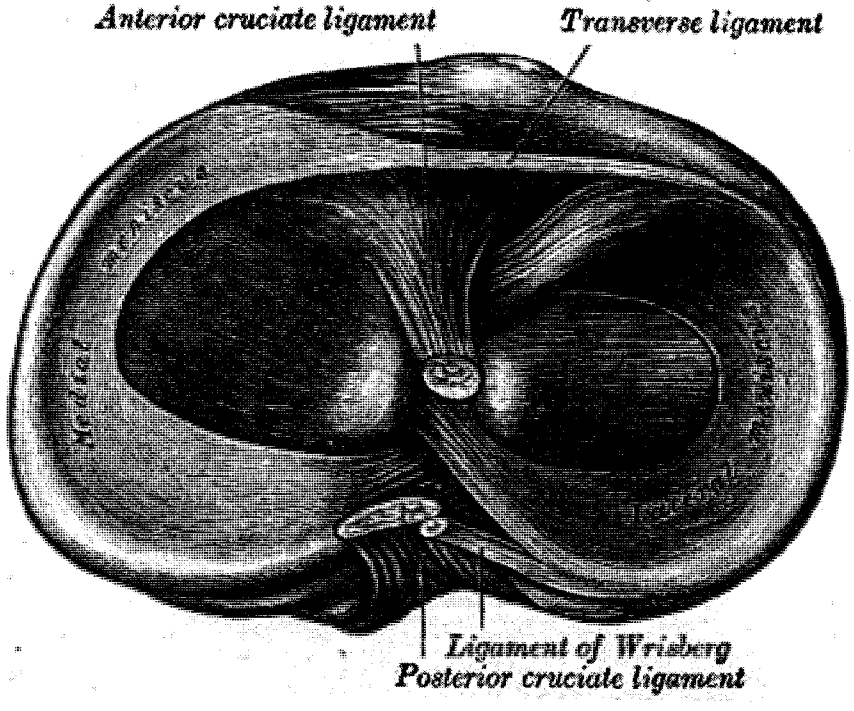

Figure 1. 4 Medial and lateral menisci of the knee joint
www.surgery-information.org

1.2.4 Ligaments

Four major ligaments (ACL, PCL, MCL and LCL), among others, control the relative movement of the tibiofemoral joint (Fig 1.5). Depending on loading conditions, one or some of these ligaments act as primary restraints in the stability of the joint. Anterior cruciate ligament (ACL) connects postero-lateral area of the femoral condyle to the anteromedial depression in front of the intercondyloid eminence of the tibia. This orientation allows the ACL to resist anterior translation of the tibia, in relation to the femur. Posterior cruciate ligament (PCL) connects the posterior intercondylar area of the tibia to the medial condyle of the femur. This configuration allows the PCL to resist forces pushing the tibia posteriorly relative to the femur. Medial (or tibial) collateral ligament (MCL) is a broad, flat, membranous band, situated slightly posterior on the medial side of the knee joint. Primarily resisting valgus deformity, MCL is attached proximally to the medial condyle of femur immediately below the adductor tubercle and distally to the medial condyle of the tibia and medial surface of its body. Its deep surface is intimately attached to the medial meniscus. The lateral collateral ligament (LCL) is thin and runs along the outside of the knee, connecting the femur to the fibula. The lateral collateral ligament provides stability against varus movements.

Ligaments, with their parallel-fibered collagenous tissues, are similar to ropes connecting femur to tibia. This arrangement renders stability and strength to the tissue. At higher strains, the waviness of fibrils decreases or disappears and so the stiffness significantly increases. For this reason, two distinct regions in the stress-strain curve of ligaments are observed; a low-load nonlinear toe region with low stiffness and a high-load linear region with higher stiffness (Chandrashekar et al., 2008).

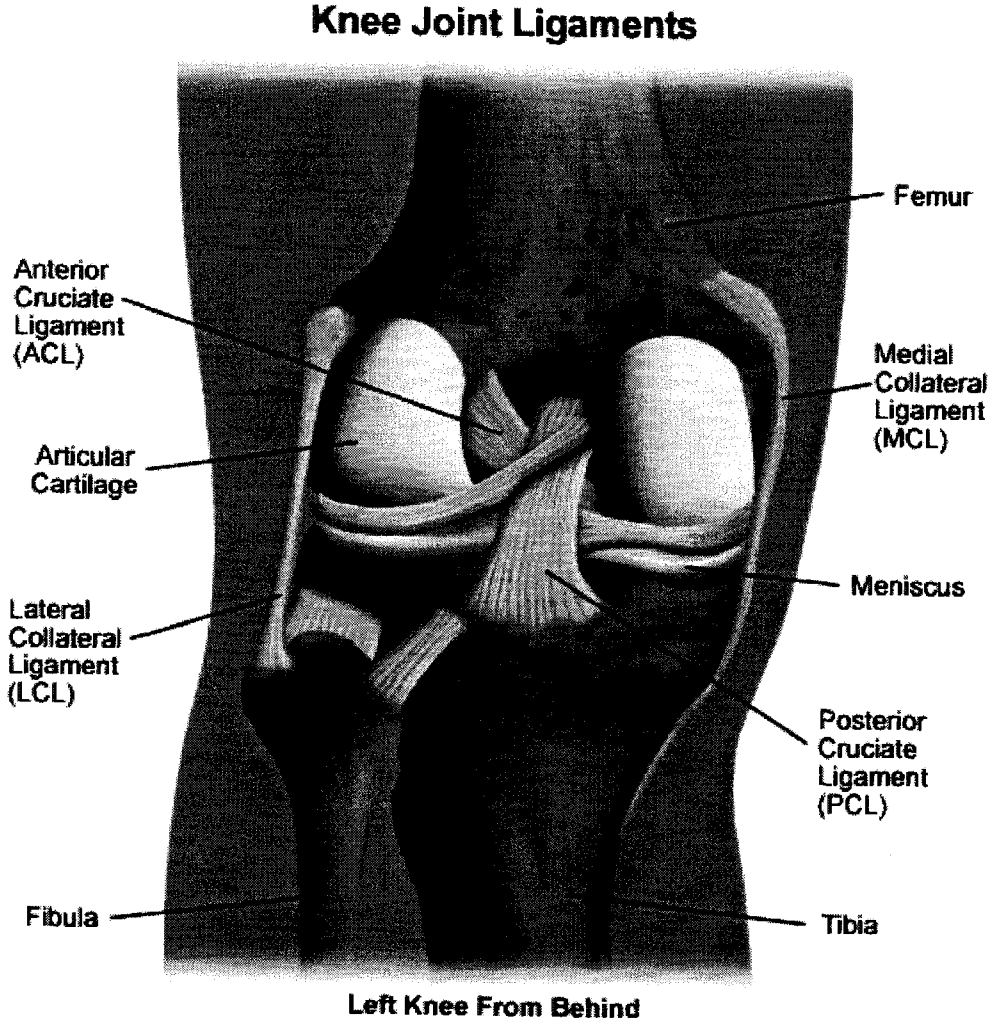

Figure 1. 5 The four major ligaments of the knee joint
http://www.healthsystem.virginia.edu

1.3 Literature Review

1.3.1 Entire Joint Experimental Studies

Numerous experimental studies have been performed on the entire knee joint with the objective to understand joint response under various flexion angles, loading, boundary conditions and tissue disruptions. We review here, however, only those directly related to the objectives of the current study, i.e. studies on the passive

tibiofemoral joint at full extension under compression and anterior-posterior drawer, acting alone or combined. For detailed review of studies on the knee joint with and without muscles, the reader may refer to recent works by our group (Mesfar, 2006; Mesfar & Shirazi-Adl, 2005, 2006a, 2006b, 2008a, 2008b; Moglo & Shirazi-Adl, 2003, 2005).

Peak and average contact stresses as well as contact areas on the tibial plateaus have been measured under a wide range of compression forces up to 2000N at full extension. Pressure sensitive film, color forming transducer, plastic micro-indentation transducer, roentgenography, casting using silicon rubber and radiography have been used for these measurements in cadaver human specimens. Range of mean maximum contact pressure under 1000N compression in different studies is reported to be between 1.6 to 3.2 MPa (Ahmed & Burke, 1983; Fukubayashi & Kurosawa, 1980; Inaba et al., 1990; Walker & Erkman, 1975). The mean average contact pressure is reported to be in the range of 0.48 to 2.2 MPa (A. Huang et al., 2003; Krause et al., 1976; Kurosawa et al., 1980; Seedhom et al., 1973). The total contact area of both plateaus has also been measured to vary in the range of 1150 to 2084 mm^2 under 1000N compression (Ahmed & Burke, 1983; T. D. Brown & Shaw, 1984; A. Huang et al., 2003; Krause et al., 1976; Kurosawa et al., 1980; Maquet et al., 1975; Seedhom & Hargreaves, 1979).

Axial displacement of the tibia relative to the femur in human cadaver specimen has been also measured to be in the range of ~0.6-0.8 mm under 1000 N uniaxial compression with all other degrees of freedom fixed (Kurosawa et al., 1980; Walker & Erkman, 1975). The scatter reported in experimental data is due likely to differences in specimens, duration of load application and measurement devices. These studies have attempted to evaluate the contribution of cartilage and meniscus on each compartment in bearing the applied load. Under 1400 N compression load, contribution of lateral and medial menisci reported, respectively, to be 81% and 77% (Seedhom & Hargreaves, 1979) while value of ~45% has also been reported as averaged over both compartments

of 16 specimens under similar loads (Shrive et al., 1978). Relative load-bearing contribution of menisci decreases with increasing compression loads (Ahmed & Burke, 1983; Walker & Erkman, 1975). For example, under 445 N and 1335 N compression, the compartmental portion of lateral meniscus reaches 82±10% and 77±7% whereas that of medial meniscus is lower at 69±17% and 62±12%, respectively (Ahmed & Burke, 1983).

Numerous experimental studies have investigated behavior of the knee joint under drawer loadings by measuring anterior-posterior laxity along with coupled degrees of freedom (such as internal-external rotations) as well as ligament forces/strains. The mean anterior tibial laxity, for example, has been reported between 2.8 mm to 6.7 mm under 100 N anterior tibial force at full extension (Fukubayashi et al., 1982; Gollehon et al., 1987; Levy et al., 1982; Markolf et al., 1981; Rudy et al., 2000; Veltri et al., 1995). Some studies have also reported tibial anterior displacement between 3.1-3.2mm and 5.3-5.5mm under greater loads of 110 N and 134N respectively (Allen et al., 2000; Kanamori et al., 2000; Markolf et al., 1981; Sakane et al., 1997; Sakane et al., 1999; S. L. Y. Woo et al., 1998). Forces in the ACL have reached 75-162 N under ~100 N drawer at full extension (Fujie et al., 1995; Kanamori et al., 2000; Markolf et al., 1995; Markolf et al., 1998; Takai et al., 1993). ACL, known as primary restraint to anterior translation of the tibia, bears up to 1.5 times of the applied anterior drawer load (Markolf et al., 1995; Takai et al., 1993). Important role of the ACL has also been demonstrated by cutting this ligament and comparing the anterior displacement of the tibia relative to the femur with the intact case (Butler et al., 1980; Fukubayashi et al., 1982; Hsieh & Walker, 1976; Kanamori et al., 2000; Markolf et al., 1976; Shoemaker & Markolf, 1985). Anterior translation increased by about twofold in ACL deficient joint.

A few experimental studies have also investigated knee joint under combined drawer and compression loads. Compression has been reported to reduce total anterior-posterior laxity (Hsieh & Walker, 1976; G. Li et al., 1998; Markolf et al., 1981; Torzilli

et al., 1994) and to protect the ACL (Ahmed et al., 1987; Markolf et al., 1990) or on the contrary to cause higher ACL strains (Fleming et al., 2001; G. Li et al., 1998; Torzilli et al., 1994). Presence of 925 N compression preload increased anterior-posterior stiffness of the joint ~two times modifying nonlinear load-displacement curve in pure drawer loading to a stiffer linear one (Markolf et al., 1981). Experimental studies have used the term "anterior neutral position shift" for anterior translation caused by a compressive load (Markolf et al., 1981; Torzilli et al., 1994), which is caused by the posterior slope of the tibia. A 34% increase in ACL force has been reported at 30° flexion when a 200 N compression preload is added to 100 N drawer loading (G. Li et al., 1998) which is in overall agreement with other measurements (Fleming et al., 2001; Torzilli et al., 1994).

1.3.2 Tissue Experimental Studies

To study the mechanical behavior of cartilage and due to its complexity, isolated cartilage samples are removed for experimental investigation. Usually a small cylindrical block is harvested from a cartilage and put in a confined chamber (Figure 1.6) or in an unconfined configuration between two impermeable platens (Figure 1.7) and compressed under a load- or displacement- control protocol. In confined compression configuration, the sample cannot expand laterally and so collagen fibrils networks do not contribute to mechanical stiffness of the tissue. In unconfined configuration, however, horizontally-oriented collagen fibrils resist lateral expansions especially in the transient period thereby augmenting the tissue stiffness. Another testing configuration involves indentation loading where an indenter compresses the tissue. These configurations are used to evaluate mechanical behavior of cartilage or estimate its mechanical properties at transient and post-transient (equilibrium) periods under different loads, strains and loading/strain rates.

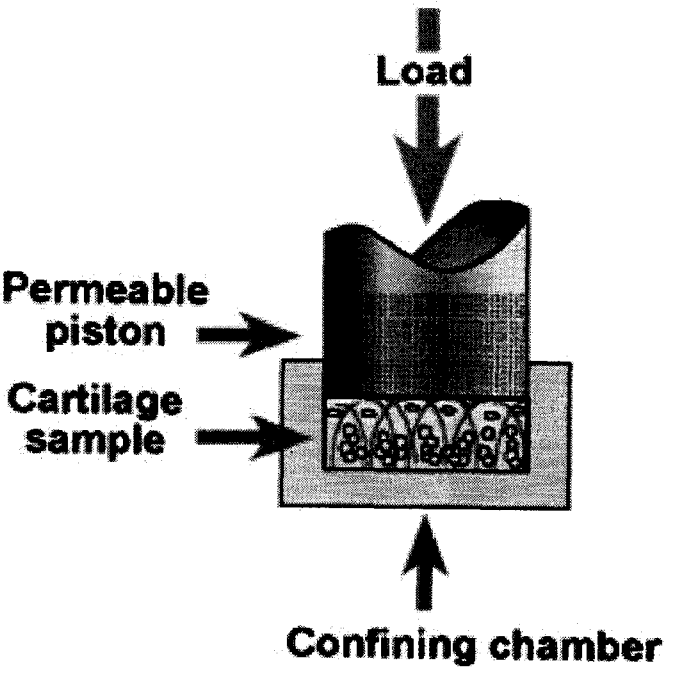

Figure 1. 6 Confined test of a cartilage sample
luotain.uku.fi/bbc/research_fields/biomechanics/

Numerous experimental studies, often combined with theoretical models, have been done under confined compression (Armstrong & Mow, 1982; Buschmann et al., 1998; Mow et al., 1980; Soltz & Ateshian, 1998), unconfined compression (Armstrong et al., 1984; Jurvelin et al., 1997; Mow et al., 1980) or indentation configuration (Athanasiou et al., 1994; Athanasiou et al., 1991; Froimson et al., 1997; Lyyra-Laitinen et al., 1999).

One study (Gore et al., 1983) performed unconfined compression tests on human patellar cartilage to reveal variation of compliance through the thickness. They found transient (short-term) modulus of 4.0 to 43.0 MPa with a mean value of 16.0 MPa under unconfined compression condition, which are typical of values found by other investigators (Johnson et al., 1977). Equilibrium modulus were measured in the range of 0.1-1 MPa (Armstrong & Mow, 1982; Athanasiou et al., 1991; Chahine et al., 2004;

Froimson et al., 1989; Zhu et al., 1993). It was also shown that the equilibrium modulus of cartilage increases when moving from articular surface to subchondral junction (Schinagl et al., 1997). A permeability of 1.18×10^{-15} (m^4/Ns) for lateral femoral condyle of human knee joint was reported (Armstrong & Mow, 1982), which is similar to 1.4×10^{-15} (mm^4/Ns) obtained by another study (Froimson et al., 1997).

Tensile tests have also been performed on animal and human specimens (Charlebois et al., 2004; Kempson et al., 1968; Kempson et al., 1973; Roth & Mow, 1980; S. L. Woo et al., 1976). For example, an average modulus of ~60 MPa was measured at the articular surface of human cartilages (Kempson et al., 1973). Nonlinear tensile properties (strain-dependency) of bovine articular cartilage and their variation with depth, age were also shown (Charlebois et al., 2004). Reporting notwithstanding concerns with sample curvature and gripping, however, they found peak and equilibrium modulus for samples not including the articular surface much lower than those found from cartilage containing the articular surface.

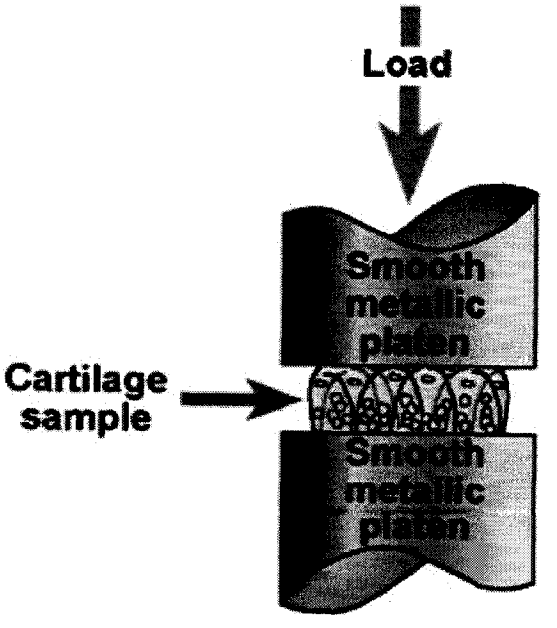

Figure 1. 7 Unconfined test of a cartilage sample
luotain.uku.fi/bbc/research_fields/biomechanics/

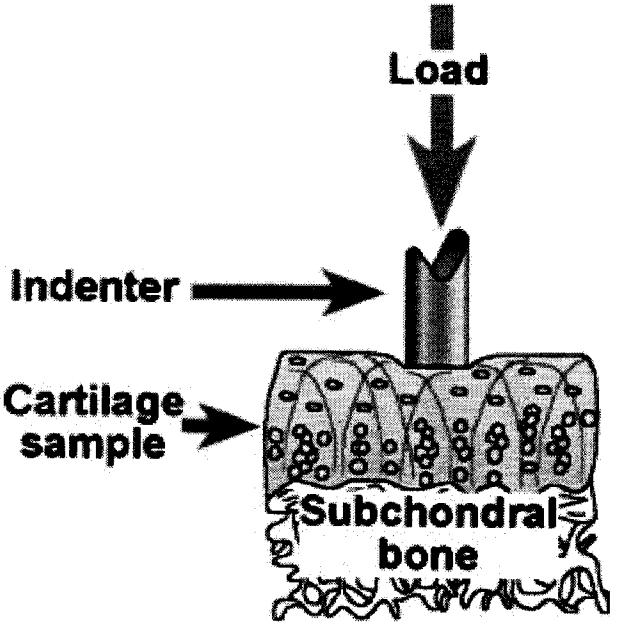

Figure 1. 8 Indentation test of a cartilage sample
luotain.uku.fi/bbc/research_fields/biomechanics/

Similarly, material properties for meniscus have been measured. These studies show that meniscus is roughly one-half as stiff and one-sixth to one-tenth as permeable in compression as articular cartilage. Modulus was measured to be between 0.1 and 0.4 MPa at equilibrium for meniscus in human and bovine specimens (Favenesi et al., 1983; Joshi et al., 1995; Proctor et al., 1989; Sweigart et al., 2004). Permeability was also measured to be between 0.7×10^{-15} and 6.2×10^{-15} $m^4N^{-1}s^{-1}$ for bovine specimens (Proctor et al., 1989; Sweigart et al., 2004). Human meniscus was reported to have a permeability of 1.5×10^{-15} $m^4N^{-1}s^{-1}$ (Sweigart et al., 2004).

Due to different arrangement of collagen fibrils at exterior surfaces of meniscus and deep zones, the tensile modulus is significantly different at each zone. Bovine 200-μm and 400-μm thick slices were harvested respectively from surface and deep zones oriented either tangential (circumferential) or normal (radial) to the predominant circumferentially oriented collagen fibrils (Figs. 9, 10). It was concluded that the surface

is isotropic in tension, which correlates well with the observation that the collagen fibers of the superficial 200 μm region appear to be randomly oriented. However, the material behavior of all deeper samples shows a high degree of dependence on orientation and thus anisotropy. Fig. 11 shows stress-strain curve for specimens at different directions for surface and deep layers. Another study of bovine specimen has shown that the tensile modulus changes from anterior to posterior region of meniscus (Fithian et al., 1990).

The maximum strain limits on tensile tests of human meniscus, reported by Tissakht and Ahmed (Tissakht & Ahmed, 1995), are significantly higher than those of the other studies. For example, the average maximum strain for circumferential specimens is 25.78% compared to ~15% reported elsewhere (Proctor et al., 1989). Moreover, collagen fibers are expected to fail at a tensile strain of less than 15% (Haut & Little, 1972; Morgan, 1960). This study was therefore excluded from our calculations to estimate collagen fibril content.

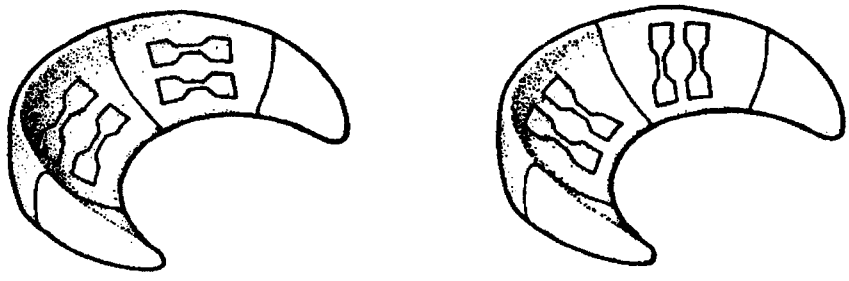

Figure 1. 9 Two dumbbell-shaped tensile specimens were obtained from each slice of tissue, oriented in either the circumferential or the radial direction. Circumferential (left); Radial (right) (Proctor et al., 1989)

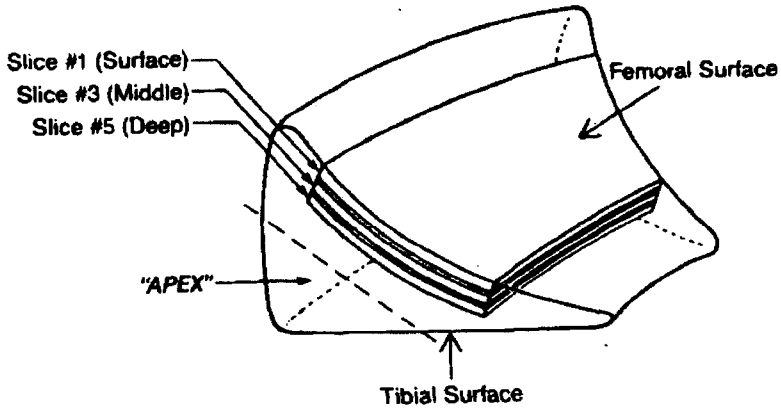

Figure 1. 10 Five serial sections were obtained using a Leitz sledge microtome. Slice 1 was 200 μm thick and contained the femoral surface layer; subsequent slices were 400 μm thick. Alternate slices (1, 3, and 5) were used for mechanical testing (Proctor et al., 1989)

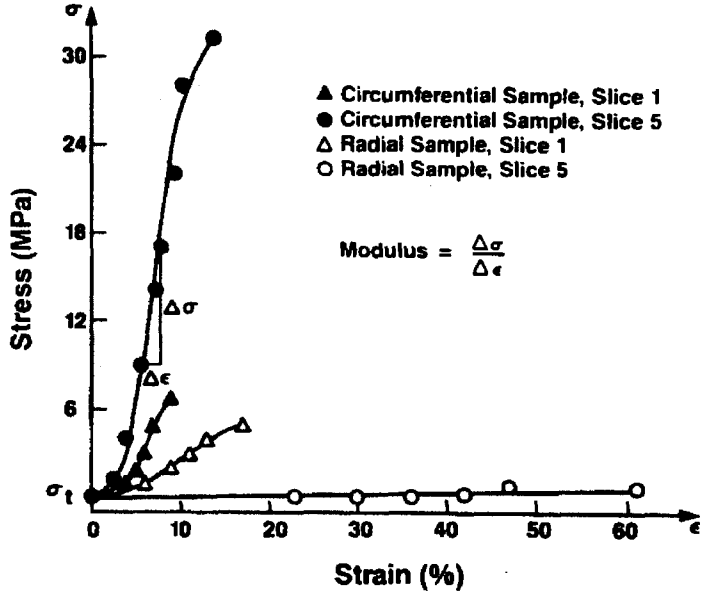

Figure 1. 11 Typical stress-strain curves demonstrating the isotropy of the surface (slice 1) and the anisotropy of the deep tissue (slice 5). The variation between the circumferential and radial direction of slice 1 for all specimens tested is not statistically significant (Proctor et al., 1989)

1.3.3 Knee Joint Model Studies

In addition to experimental measurements, computational approaches are complementary tools that can predict all variables of interest such as primary/coupled displacements, stress, strain and contact area/pressure. Therefore, a theoretical model is an indispensable alterative to provide new insights into understanding the biomechanical behavior of the knee joint and its components, i.e. cartilage, meniscus and ligaments as well as their interactions in different loading conditions.

Earlier theoretical models of knee joint simulated only tibial and femoral surfaces while neglecting menisci (Blankevoort et al., 1991; Crowninshield et al., 1976; Grood & Hefzy, 1982; Wismans et al., 1980). Wismans et al. introduced a mathematical model that simulated the quasi-static behaviour of the tibio-femoral joint by calculating the relative equilibrium positions of the tibia and femur for given external loads and kinematics constraints (Wismans et al., 1980). The articular surfaces were assumed to be rigid and approximated by surface polynomials of degree 3 and 4. Blankevoort et al. developed a three-dimensional mathematical model of human knee joint to determine different mathematical descriptions of articular contact and articular surface geometry (Blankevoort et al., 1991). Deformable and rigid contact description for articular contact was implemented. The difference between linear and nonlinear deformable contact was very small for moderate loading conditions. It was concluded that for simulation of the passive motion characteristics of the knee, the simplified description for contact of a thin linear elastic layer on a rigid foundation is a valid approach when aiming at the study of the motion characteristics for moderate loading conditions.

More recent model studies have used imaging techniques to obtain more precise surface geometry and have included menisci to study biomechanics of the tibiofenmoral joint in its intact and disrupted states (Bendjaballah et al., 1995; Donahue et al., 2002; Pena et al., 2005). Bendjaballah et al. used computerized tomography to reconstruct bony structures and employed a numerically controlled machine to directly digitize

articular surfaces of cartilage layers and menisci (Bendjaballah et al., 1995). This study simulated anisotropic nature of the menisci by using distinct tension-only elements to represent collagen fibrils (Bendjaballah et al., 1995, 1997, 1998). Cartilage was however considered to be isotropic with stiffness of the tissue (Hayes & Mockros, 1971) lumped into one element including both solid matrix and collagen fibrils. The subchondral bones were taken rigid due to their much greater stiffness compared to joint soft tissues (Mente & Lewis, 1994). Donahue et al. used a noncontacting laser-based digitizing system with a root mean squared error of less than 8 microns to create accurately the menisci and articular surfaces (Donahue et al., 2002). They investigated the effect of assuming rigid versus deformable cortical and trabecular bone of the femur and tibia and found that none of the contact variables changed by more than 2% when the femur and tibia were represented as rigid. The menisci were assumed to be transversely isotropic and linearly elastic whereas the cartilages were assumed linear isotropic. In another and more recent study, the geometrical data of the model were obtained by computerized tomography and magnetic resonance images taken from a normal volunteer (Pena et al., 2005). Both cartilage and meniscus were assumed to be linearly elastic and isotropic.

1.3.4 Tissue Model Studies

Cartilage was simulated as elastic (Hayes et al., 1972), viscoelastic (Parsons & Black, 1977) and a poroelastic material composed of an isotropic homogeneous porous media filled with a permeating fluid (Buschmann & Grodzinsky, 1995; Frank & Grodzinsky, 1987; Mow et al., 1980). The measured global load-displacement behaviour of cartilage specimens in confined tests was adequately predicted by these models. While offering new insights into biomechanics of cartilage, this model however failed to describe the overall cartilage mechanical behaviour measured in unconfined compression, a geometry that simulates with a better approximation the tissue physiological conditions in the joint (Armstrong et al., 1984; T. D. Brown & Singerman, 1986). The inherent differences in behaviour of cartilage in tension and compression demanded a more robust model that could automatically simulate both tissue isotropy in

compression (for confined test geometry) and tissue transverse anisotropy in tension (for unconfined test geometry). Additional stiffness in the lateral direction introduced via an orthotropic model was, therefore, found successful in more accurate evaluation of transient response of specimens in unconfined compression test (Cohen et al., 1992).

Subsequently and based on earlier simulations of other fibrous tissues such as intervertebral discs and menisci, a fibril-reinforced composite model of the articular cartilage was developed in which the collagen fibrils were simulated distinctly from the porous isotropic solid matrix (L. P. Li et al., 2000; L. P. Li et al., 1999; Soulhat et al., 1999). The collagen fibrils were represented by radial springs with linear and nonlinear elastic material properties and no resistance in compression. Collagen fibrils were distributed horizontally all along the depth without any change in orientation. Such composite models have also extensively been employed in recent model studies on mechanics of articular cartilage (Julkunen et al., 2007; Wilson et al., 2005; Wilson et al., 2004). Consequently the orientation change in collagen fibrils with its arcade-like structure at the transitional zone that turn gradually horizontal at the surface and vertical at the deep zone was considered in a finite element model (Wilson et al., 2004). Both the non-fibrillar and the fibrilla part of the solid matrix were included in one continuum element in this study. In these models and in the fiber direction, despite the fact that both matrix and collagen fibrils were subjected to the same normal strain, the normal stresses in constituent materials in the same direction were completely different and at times even exhibited opposite signs. These models were successfully applied to both confined and unconfined tests yielding satisfactory results in agreement with measurements.

1.4 Objectives

The overall objective of this study was to develop a novel knee joint model incorporating anisotropic and nonhomogeneous nature of cartilage as well as meniscus. To do so, cartilage fibril-reinforced model developed earlier in our group was substantially improved to be used in our existing 3-D model of entire knee joint.

In the fibril-reinforced axisymmetric model developed earlier in our group, the stiffness of fiber network in the radial direction was so adjusted as to also represent the stiffness of circumferential fibers, which were absent in this model. Moreover, the nonlinear mechanical properties used for the radial fibers did not explicitly account either for the collagen volume fraction in the tissue or the strain-dependent material properties for the pure collagen fibers. To overcome these shortcomings, the objective of the first phase of this study was to develop nonlinear membrane elements to represent fibril networks with strain-dependent material properties and uniform in-plane distribution of fibrils in all directions. In this manner, the physical parameters of the tissue such as the collagen fibril volume fraction and collagen stress-strain properties are explicitly considered in the formulation.

Another shortcoming of earlier fibril-reinforced model was the lack of consideration of change in the orientation of collagen fibrils with depth. The mechanical role of deep vertical fibrils network had been either completely neglected or overlooked in earlier model studies. The objective of the second phase of this study was to appropriately simulate collagen fibrils at different zones along cartilage depth and evaluate role of each zone. To do so, continuum and membrane elements were developed and used.

The objective of the third phase was set to initially incorporate the detailed nonhomogeneous fibrils network structure of the articular cartilage and menisci based on the first and second phases into our existing model of the human knee joint (Bendjaballah et al., 1995; Mesfar & Shirazi-Adl, 2006b) developing thus a novel model of the entire tibiofemoral joint. The transient (i.e., short-term) response of the passive knee joint was subsequently investigated under axial compression forces up to 2000 N with special focus on the mechanical role of fibrils networks in femoral and tibial articular cartilage layers.

In the final phase of this study, using the detailed refined model developed in the third phase as an appropriate computational tool, we investigated the effect of isolated or concurrent ACL reconstruction and unilateral partial meniscectomy under drawer and compression loads acting alone or combined.

1.5 Plan of Thesis (Thesis Organization)

The following articles have been submitted for publication during the course of my PhD studies:

Shirazi R, Shirazi-Adl A. Analysis of articular cartilage as a composite using nonlinear membrane elements for collagen fibrils. Med Eng Phys. 2005 Dec; 27(10):827-35.

Shirazi R, Shirazi Adl A. Deep vertical collagen fibrils play a significant role in mechanics of articular cartilage. J Orthop Res. 2008 May; 26(5):608-15.

Shirazi R, Shirazi Adl A., Hurtig M. Role of cartilage collagen fibrils networks in knee joint biomechanis under compression. Accepted for publication in Journal of Biomechanics 2008; 41(16):3340-8

Shirazi R, Shirazi-Adl A. Analysis of partial meniscectomy and ACL reconstruction in knee joint biomechanics under combined loading Submitted to the American Journal of Sports Medicine, 2008 November (Under Review)

At the end, the codes written in subroutines to appropriately incorporate the material properties' formulation of membrane and brick elements in axisymmetric and 3-D models of cartilage and menisci are explained in the appendix. Also, some additional relevant results for the first study will be presented in the appendix at the end of the thesis.

Chapter two

Article I: Analysis of articular cartilage as a composite using nonlinear membrane elements for collagen fibrils

R. Shirazi and A. Shirazi-Adl

Division of Applied Mechanics, Department of Mechanical Engineering
École Polytechnique, Montréal, Québec, Canada

Article published in
Medical Engineering & Physics
2005; 27(10):827-35

Keywords: Cartilage; Composite, Collagen Fibrils; Membrane Element; Unconfined Compression; Volume Fraction; Finite Element Analysis

2.1 Abstract

To develop a composite fibre-reinforced model of the cartilage, membrane shell elements were introduced to represent collagen fibrils reinforcing the isotropic porous solid matrix filled with fluid. Nonlinear stress-strain curve of pure collagen fibres and collagen volume fraction were explicitly presented in the formulation of these membrane elements. In this composite model, in accordance with tissue structure, the matrix and fibril membrane network experienced dissimilar stresses despite identical strains in the fibre directions. Different unconfined compression and indentation case studies were performed to determine the distinct role of membrane collagen fibrils in nonlinear poroelastic mechanics of articular cartilage.

The importance of nonlinear fibril membrane elements in the tissue relaxation response as well as in temporal and spatial variations of pore pressure and solid matrix stresses was demonstrated. By individual adjustments of the collagen volume fraction and collagen mechanical properties, the model allows for the simulation of alterations in the fibril network structure of the tissue towards modelling damage processes or repair attempts. The current model which is based on a physiological description of the tissue structure is promising in improvement of our understanding of the cartilage pathomechanics.

2.2 Introduction

The breakdown of articular cartilage and its underlying bone leading to osteoarthritis (OA) and pain can result from a multitude of interacting mechanical and biological factors that can occur in an acute and traumatic form or cumulatively in a chronic fashion over many years (Mow & Hayes, 1997). An improved knowledge in biomechanics of articular cartilage including interactions between its various constituent materials under different loading conditions is essential for both a better understanding of pathomechanics of OA and more effective preventive as well as treatment procedures.

The major mechanical function of articular cartilage is to facilitate, without much resistance, the articulation of joints while undergoing different loading and movement conditions. In doing so, the articular cartilage itself is constantly subjected to large loads and finite deformations, even in regular daily living activities. The articular cartilage is a highly nonhomogeneous, anisotropic and multiphasic complex biomaterial (Chahine et al., 2004; Charlebois et al., 2004; Huang et al., 2005; Verteramo & Seedhom, 2004; Wang et al., 2003) with three mechanically important constituents; i.e. water, collagen fibrils and nonfibrillar matrix (proteoglycans), which interact with each other in a manner to maintain the high performance of the cartilage without impairments for decades under repetitive static and dynamic loads. In the earlier attempts in which the articular cartilage was modelled as a poroelastic material composed of an isotropic homogeneous porous media filled with permeating fluid, the measured global load-displacement behaviour of cartilage specimens in confined compression tests was adequately predicted (Buschmann et al., 1998; Frank & Grodzinsky, 1987; Mow et al., 1980). On the contrary, however, this model subsequently failed to describe the overall cartilage mechanical behaviour measured in unconfined compression testing configuration, a geometry that simulates with a better approximation the tissue physiological conditions in the joint (Armstrong et al., 1984; Brown & Singerman, 1986). The inherent differences in behaviour of cartilage in tension and in compression

demanded a more robust model that could automatically simulate both tissue isotropy in compression (for confined test geometry) and tissue transverse anisotropy in tension (for unconfined test geometry). Additional stiffness in the lateral direction introduced via an orthotropic model was, therefore, found successful in more accurate evaluation of transient response of specimens in unconfined compression tests (Cohen et al., 1992).

Following our earlier model studies of connective fibrous tissues such as the intervertebral disc anulus and knee joint meniscus (Bendjaballah et al., 1995; S. A. Shirazi-Adl et al., 1984), a fibre-reinforced composite model of the articular cartilage was developed in which the collagen fibrils were simulated distinctly from the porous isotropic solid matrix (Li et al., 2000; Li et al., 1999; Soulhat et al., 1999). The collagen fibrils were represented by radial springs with linear and nonlinear elastic material properties and no resistance in compression. In this model and in the fibre direction, despite the fact that both matrix and collagen fibrils were subjected to the same normal strain, the normal stresses in constituent materials in the same direction were completely different and at times even exhibited opposite signs. The model was successfully applied to both confined and unconfined tests yielding satisfactory results in agreement with measurements.

In foregoing axisymmetric model studies (Soulhat et al., 1999), the stiffness of fibre network in the radial direction was so adjusted as to also represent the stiffness of circumferential fibres which were absent in the model. Moreover, the nonlinear mechanical properties used for the radial fibres did not explicitly account either for the collagen fibril volume fraction in the tissue or the strain-dependent material properties reported in the literature for the pure collagen fibres. In continuation of our earlier model studies in which the anulus collagen fibres were represented by membrane elements with single fibre directions (A. Shirazi-Adl, 1988, 1989, 1994), the objective of the present work was, hence, set to develop nonlinear membrane shell elements to represent fibril networks with strain-dependent material properties and uniform in-plane distribution of

fibrils in all directions. In this manner, the physical parameters of the tissue such as the collagen fibril volume fraction and collagen stress-strain properties are explicitly considered in the formulation. In the current investigation, this element is introduced in the ABAQUS software and used to simulate fibril network of the articular cartilage in both axisymmetric and 3-D poroelastic nonlinear response studies under different loading conditions.

2.3 Method

2.3.1 Membrane Element

The solid isotropic porous matrix of the articular cartilage filled with water is represented, in a 3-D mesh, by 8-node or 20-node elements with regular or reduced integrations (the integration order did not have much effect on predictions in all cases studied in this work). The pressure field is taken linear in different directions while the displacement fields are either linear or quadratic. The fibrils, on the other hand, are introduced by 4-node or 8-node shell membrane elements with, respectively, linear and quadratic displacement fields.

The collagen fibrils in the plane of membranes are assumed to be homogeneously distributed in all directions. Despite such distribution, however, a direction-dependent response prevails due to the strain-dependency in the fibrils material properties and anisotropy in the strain field. At each step of loading, principal strain directions in the plane of membranes are taken as the material principal axes. The stresses in these principal directions are subsequently evaluated based on the total principal strains (Fig. 2.1) and fibrils stress-strain curve (Fig. 2.2). This latter nonlinear curve presents the mechanical property of pure collagen fibres in accordance with the reported data in the literature (Haut & Little, 1972; Morgan, 1960). Equal principal strains would generate an isotropic material modulus matrix while any non-positive principal strain results in a zero (or near-zero) diagonal component in the corresponding modulus and stress

matrices. Finally these tensors are transformed back to the local membrane directions and used in subsequent manipulations.

For the axisymmetric models, the principal directions lie along the membrane element in the radial plane and along global circumferential direction. In the initial configuration, membrane elements can arbitrarily be oriented in any direction in the radial plane. The formulation of these membrane elements with nonlinear material properties were introduced in the ABAQUS via the subroutine UMAT. The results were validated by comparison of predictions for different existing constitutive relations.

In the finite element mesh, the thickness of the entire membrane element for each solid matrix element is initially calculated based on the fibril volume fraction in that direction. This thickness is subsequently subdivided either equally between 2 membrane elements when using solid elements with linear displacement fields or with proportions of 2/3 for the middle element and 1/6 for the side elements when considering solid elements with quadratic displacement fields (Fig. 2.3). All analysed cases considered in this work have incorporated three nonlinearities; fibril strain-dependant material properties (Fig. 2.2), finite deformation and strain-dependent permeability. The initial void ratio is taken as 4 with drained matrix isotropic moduli E_m=0.26 MPa and v_m=0.42, permeability $k_0=3\text{x}10^{-15}$ m^4/Ns and M=30 in the nonlinear permeability relation $k = k_0 \exp(M\frac{e-e_0}{1+e_0})$. No axially oriented membranes are considered in current studies.

2.3.2 Cases Studied

Four different cases are considered in this investigation.

Case 1: To compare the results obtained using two different models for the network of reinforcing fibrils (i.e. the present model using membrane elements and that of Li et al. (Li et al., 1999) using spring elements), an axisymmetric model of an unconfined

compression test similar to that used by Li et al. (Li et al., 1999) is considered in this case (Fig. 2.3).

For the Li et al. model (Li et al., 1999), the results are obtained using $E=2400\times\varepsilon+3$ for the radially-oriented fibril springs that occupy the entire volume. Since the collagen volume fraction and fibril material properties are not explicitly used in this model (Li et al., 1999), an equivalent volume fraction for which nearly similar results (for the same load and load rate) are obtained is initially evaluated. The loading is considered in accordance with Li et al. (Li et al., 1999); 20 steps of equal ramp compression displacement of 5 μm each in the axial direction. The compression rate is taken at 2 μm/s and each increment is followed by a relaxation period.

An additional case is also studied in which the total axial displacement of 100 μm is applied in only one ramp step at 0.5 s, i.e. at a strain rate of 20%/s. Initially, the model with fibril network represented by radial spring elements is applied to compute the response using $E=2420\times\varepsilon+3$. Subsequently, an equivalent fibril volume fraction is estimated for the membrane element of the present model in order to yield comparable relaxation response.

Finally, to verify the 3-D version of the membrane element, a 3-D model of an unconfined compression test using a specimen with 1 mm height and 30 mm×30 mm base dimensions (as a rough representation of a tibial plateau) are developed and subjected to a 0.1 mm uniform ramp axial displacement at 0.5 s. An axisymmetric model with nearly equal cross-sectional area (radius of 17 mm) is also analysed to compare predictions.

Case 2: In this case, for the unconfined testing configuration in compression with a ramp displacement of 100 μm at 0.5s (strain rate at 20 %/s), the fibril volume fraction is varied and its effect on the response is predicted. For this purpose, the volume fraction

obtained in previous case study is taken as the reference value which is then altered by ±33%.

Case 3: The third case, under the same ramp displacement, investigates the effect of changes in the radius of specimens in unconfined compression tests on results. The radius of the model shown in Fig. 2.3 which is 1.4 mm is increased by 2, 4 or 8 folds to 2.8 mm, 5.6 mm or 11.2 mm. The mesh density remains identical for all four cases considered. It was verified for the largest specimen that further refinement of the mesh beyond the current one did not influence the results.

Case 4: In this case study, an indentation test is simulated. A specimen with a height of 2 mm and radius of 17 mm is considered. A rigid semi-spherical permeable punch with a diameter of 2.5 mm (slightly larger than the thickness of the specimen) indents the specimen by a maximum of 0.2 mm in 0.5 second ramp displacement resulting in a nominal axial strain of 10% at the centre. The centre of the punch is on the axis of the symmetry. To improve accuracy and avoid excessive distortion, a finer mesh is adopted for the areas in and around the contact. The bottom surface of the specimen is assumed completely fixed, a condition that could simulate the cartilage attachment to the subchondral bone. The bottom surface is taken impermeable while both the permeable and impermeable conditions are assumed for the top surface. An open surface and not a sealed one has been reported to yield better agreement with experiments in terms of relaxation time and load sharing between the solid and fluid phases (Federico et al., 2004). The contact surfaces are assumed to be frictionless.

2.4 Results and Discussion

It is to be noted that in all cases considered in this work, the depth-dependent changes in the material properties of the articular cartilage (i.e., changes in fibril volume fraction, fibril material properties and matrix material properties with location within the

tissue) were not considered (Buschmann & Grodzinsky, 1995; Erne et al., 2005; Kempson et al., 1973; Kempson et al., 1970; Pins et al., 1997; Roth & Mow, 1980; Woo et al., 1976; Woo et al., 1979).

Case 1: Based on a trial-and-error attempt, a collagen fibril volume fraction of ~4% is found to yield results (Fig. 2.4) similar to those reported elsewhere (Li et al., 1999). It is to be noted that perfect agreement cannot be expected due to differences in models such as the stress-strain curves with nonlinear modulus used in this work (Fig. 2.2) and that with linear modulus used earlier (Li et al., 1999). Fibril volume fraction of 3.2% has been estimated by Simha et al. (Simha et al., 1999) by comparison of a composite model of cartilage tissue with measurements on a tissue culture using chondrocytes from cartilage of young rabbits.

In agreement with measurements (Fortin et al., 2000), the nonlinear compression-offset dependent stiffening of the transient response is evident in which the transient peak to equilibrium load ratio increases from a cycle to the next as displacement loading progresses. In other words, the relaxation behaviour becomes increasingly more apparent with the applied strain. This behaviour is primarily due to the strain-dependent properties of fibril membrane elements (Li et al., 1999).

Under a single ramp displacement at 0.5 s, an equivalent collagen content of ~7.5% is evaluated (Fig. 2.5) in order to match the transient response using the model with fibril network as uniaxial spring elements (Li et al., 1999). In this case, due to much larger strain and strain-rate applied at one single ramp step, the fibrils undergo much greater strains; for example the radial/circumferential strains at the centre reach 5.3% at transient peak which diminish to 1.5% at equilibrium compared with 0.8% at the peak and 0.5% at equilibrium for the 20^{th} cycle in previous loading case.

Finally, similar results are computed when using a 3-D model rather than an axisymmetric one for the unconfined test subject to a single ramp compression.

Case 2: The transient response significantly stiffens as the fibril volume fraction increases from 5% to 7.5% and further to 10% (Fig. 2.6) which is in agreement with earlier investigations (Li et al., 1999). The equilibrium load remains, however, nearly the same irrespective of foregoing variations in the volume fraction (Fig. 2.6a). The pore pressure also substantially increases with the fibril volume fraction early during the loading (Fig. 2.6b), a trend that disappears later at t>15s. As time progresses (say at t=30s), this trend even reverses so that the pore pressure, even though small, is largest for the case with smallest volume fraction. This is due to much larger pore pressure at the transient stage in the case with larger volume fraction (Fig. 2.6b) which results in greater exudation of fluid out of the specimen in the early stages.

The radial strain in both the matrix and fibril network remains always tensile and decreases from its maximum at the transient period to its minimum at equilibrium (Fig. 2.7a). The radial stress in the fibril network demonstrates a similar trend with the maximum of ~45 MPa at the transient peak (not shown). In contrast, however, the solid matrix experiences tensile radial stress only for a short period after the ramp loading is applied and becomes increasingly compressive as time advances towards equilibrium (Fig. 2.7b). Changes in the fibril volume fraction influences the strain and stress in membrane elements and solid matrix only at post transient period to equilibrium. At transient peak, the added horizontal forces under greater fibril volume fraction are supported solely by the pore fluid resulting in a substantial increase in this latter which in turn augments the stiffness and transient load (Fig. 2.6a,b). As the pore pressure decreases with time in post transient period, the radial stress caused by fibril network is transferred from the pore fluid to the solid matrix.

Case 3: This case considers the effect of changes in the radial dimension of specimens on results in unconfined compression tests. The radius of 1.4 mm, used in previous cases, was increased by 2, 4 and 8-folds and analyses were repeated under identical ramp displacement loading. The fibril volume fraction remained constant at 7.5% in this case. The normalised transient and post transient stiffness and pore pressure responses are significantly influenced by changes in the size of specimens (Fig. 2.8). In contrast to the results in previous case, the effect is much more pronounced at the post transient period than at the transient peak (t=0.5s). In specimens with smaller radius, the peak pore pressure is reached shortly after the transient period and drops rapidly after to equilibrium. In contrast in larger specimens, this peak pressure is attained with a substantial delay after the transient period. The drop in the stiffness (relaxation) and pore pressure is much more rapid at smaller specimens than at larger ones where the pore pressure is preserved at near the peak values for much longer times. For instance, the relaxation time defined in each case as the time needed for the applied stress to reach 5% of its respective peak transient value (t=0.5s) is found as ~97 s for R=1.4 mm, 358 s for R=2.8 mm, 1372 s for R=5.6 mm and 5391 s for R=11.2 mm. The change in the relaxation time from a specimen to another is, hence, roughly proportional to the square of the specimen radius, a relationship that has been observed in linear cases (Soulhat et al., 1999). This phenomenon is due to the greater pore fluid outflow distance to outer free boundaries in larger specimens.

The fibril membranes experience tensile strain and stress that remain nearly constant in early post transient period in the largest specimen (Fig. 2.9a). In contrast, the relaxation in strain and stress is much more rapid in specimens with smaller radius. Similarly, the radial stress in the solid matrix of the specimen with largest radius remains tensile for a relatively long period of time ($t \approx 187s$) following transient period (Fig. 2.9b). Similar to the situation in previous case, the radial stress in the solid matrix is dependent on the interplay between the membrane stresses and pore fluid pressure. Any

marked decrease in the pore pressure observed in smaller specimens tends to relegate the support of the horizontal fibril network tensile stresses to the solid matrix.

Case 4: Indentation of an axisymmetric specimen with 17 mm radius and 2 mm thickness by a spherical permeable indenter of 2.5 mm radius is considered in this case. Much greater transient stiffness and pore pressure are computed when the upper surface is impermeable (i.e., sealed) and, hence, the outflow of fluid at the top surface is not allowed (Fig. 2.10). For both cases and at the transient time (0.5 s), only a small portion of the specimen (radius of ~1.2 mm) experiences a non-negligible pore pressure. As time progresses, fluid pressure substantially drops at the centre and throughout while extending radially. For example at 1000 s, the pore pressure, while reaching nearly as far as the mid-radius position, diminishes to maximum values of only 1.6 KPa and 4 KPa at the centre respectively for cases with permeable and sealed conditions.

At the transient period, the fibril network experiences much larger radial tensile strain in the sealed boundary condition compared with the permeable condition. Though the strain in the fibril network continuously diminishes with time, it remains always positive (i.e., tensile) (Fig. 2.11a). The solid matrix, on the other hand while under the same strain field (Fig. 2.11a), initially experiences tensile radial stress which becomes compressive as time progresses and pore pressure drops (Fig. 2.11b). This compressive stress remains greater in the sealed case which is due to larger tensile radial strain in fibril network in this case.

2.5 Concluding Remarks

The fibril-reinforced composite model of the articular cartilage has been successful in describing the experimentally-observed temporal response characteristics of the articular cartilage in confined and unconfined testing configurations (Li et al., 2000, 2003; Li et al., 1999; Soulhat et al., 1999). The ever-important mechanical role of collagen fibrils in tension and its interaction with the pore fluid flow have been found

responsible for the strain and strain-rate dependencies of the cartilage tissue (Li et al., 2003). In this composite model, the matrix (i.e., proteoglycan) and fibril network (i.e., collagen) experience dissimilar stresses despite identical strains in the fibre directions (neglecting interfacial slips). Evidently, such differences in stress values depend on the strain and relative stiffness of these constituents which are both expected to increase under larger loads and displacements. The fibril networks while under tension, in turn, confine and apply compression on the matrix thus influencing the stress field in the tissue as a whole as compared with that in homogeneous orthotropic models. The prediction of tensile stresses in fibril networks and of compressive stresses in the matrix appears desirable in employing each component to resist stresses for which it is best structured.

In our earlier model studies of the articular cartilage, the fibril networks in the radial direction were represented by uniaxial spring elements with nonlinear properties in tension and no resistance in compression. These studies, however, did not explicitly account for the important physical properties of the tissue such as the volume fraction and nonlinear stress-strain curves of the fibril networks at different locations and directions. Moreover, the radial fibrils were modified to also account for the circumferential fibrils by using equivalent strain energies in a disc under a uniform state of stress. In this investigation, however, membrane shell elements are used to directly represent fibril networks in both axisymmetric and 3-D model studies. The formulation of the membrane element also explicitly accounts for the tissue collagen fibre properties such as volume fraction and stress-strain curve. This approach appears more meaningful in not lumping various fibril properties into one stiffness term which risks losing its physical interpretation and, hence, significance. In the current study, the cross coupling between membrane strains and stresses in material principal directions (Fig. 2.1) were neglected by assuming a Poison's ratio of nil for membrane elements. Moreover, the axially oriented fibril membranes were not represented in none of cases investigated.

Alterations in the fibril network structure of the tissue towards the realistic simulation of a damage process or repair attempt can be controlled by separate variations in the collagen volume fraction and in the collagen mechanical properties. In this manner the individual role of each physical parameter can be considered and identified. The structure-based description of the tissue proposed in this work is promising in delineating the tissue pathomechanics. Finally, the developed membrane elements can in future be used to simulate fibril networks in the articular cartilage and menisci of our existing knee joint models towards the nonlinear poroelastic investigations of the entire tibiofemoral and patellofemoral joint mechanics.

2.6 Acknowledgment

The research work is supported by a grant from the Natural Sciences and Engineering Research Council of Canada (NSERC).

2.7 References

Armstrong, C. G., Lai, W. M., and Mow, V. C. (1984). An analysis of the unconfined compression of articular cartilage. *J Biomech Eng, 106*(2), 165-173.

Bendjaballah, M. Z., Shirazi-Adl, A., and Zukor, D. J. (1995). Biomechanics of the human knee joint in compression: reconstruction, mesh generation and finite element analysis. *The Knee, 2*(2), 69-79.

Brown, T. D., and Singerman, R. J. (1986). Experimental determination of the linear biphasic constitutive coefficients of human fetal proximal femoral chondroepiphysis. *J Biomech, 19*(8), 597-605.

Buschmann, M. D., and Grodzinsky, A. J. (1995). A molecular model of proteoglycan-associated electrostatic forces in cartilage mechanics. *J Biomech Eng, 117*(2), 179-192.

Buschmann, M. D., Soulhat, J., Shirazi-Adl, A., Jurvelin, J. S., and Hunziker, E. B. (1998). Confined compression of articular cartilage: linearity in ramp and sinusoidal tests and the importance of interdigitation and incomplete confinement. *J Biomech, 31*(2), 171-178.

Chahine, N. O., Wang, C. C., Hung, C. T., and Ateshian, G. A. (2004). Anisotropic strain-dependent material properties of bovine articular cartilage in the transitional range from tension to compression. *J Biomech, 37*(8), 1251-1261.

Charlebois, M., McKee, M. D., and Buschmann, M. D. (2004). Nonlinear tensile properties of bovine articular cartilage and their variation with age and depth. *J Biomech Eng, 126*(2), 129-137.

Cohen, B., Lai, W. M., Chorney, G. S., Dick, H. M., and Mow, V. C. (1992). *Unconfined compression of transversely-isotropic biphasic tissues*. vol. 22. 187-190, Anaheim, CA, USA.

Erne, O. K., Reid, J. B., Ehmke, L. W., Sommers, M. B., Madey, S. M., and Bottlang, M. (2005). Depth-dependent strain of patellofemoral articular cartilage in unconfined compression. *J Biomech, 38*(4), 667-672.

Federico, S., La Rosa, G., Herzog, W., and Wu, J. Z. (2004). Effect of fluid boundary conditions on joint contact mechanics and applications to the modeling of osteoarthritic joints. *J Biomech Eng, 126*(2), 220-225.

Fortin, M., Soulhat, J., Shirazi-Adl, A., Hunziker, E. B., and Buschmann, M. D. (2000). Unconfined compression of articular cartilage: nonlinear behavior and comparison with a fibril-reinforced biphasic model. *J Biomech Eng, 122*(2), 189-195.

Frank, E. H., and Grodzinsky, A. J. (1987). Cartilage electromechanics--II. A continuum model of cartilage electrokinetics and correlation with experiments. *J Biomech, 20*(6), 629-639.

Haut, R. C., and Little, R. W. (1972). A constitutive equation for collagen fibers. *J Biomech, 5*(5), 423-430.

Huang, C. Y., Stankiewicz, A., Ateshian, G. A., and Mow, V. C. (2005). Anisotropy, inhomogeneity, and tension-compression nonlinearity of human glenohumeral cartilage in finite deformation. *J Biomech, 38*(4), 799-809.

Kempson, G. E., Muir, H., Pollard, C., and Tuke, M. (1973). The tensile properties of the cartilage of human femoral condyles related to the content of collagen and glycosaminoglycans. *Biochim Biophys Acta, 297*(2), 456-472.

Kempson, G. E., Muir, H., Swanson, S. A., and Freeman, M. A. (1970). Correlations between stiffness and the chemical constituents of cartilage on the human femoral head. *Biochim Biophys Acta, 215*(1), 70-77.

Li, L. P., Buschmann, M. D., and Shirazi-Adl, A. (2000). A fibril reinforced nonhomogeneous poroelastic model for articular cartilage: inhomogeneous response in unconfined compression. *J Biomech, 33*(12), 1533-1541.

Li, L. P., Buschmann, M. D., and Shirazi-Adl, A. (2003). Strain-rate dependent stiffness of articular cartilage in unconfined compression. *J Biomech Eng, 125*(2), 161-168.

Li, L. P., Soulhat, J., Buschmann, M. D., and Shirazi-Adl, A. (1999). Nonlinear analysis of cartilage in unconfined ramp compression using a fibril reinforced poroelastic model. *Clin Biomech, 14*(9), 673-682.

Morgan, F. R. (1960). Mechanical properties of collagen and leather fibres. *American Leather Chemists Association Journal, 55*(1), 4-23.

Mow, V. C., and Hayes, W. C. (1997). *Basic Orthopaedic Biomechanics* (2nd ed.). New York: Lippincott-Raven.

Mow, V. C., Kuei, S. C., Lai, W. M., and Armstrong, C. G. (1980). Biphasic creep and stress relaxation of articular cartilage in compression? Theory and experiments. *J Biomech Eng, 102*(1), 73-84.

Pins, G. D., Huang, E. K., Christiansen, D. L., and Silver, F. H. (1997). Effects of static axial strain on the tensile properties and failure mechanisms of self-assembled collagen fibers. *Journal of Applied Polymer Science, 63*(11), 1429-1440.

Roth, V., and Mow, V. C. (1980). The intrinsic tensile behavior of the matrix of bovine articular cartilage and its variation with age. *J Bone Joint Surg Am, 62*(7), 1102-1117.

Shirazi-Adl, A. (1988). *Finite element stress analysis of disc annulus using different composite material models*. vol. 9. 449-460, Chicago, IL, USA.

Shirazi-Adl, A. (1989). On the fibre composite material models of disc annulus--comparison of predicted stresses. *J Biomech, 22*(4), 357-365.

Shirazi-Adl, A. (1994). Biomechanics of the lumbar spine in sagittal/lateral moments. *Spine, 19*(21), 2407-2414.

Shirazi-Adl, S. A., Shrivastava, S. C., and Ahmed, A. M. (1984). Stress analysis of the lumbar disc-body unit in compression. A three-dimensional nonlinear finite element study. *Spine, 9*(2), 120-134.

Simha, N. K., Fedewa, M., Leo, P. H., Lewis, J. L., and Oegema, T. (1999). A composites theory predicts the dependence of stiffness of cartilage culture tissues on collagen volume fraction. *J Biomech, 32*(5), 503-509.

Soulhat, J., Buschmann, M. D., and Shirazi-Adl, A. (1999). A fibril-network-reinforced biphasic model of cartilage in unconfined compression. *J Biomech Eng, 121*(3), 340-347.

Verteramo, A., and Seedhom, B. B. (2004). Zonal and directional variations in tensile properties of bovine articular cartilage with special reference to strain rate variation. *Biorheology, 41*(3-4), 203-213.

Wang, C. C., Chahine, N. O., Hung, C. T., and Ateshian, G. A. (2003). Optical determination of anisotropic material properties of bovine articular cartilage in compression. *J Biomech, 36*(3), 339-353.

Woo, S. L., Akeson, W. H., and Jemmott, G. F. (1976). Measurements of nonhomogeneous, directional mechanical properties of articular cartilage in tension. *J Biomech, 9*(12), 785-791.

Woo, S. L., Lubock, P., Gomez, M. A., Jemmott, G. F., Kuei, S. C., and Akeson, W. H. (1979). Large deformation nonhomogeneous and directional properties of articular cartilage in uniaxial tension. *J Biomech, 12*(6), 437-446.

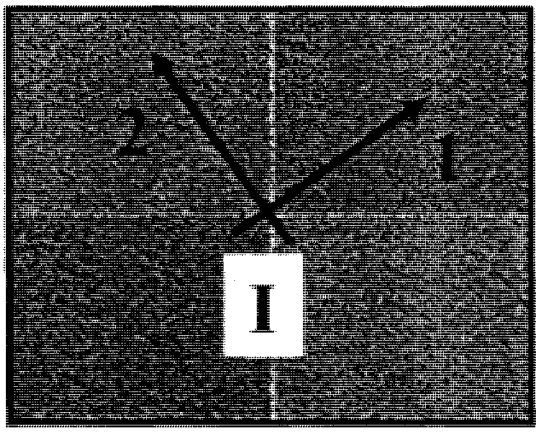

$$[E_T] = \begin{bmatrix} E_1 & 0 & 0 \\ 0 & E_2 & 0 \\ 0 & 0 & G_{12} \end{bmatrix}$$

$$G_{12} = \frac{E_1 + E_2}{4}$$

Figure 2. 1 A typical shell membrane element with material principal axes that are oriented along the principal strain directions in the plane of the membrane at any given integration point I. The tangent modulus matrix in this system is also shown neglecting the cross coupling terms between incremental normal stresses and strains (i.e. ν=0).

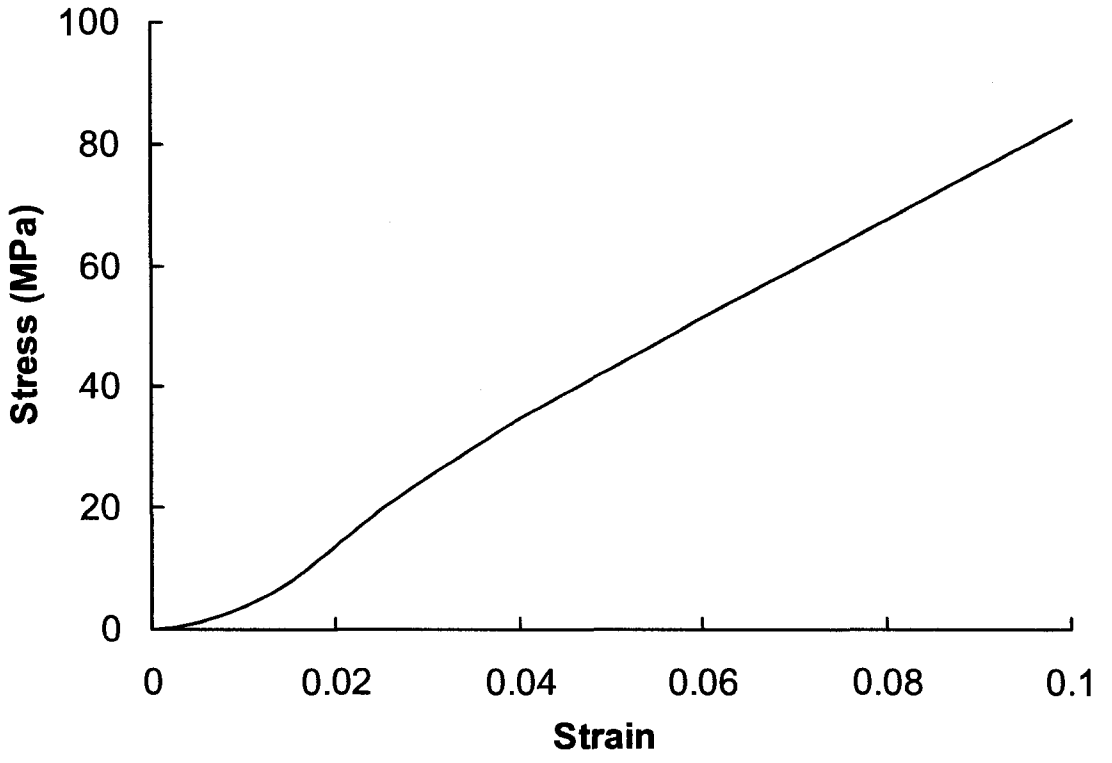

Figure 2. 2 Nonlinear stress-strain curve for pure collagen employed for articular cartilage fibrils (Haut & Little, 1972; Morgan, 1960). The slope of the curve monotonically increases at smaller strains and becomes constant at larger strains.

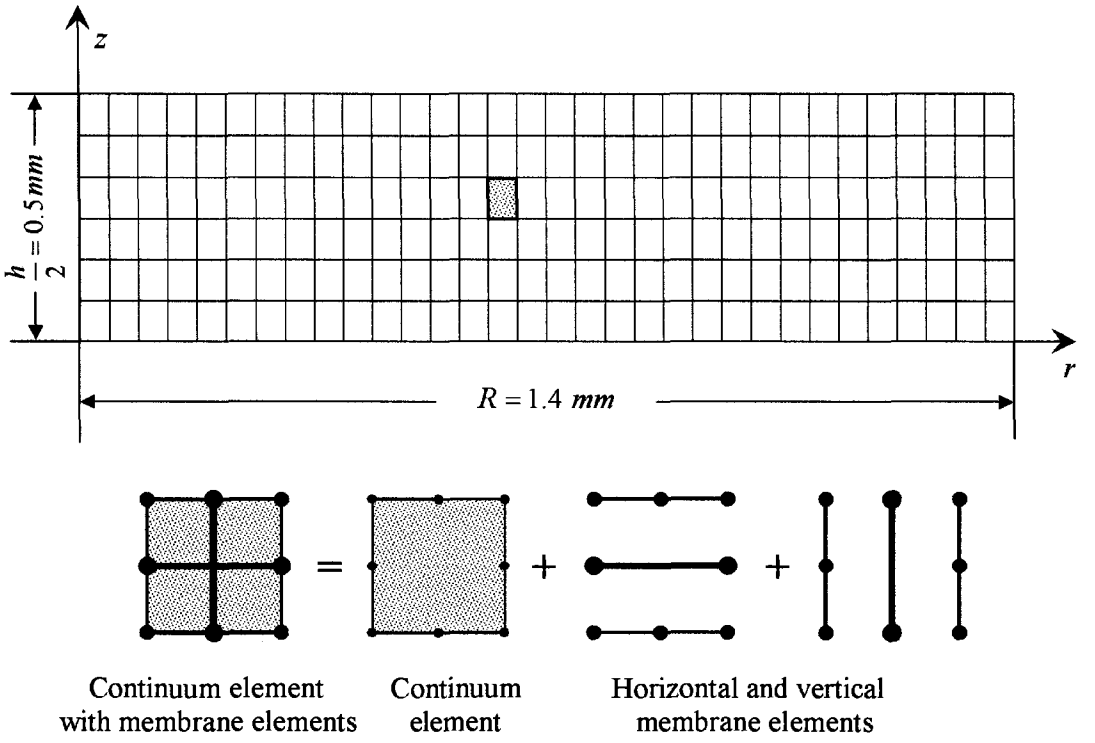

Figure 2. 3 Finite element mesh of the model used in the Case 3 showing also the arrangement of horizontal and vertical membrane elements in a typical axisymmetric porous continuum element.

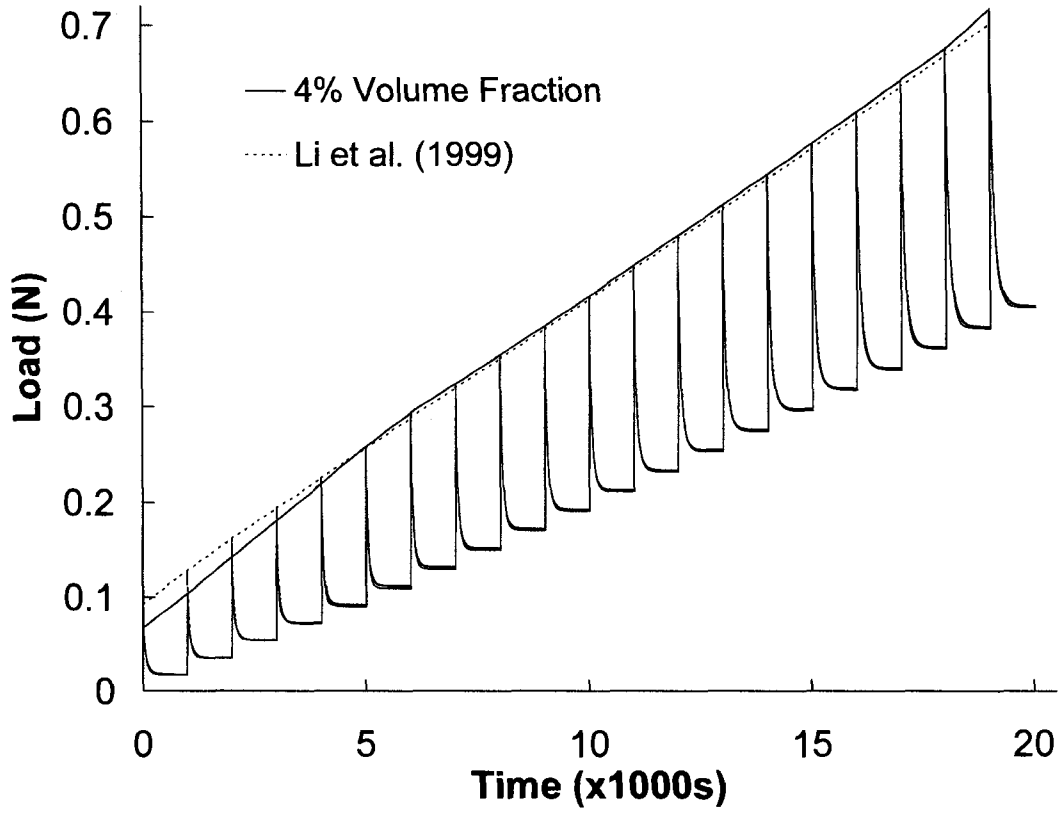

Figure 2. 4 Computed variation of the total load with time for 20 increments of prescribed ramp displacements using a fibril volume fraction of 4%. Li et al.'s results (Li et al., 1999) are also given for comparison.

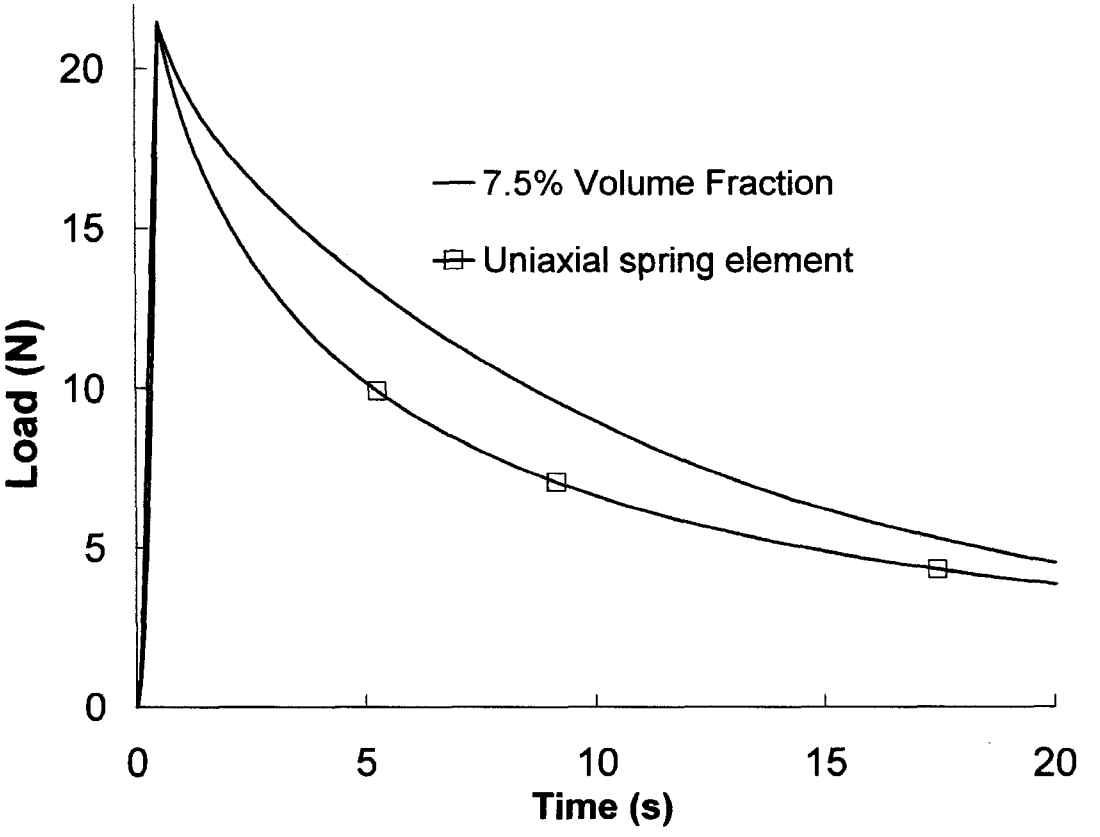

Figure 2. 5 Variation of the total load with time for the case with the displacement applied in one single ramp using the equivalent fibril volume fraction of 7.5%. For the sake of comparison, results based on the model with uniaxial spring elements are also given.

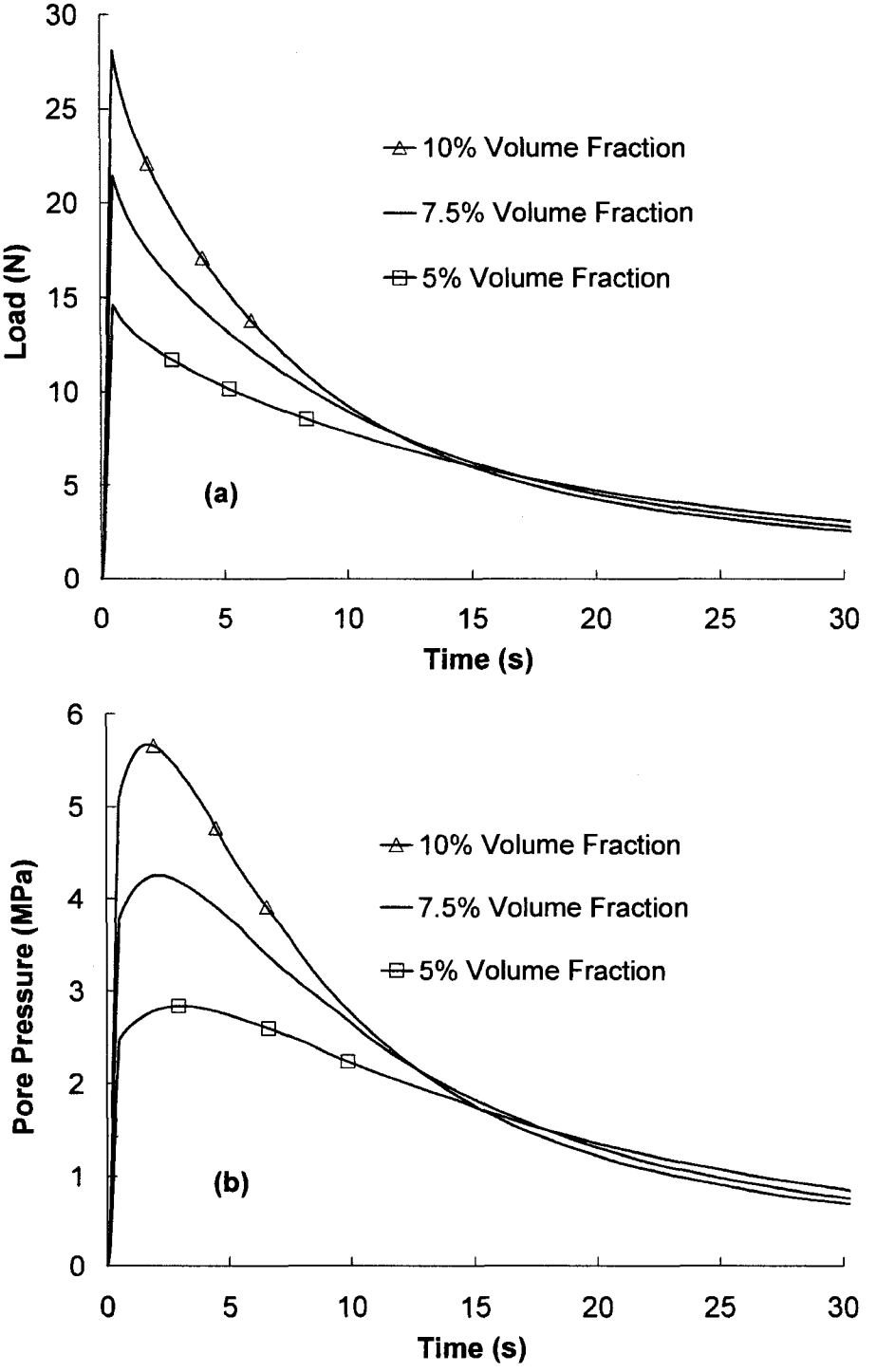

Figure 2. 6 Temporal variation of results in the unconfined compression test for different fibril volume fractions; a) total load, b) pore pressure at the disc centre.

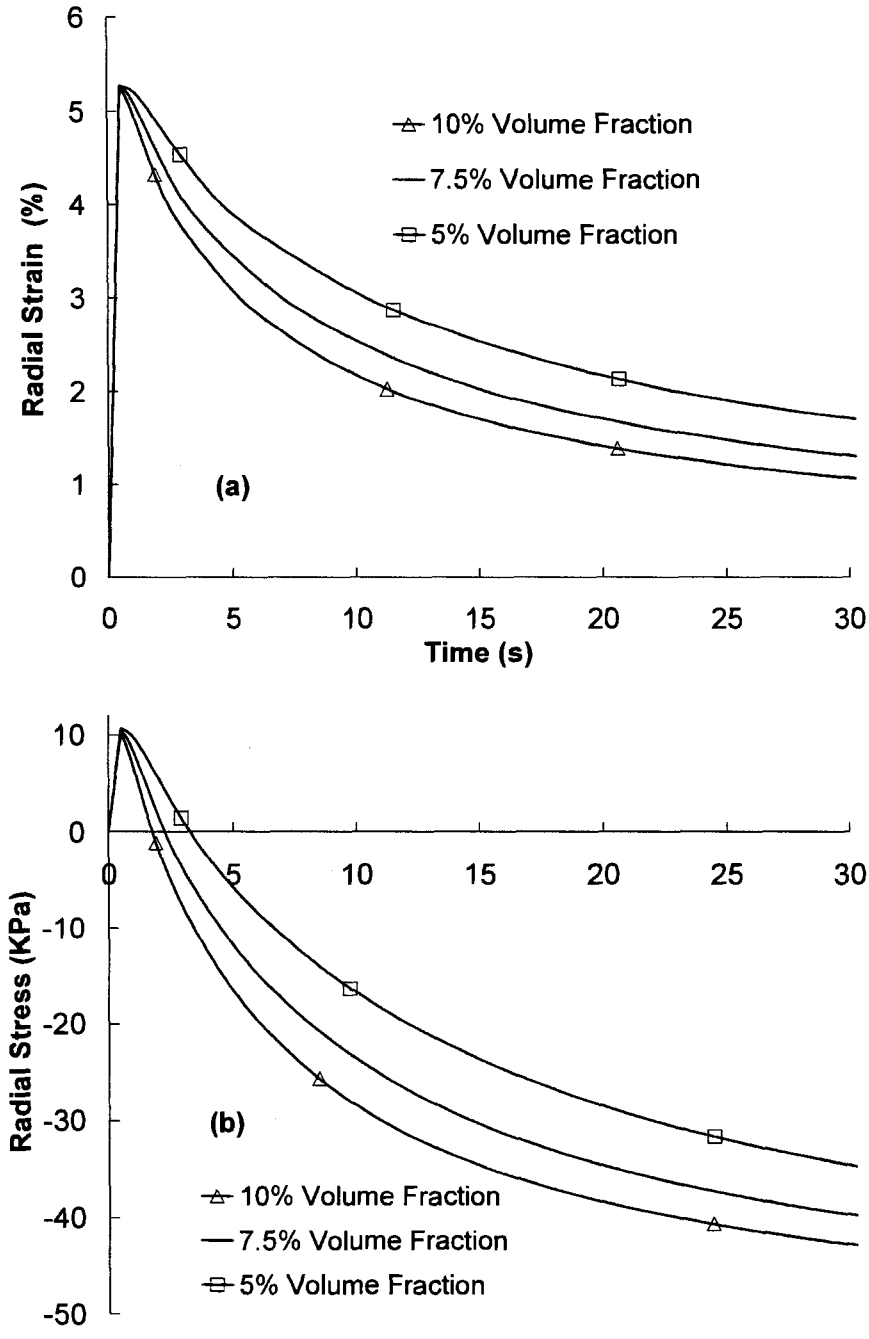

Figure 2. 7 Temporal variation of results in the unconfined compression test for different fibril volume fractions; a) radial strain at the disc centre which is identical in both fibril membranes and solid matrix, b) radial stress at the disc centre in the solid matrix. The radial stress in fibril membranes follow the same trend as in (a) in proportion to the stress-strain curve given in Figure 2.2.

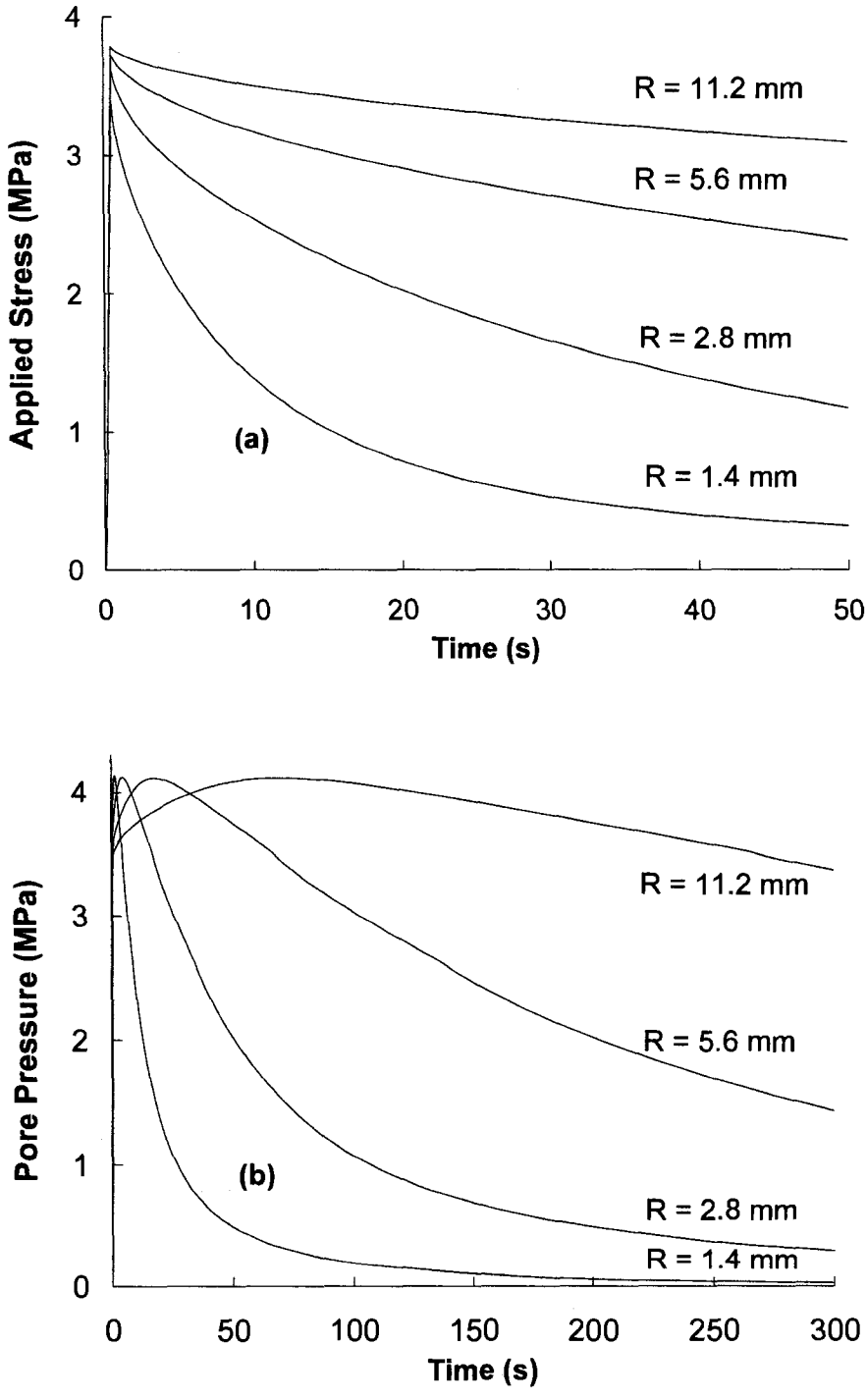

Figure 2. 8 Temporal variation of results in the unconfined compression test for different specimen sizes (R is the radius); a) applied stress as total load normalised to initial cross-sectional areas, b) pore pressure at the disc centre.

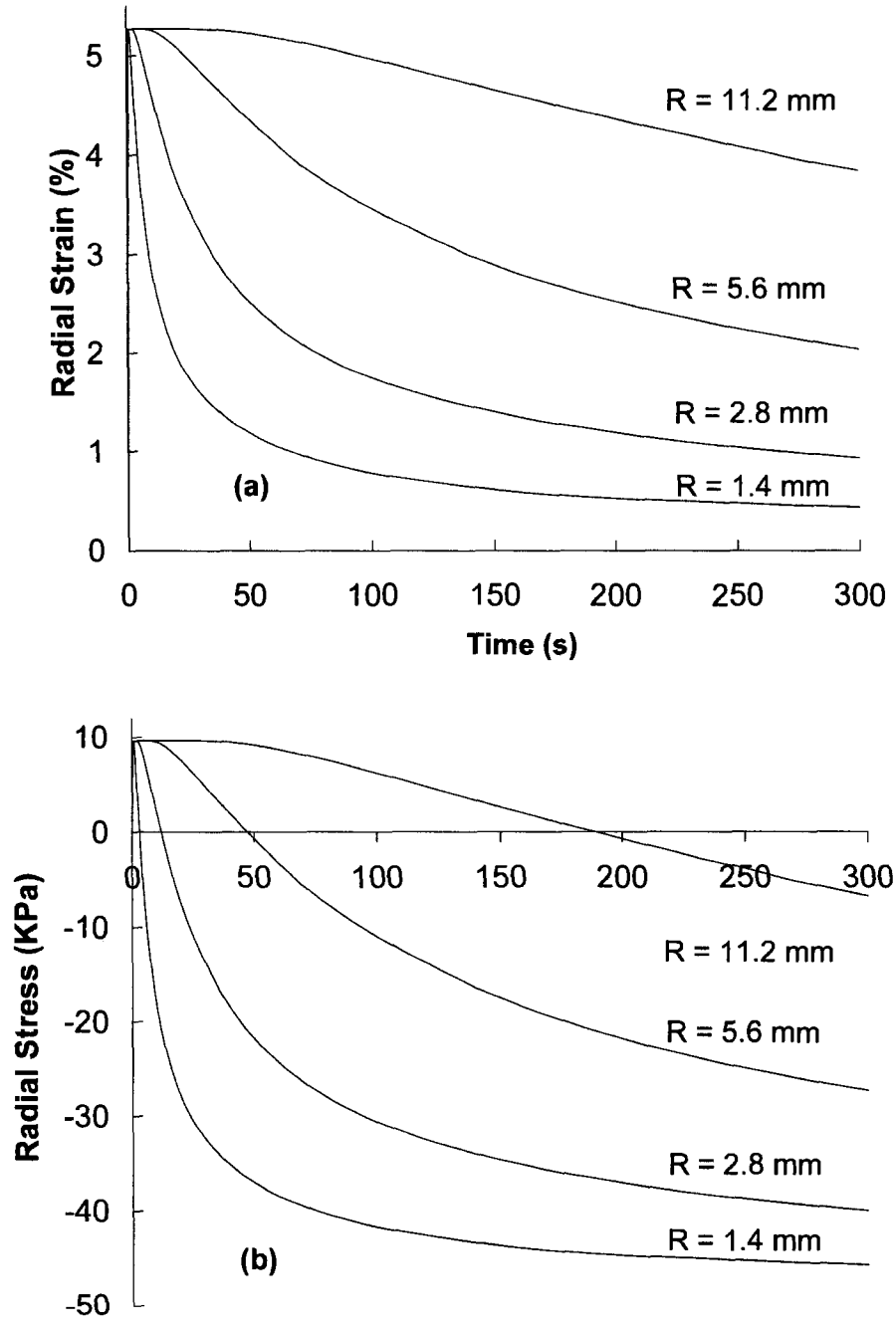

Figure 2. 9 Temporal variation of results in the unconfined compression test for different specimen sizes (R is the radius); a) radial strain at the disc centre which is identical in both fibril membranes and solid matrix, b) radial stress at the disc centre in the solid matrix. The radial stress in fibril membranes follow the same trend as in (a) in proportion to the data given in Figure 2.2.

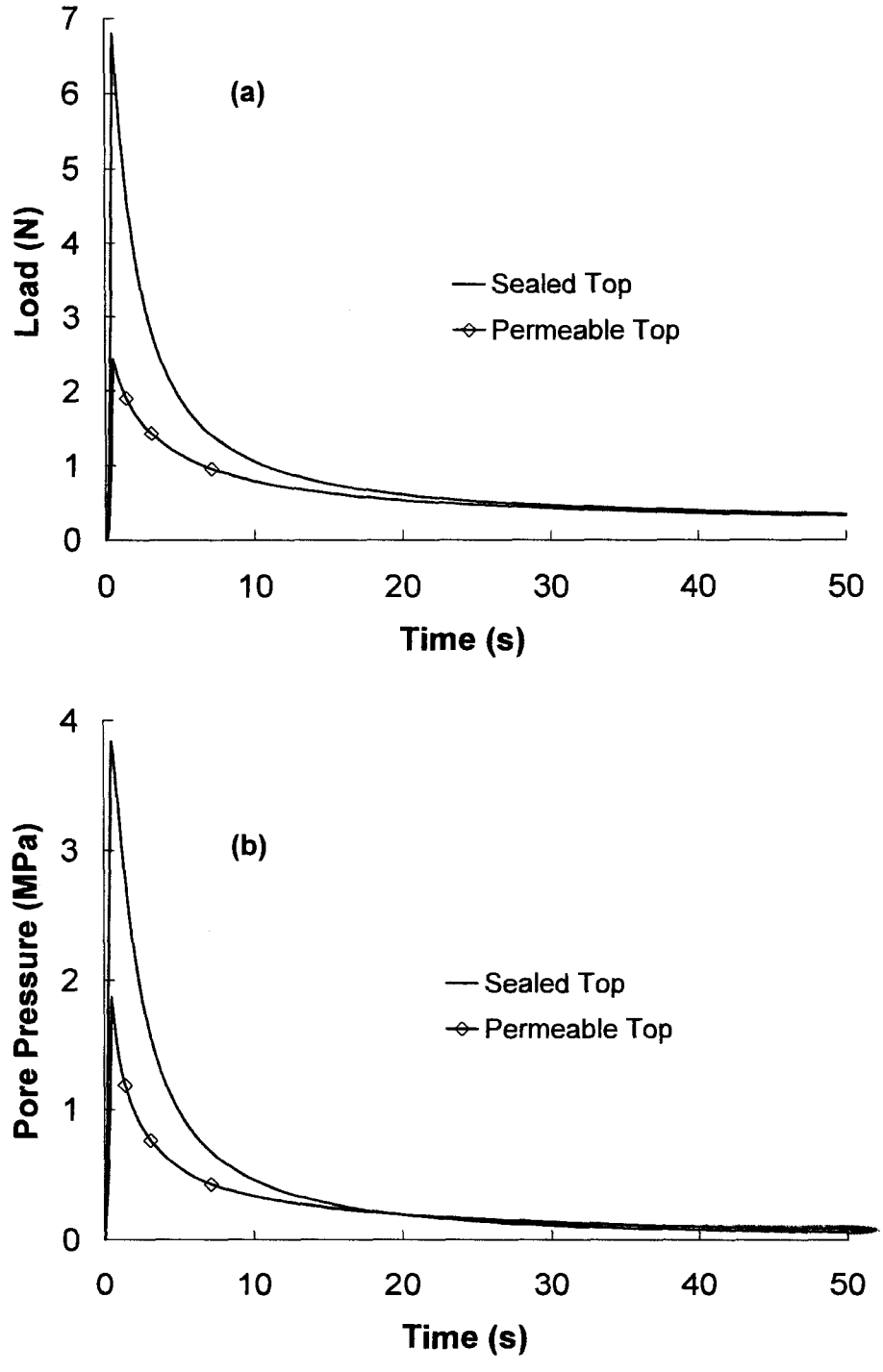

Figure 2. 10 Temporal variation of results in the indentation test for two boundary conditions at the top surface; a) total load, b) pore pressure on the axis at the disc mid-height.

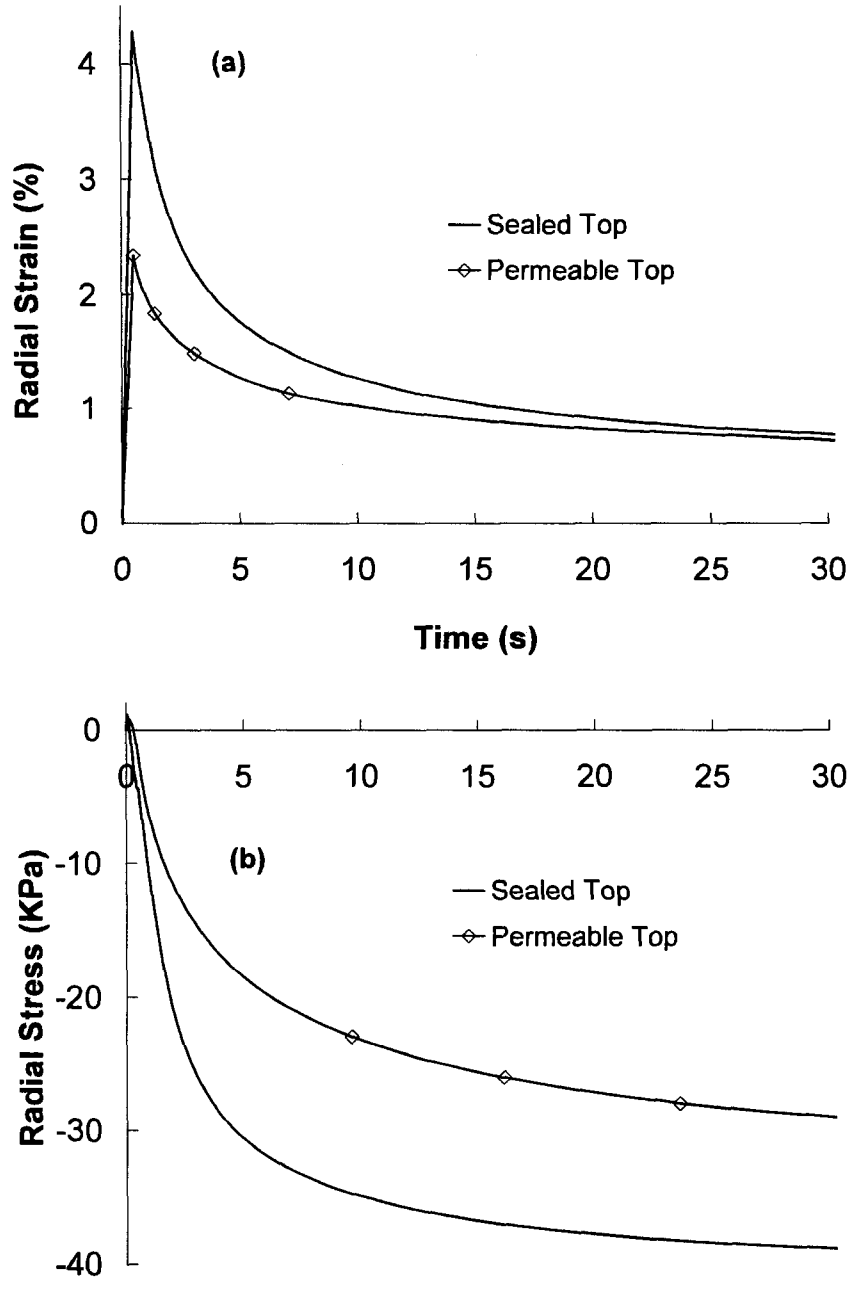

Figure 2. 11 Temporal variation of results in the indentation test for two boundary conditions at the top surface; a) radial strain at the disc mid-height close to the axis which is identical in both fibril membranes and solid matrix, b) radial stress at the disc mid-height close to the axis in the solid matrix. The radial stress in fibril membranes follow the same trend as in (a) in proportion to the data given in Figure 2.2.

Chapter three

Article II: Deep vertical collagen fibrils play a significant role in mechanics of articular cartilage

R. Shirazi and A. Shirazi-Adl

Division of Applied Mechanics, Department of Mechanical Engineering
École Polytechnique, Montréal, Québec, Canada

Article published in
JOURNAL OF ORTHOPAEDIC RESEARCH
2008 May; 26 (5): 608-15

Keywords: Vertical fibrils, Collagen networks, Cartilage, Indentation, Finite element method

3.1 Abstract

The primary orientation of collagen fibrils alters along the cartilage depth; being horizontal in the superficial zone, random in the transitional zone and vertical in the deep zone. Commonly used confined and unconfined (when with no underlying bone) testing configurations cannot capture the mechanical role of deep vertical fibril network. To determine this role in cartilage mechanics, an axisymmetric nonlinear fibril-reinforced poroelastic model of tibial cartilage plateaus was developed accounting for depth-dependent properties and distinct fibril networks with physical material properties. Both creep and relaxation indentation models were analysed which results were found equivalent in the transient period but diverged in post-transient periods. Vertical fibrils played a significant role at the transient period in dramatically increasing the stiffness of the tissue and in protecting the solid matrix against large distortions and strains at the subchondral junction. This role, however, disappeared both with time and at loading rates slower than those expected in physiological activities such as walking. The vertical fibrils demonstrated a chevron-type deformation pattern that was further accentuated with time in creep loading. Damages to deep vertical collagen fibril network or their firm anchorage to the bone, associated with bone bruises for example, would weaken the transient stiffness and place the tissue at higher risk of failure particularly at the deep zone.

3.2 Introduction

Articular cartilage covers the bony ends in diarthrodial joints to facilitate motions and distribute loads. Its integrity depends primarily on networks of collagen fibrils that resist tension and embed the water and nonfibrillar matrix (mainly proteoglycans) resulting in a highly nonlinear, nonhomogeneous and anisotropic tissue (Huang et al., 2005). The arrangement of collagen fibril networks markedly alter along the depth (Benninghoff, 1925; Kaab, Gwynn et al., 1998). At the superficial zone, the fibrils are horizontally oriented parallel to the articular surface (Minns & Steven, 1977) whereas they become rather random in the transitional zone (Broom & Marra, 1986) and finally turn perpendicular to the articular surface in the deep zone (Benninghoff, 1925; Kaab, Gwynn et al., 1998; Lane & Weiss, 1975; Minns & Steven, 1977) to anchor the tissue firmly to the subchondral bone (Broom & Marra, 1986; Redler et al., 1975).

Damages to the collagen fibril networks likely initiate or accelerate the cartilage failure, disintegration and degeneration (Wilson et al., 2006). To accurately capture the microstructure of the tissue and following our earlier simulations of other similar connective tissues (Bendjaballah et al., 1995; Shirazi-Adl et al., 1984), we introduced and validated fibril-reinforced composite models of the cartilage that represented the constituents as distinct elements each playing a mechanical role for which it is best structured (Fortin et al., 2000; Li et al., 2003; Li et al., 1999; Soulhat et al., 1999). Such models have also extensively been employed in more recent model studies on mechanics of the articular cartilage e.g. (Julkunen et al., 2007; Laasanen et al., 2003; Wilson et al., 2006; Wilson et al., 2004). Despite numerous earlier investigations, the mechanical role of vertical fibrils in the deep zone has often been either completely neglected or simply overlooked. It is evident that, due to the uniform pattern of compressive deformation at different heights, the commonly used confined and unconfined (when with no underlying bone) testing configurations cannot capture the primary mechanical role of deep vertical fibril network.

In the knee joint, for example, the cartilage is subject to localised, non-uniform, contact pressure loading that could more closely be represented by indentation testing configurations. The rapid localised physiological contact loading and unloading cycles could cause large tensile strains in the deep fibres as indirectly evident from recent micro-anatomy studies of the cartilage under compression load (Kaab, Ito et al., 1998; Notzli & Clark, 1997; Thambyah & Broom, 2006). The micro-deformation patterns of the intact and fibrillated cartilage specimens under loading points to the likely crucial role of deep fibril network especially in the neighbourhood of loading edge where shear strains are large.

In this work and in order to properly investigate the role of deep vertical fibres in cartilage mechanics, we have developed an axisymmetric nonlinear fibril-reinforced finite element model of cartilage incorporating the tissue fibril network as three distinct groups; horizontal at superficial region, random in transitional region and vertical in deep zone. To adequately represent these collagen networks, we have used continuum and membrane elements employing tissue physical quantities such as collagen fibre volume fractions and nonlinear stress-strain relation (Shirazi & Shirazi-Adl, 2005). Using an indentation geometry similar to that of tibial plateaus, the role of changes in the volume fraction of fibril networks, boundary condition at the osteochondral junction and loading rate are investigated under both relaxation and creep loading conditions. We hypothesize that vertical fibres play a crucial role in cartilage mechanics by supporting and protecting the tissue under physiological loading conditions. Determination of the extent of this role and parameters affecting it constitute, hence, the specific objective of this investigation.

3.3 Method

3.3.1 Finite Element Mesh

A cylindrical model with radius R=17 mm and height H=2.5 mm is considered which roughly represents the cartilage at the medial tibial plateau based on our detailed model of the human knee joint (Bendjaballah et al., 1995). The indenter is assumed rigid and impermeable with a profile identical to that of the femoral medial condyle at the sagittal plane. The subchondral bone is assumed rigid due to its much greater stiffness as compared with the cartilage (Mente & Lewis, 1994).

The cartilage is modelled as an isotropic porous solid matrix filled with water and reinforced by fibrillar networks (Fig. 3.1). The porous matrix is represented by axisymmetric elements with linear pressure and displacement fields while the fibrillar networks are simulated either by membrane or continuum elements (Fig. 3.1). In the superficial zone, the collagen fibrils are isotropically distributed in the plane of membrane elements (Shirazi & Shirazi-Adl, 2005). Despite such distribution, however, a direction-dependent response prevails due to the strain-dependency in the fibrils material properties and anisotropy in the strain field. The stresses in each of the radial and circumferential directions, are evaluated using the nonlinear stress-strain curve assumed for collagen type II based on earlier works (Haut & Little, 1972; Morgan, 1960). Equal principal strains would generate an isotropic material while any negative principal strain results in a zero principal stress (i.e., tension only membranes).

In the transitional zone with random fibres and no dominant orientation, continuum elements that take the principal strain directions as the material principal axes represent collagen fibrils. In the deep zone, vertical fibrils are represented with vertical membrane elements similar to horizontal superficial ones except that they do not offer any resistance in circumferential direction. Tensile stresses can, hence, be generated in these vertical fibrils only in their direction, which is initially vertical. The formulation of

these fibril networks is introduced in the ABAQUS finite element commercial program (Hibbit, Karlsson & Sorensen, Inc., Pawtucker, RI).

3.3.2 Material Properties

The thickness of membrane elements in the superficial and deep zones is evaluated based on the fibril volume fraction in these zones. The equivalent collagen fibre content at the superficial zone is estimated based on the reported tissue properties in tension (Kempson et al., 1973) and collagen stress-strain curve using the following relation:

$$E_T^{SEC} = \alpha E_F^{SEC} + E_M$$

where α is the collagen fibre volume fraction content, E_M is the drained modulus of the matrix and E_T^{SEC} and E_F^{SEC} are the strain-dependent nonlinear tensile secant moduli of the cartilage tissue and collagen fibres, respectively. A total volume fraction of 15% is estimated in the superficial zone which is in agreement with the mean value of 14% reported as its wet weight (Hollander et al., 1994). The volume fractions in transitional and deep zones are subsequently estimated based on the reported decrease in collagen content per dry weight along the depth (Mow & Guo, 2002). Based also on the reported simultaneous decrease in the water content along the depth (Maroudas, 1970; Mow & Guo, 2002; Venn & Maroudas, 1977) as well as low collagen content in the middle zone (Bi et al., 2006), volume fractions of 10.5% for the transitional zone and 9% for the deep zone are assumed. Different fraction values are also considered as described later.

The solid matrix drained modulus and Poisson's ratio increase linearly from 0.3 MPa and 0.12 at the superficial layer to 1.2 MPa and 0.42 at the bottom, respectively (Schinagl et al., 1997). The water content linearly decreases in the model from 80% at the surface to 60% at the bone/cartilage interface (Maroudas, 1970; Mow & Guo, 2002; Venn & Maroudas, 1977). The permeability is assumed to be isotropic and strain-

dependent (Lai et al., 1981) using the nonlinear relation $k = k_0 \exp(M \frac{e - e_0}{1 + e_0})$ with k_0=4.7×10^{-15} (mm^4/Ns) (Armstrong & Mow, 1982), e_0 as the initial void ratio and M=10.

3.3.3 Loading and Boundary Conditions

Two loading protocols are used in this study: stress relaxation and creep. In the former, 20% nominal strain is applied at the centre of the indenter in 0.5 second yielding a near-physiological rate expected during walking (Sathasivam & Walker, 1997). In the creep simulations, however, a compression load of 500 N is applied via the indenter in 0.5 second that remains constant thereafter for 60 minutes. This compression force is verified to fall in the range of transient compression loads in the relaxation models. The bottom surface at the subchondral bone is completely fixed and impermeable. The cartilage surface is impermeable only at the areas in contact with the indenter.

3.3.4 Parametric Studies

To examine the role of the deep vertical fibrils, their volume fraction content is varied from the reference 9% either to 12 and 15% or to 6, 3 and finally 0% (nil). Cases are also considered while varying the volume fraction of superficial fibrils from 15 to 10 and 20% and that of transitional fibres from 10.5 to 6 and 15%. The effects of the boundary condition at the osteochondral junction (free sliding rather than constrained) and strain rate (4000, 2, 0.2 and 0.04 %s^{-1} rather than 40 %s^{-1} used in the reference case) are also investigated in the relaxation model.

3.4 Results

Vertical fibrils significantly increased the transient (t=0.5 s) stiffness of the cartilage in the relaxation model, an effect that completely disappeared at equilibrium (Fig. 3.2). This stiffening effect was associated with changes in the pore pressure that dramatically increased at the mid-height centre from 2.62 to 4.43, 5.36, 6.14, 6.83 and 7.48 MPa, respectively, as the volume fraction increased from 0 to 3, 6, 9, 12 and 15%. The transient horizontal (radial) reaction force at the base also substantially increased,

respectively, from 105 to 307, 436, 550, 656 and 755 N that almost totally diminished thereafter to equilibrium. Despite the considerable increase in the axial/radial reaction forces and pore pressure, the maximum principal strain in the solid matrix and the maximum tensile strain in vertical fibrils themselves actually markedly dropped as higher volume fractions were considered (Fig. 3.3). The tissue deformation field was also substantially altered in presence of vertical fibrils (Fig. 3.4). In contrast, however, the maximum strains in other fibril networks at the superficial and transitional zones increased (Fig. 3.3). The foregoing predicted effects were found greater as the volume fraction altered from 0% to 3% compared with subsequent incremental changes. The case with unconstrained sliding at the cartilage-bone junction demonstrated the least axial reaction force, pore pressure and maximum strains in the matrix as well as fibril networks (Figs. 3.2-3.4). The role of vertical fibres almost disappeared in equilibrium where relatively negligible strains were calculated in the solid matrix (<2%) and fibril networks (<1%) (see Fig. 3.5 for deformation patterns).

Alterations in the volume fraction of superficial and transitional fibril networks yielded much smaller effects on predictions at transient in the relaxation model. Alterations in the volume fraction of superficial fibrils from 15 (reference case) to 10 and 20% changed the axial reaction force from 762 only to 702 and 818 N and the maximum radial strain in horizontal fibrils themselves from 13.3 to 13.6 and 13.0%, respectively. Under the alterations in the volume fraction of random fibrils in the transitional zone from 10.5 (reference case) to 6 and 15%, the axial reaction force and maximum principal strain in random fibrils themselves also varied slightly from 762 to 702 and 819 N and from 14.3 to 14.6 and 14.1%, respectively. Likewise, strains in the solid matrix and other fibril networks changed only slightly.

The foregoing dramatic role of vertical fibrils on transient mechanics of the cartilage was highly sensitive to the strain-rate in the relaxation model (Fig. 3.6). As the indenter velocity decreased from 1000 μm/s (reference case) to 50, 5 and further to 1

μm/s, both transient axial and radial reaction forces substantially dropped and the mechanical effectiveness of vertical fibrils disappeared. On the contrary, much greater strain rate (by 100-fold) had nearly no effects on predictions (Fig. 3.6).

Due to smaller load applied in the creep model as compared with that reached in the relaxation model, alterations in the volume fraction of vertical fibrils from 9 to 3 and 15% demonstrated less effects on the transient response (t=0.5 s) in the creep model. For the volume fractions increasing from 3 to 9 and 15%, respectively, the transient nominal strain at the centre decreased from 19.8 to 17.9 and 17.1%. The transient maximum principal strain in the matrix also decreased from 25.8 to 20.0 and 18.6%. Similarly, the transient maximum strain dropped, respectively, from 11.9 to 10.9 and 10.5% in horizontal fibrils, from 13.1 to 12.0 and 11.6% in transitional fibrils and finally from 11.6 to 5.9 and 4.0% in vertical fibrils themselves. At near-equilibrium, the maximum principal strains in the solid matrix increased whereas the maximum tensile strains in the fibril networks decreased (more so in the vertical fibrils whereas only slightly in remaining fibril networks). The radial reaction force diminished from 295, 361 and 393 N at t=0.5 s, respectively for volume fractions of 3, 9 and 15%, to ~160 N at t=30 min and further to ~146 N at t=60 min. As time progressed, superficial layers under load were further compressed and the chevron deformation pattern of vertical fibres in the neighbourhood of the loading edge became more and more evident (Fig. 3.5).

3.5 Discussion

In this model study and in accordance with its stated objective, role of the vertical collagen fibril network on mechanics of the articular cartilage was evaluated. To do so, the effects of changes in volume fraction of various fibril networks, strain rate, boundary conditions at the base, and testing configuration (relaxation versus creep) on predictions were investigated.

3.5.1 Stress Relaxation

The vertical fibril network substantially increased the transient stiffness of the cartilage; the ratio of transient to equilibrium force (i.e., dynamic to static stiffness) increased by ~ three-fold (from ~18 to 51) when the volume fraction of vertical fibrils increased from 0 to 9%. This ratio for the case neglecting vertical fibrils is in the higher range of those reported in unconfined compression tests under similar strain magnitudes and rates (Li et al., 2003). It is evident that vertical fibrils do not play any noticeable mechanical role in confined and unconfined (with no underlying bone) tests.

The vertical fibrils also protected the solid matrix from excessive strains and, hence, damage and rupture (Figs. 3.3 and 3.4); the transient maximum principal strain diminished from 51.3% to 22.8% in presence of 9% vertical fibril content and that despite a concurrent near three-fold increase in the applied force. Maximum shear and principal strains in the solid matrix occurred indeed at the osteochondral junction in the deep zone in which site horizontal split fractures have been reported (Meachim & Bentley, 1978). This area underneath the loading edge also experienced the largest radial and axial reaction forces. In contrast to the vertical fibrils close to the centre of loading that were compressed, those located away from the centre towards the loading edge were stretched contributing to the tissue stiffness. The prediction of crimped fibrils near the centre of loading and not away from it is corroborated by experimental studies (Broom & Poole, 1982; Glaser & Putz, 2002). It is, therefore, evident that the presence of vertical fibrils in the deep zone is crucial to the integrity of the tidemark region (Broom & Poole, 1982; Redler et al., 1975) especially at the regions of highest distortions beneath the loading edge neighbourhood.

The predictions for the case with sliding boundary condition at the bottom demonstrated a dramatic drop in both the load-bearing capacity of the tissue (Fig. 3.2) and strains in all components (Fig. 3.3). The tissue deformation pattern was also altered (Fig. 3.4). In presence of localised horizontal splits or bone bruises observed at the

osteochondral junction, the neighbouring intact areas of the cartilage are likely subject to even greater stresses and distortions and, hence, risk of failure propagation and disintegration.

Interestingly, the presence of vertical fibril network in the model increased the tensile strain in the remaining superficial and transitional fibril networks thereby increasing their mechanical effectiveness in supporting additional load and protecting the solid matrix (Fig. 3.3). For example, a 9% vertical volume fraction markedly increased the maximum strain in superficial and transitional fibrils from 9.4% and 10.9% to 13.3% and 14.3%, respectively. Moreover, results for all vertical fibril volume fractions in the range of 3-15%, demonstrated that these fibrils were always subject to smaller strains than were the superficial and transitional fibrils. It appears, hence, that they should also be at lesser risk to direct failure than the latter fibrils, an observation supported by earlier studies (Hollander et al., 1994; Wilson et al., 2006).

Results of parametric studies demonstrated that, for nearly the same relative change, vertical fibrils had greater influence on cartilage mechanics than had the superficial and transitional fibril networks. For example, the reaction force varied by as much as 60 N when the volume fraction of superficial fibrils increased by 5% whereas it changed by more than 110 N when the vertical fibrils were altered by only 3%.

The role of vertical fibrils in supporting the external load and protecting the tissue matrix was strongly time and strain-rate dependent; it was dramatically compromised at slower strain rates and as time progressed. In contrast, almost no difference in response was predicted as the strain rate increased 100 times from $40\%s^{-1}$ to $4000\%s^{-1}$ (Fig. 3.6). These predictions are corroborated with earlier measurements (Oloyede et al., 1992) reporting a progressive increase in tissue stiffness at low and medium strain rates while nearly no change at high strain rates. The influence of vertical fibrils, being directly coupled to the fluid pressurization, increased in faster rates in

absence of any appreciable water exodus, an interaction that was recognized in earlier studies as well (Li et al., 2003). The results of this study, therefore, stress the important role of vertical fibrils in cartilage mechanics under physiological loading rates expected in walking, running and jumping. The much slower rates that have often been considered in earlier measurement and model studies cannot, hence, be expected to adequately identify the mechanical influence of vertical collagen fibrils. Along with the drastic reduction in large strains in both solid matrix and fibril networks as time progressed to the equilibrium, the chevron deformation pattern in vertical fibres disappeared (Fig. 3.5). The foregoing loss in the mechanical role of vertical fibres and lower risk of tissue failure is however of lesser practical and clinical importance due to the non-physiological nature of the slow or long-term relaxation loadings.

3.5.2 Creep

Overall at transient period (t=0.5 s), the creep results under 500 N that yielded a nominal axial strain of 17.9% at the centre were similar (in trends but naturally smaller in magnitudes) to relaxation results under 20% axial strain generating a total reaction force of 762 N. For all practical reasons, the transient responses and observations in creep and relaxation testing models are hence equivalent. The foregoing crucial effects of the vertical fibres in cartilage mechanics at the transient period predicted in the relaxation model withhold in the creep model as well. Any increase in applied strain in the relaxation model or in applied compression load in the creep model would further accentuate the mechanical role of vertical fibrils. Post-transient trends in the creep model however diverged from those in the relaxation model; in the creep model the maximum strain in the solid matrix increased with time while the reductions in superficial and transitional fibril networks strains as well as in reaction forces were of much smaller magnitudes. These smaller post-transient decreases in horizontal and transitional fibrils strains suggest a more prominent role for these fibrils at longer time creep loading conditions.

The role of vertical fibrils diminished with time as their tensile strain dramatically decreased thus leaving the solid matrix at the deep zones prone to greater shear strains. In contrast to the relaxation model in which the chevron deformation pattern of vertical fibrils disappeared after the transient period, in creep this pattern was further accentuated with the time (Fig. 3.5). This computed pattern is in agreement with reported observations on post-transient micro-deformation of cartilage in creep (Kaab, Ito et al., 1998; Notzli & Clark, 1997; Thambyah & Broom, 2006) despite differences in indenter profile, load magnitude and tissue geometry. At longer time periods, hence, the vertical fibres played negligible mechanical role in both relaxation and creep models despite their distinct patterns; being straight in the former whereas chevron-type in the latter (Fig. 3.5).

Finally in conclusion, using an indentation model with a simplified geometry simulating tibial plateaus, we investigated the role of vertical fibril network in cartilage mechanics. Vertical fibrils, in confirmation of our hypothesis, played a significant role in increasing the stiffness of the tissue and in protecting the solid matrix against large distortions and strains at the subchondral junction at the transient period in both relaxation and creep indentation models. These observations are of prime importance bearing in mind the nature of loading/unloading cycles (i.e., high loading rates, short durations, high strain/stress magnitudes) in common daily activities. These roles, however, disappeared both with time and at loading rates slower than those expected in physiological activities such as walking and running. The vertical fibres also demonstrated a chevron-type deformation pattern that was further accentuated in creep loading with time. Damages to deep vertical collagen fibril network or their anchorage to the bone, associated with bone bruises for example, would weaken the transient stiffness and place the tissue at higher risk of failure particularly at the deep zone. Due consideration of the crucial role of fibril networks is essential in successful prevention and treatment management of tissue degenerative processes and in tissue engineering transplants.

3.6 Acknowledgment

This research work is supported by grants from the Canadian Institute of Health Research (CIHR) and the National Sciences and Engineering Research Council of Canada (NSERC).

3.7 References

Armstrong, C. G., and Mow, V. C. (1982). Variations in the intrinsic mechanical properties of human articular cartilage with age, degeneration, and water content. *J Bone Joint Surg Am, 64*(1), 88-94.

Bendjaballah, M. Z., Shirazi-Adl, A., and Zukor, D. J. (1995). Biomechanics of the human knee joint in compression: reconstruction, mesh generation and finite element analysis. *The Knee, 2*(2), 69-79.

Benninghoff, A. (1925). Form und Bau der Gelenkknorpel in ihren Beziehungen zur Funktion. *Zeitschrift für Zellforschung, 2*, 783-862.

Bi, X., Yang, X., Bostrom, M. P., and Camacho, N. P. (2006). Fourier transform infrared imaging spectroscopy investigations in the pathogenesis and repair of cartilage. *Biochim Biophys Acta, 1758*(7), 934-941.

Broom, N. D., and Marra, D. L. (1986). Ultrastructural evidence for fibril-to-fibril associations in articular cartilage and their functional implication. *J Anat, 146*, 185-200.

Broom, N. D., and Poole, C. A. (1982). A functional-morphological study of the tidemark region of articular cartilage maintained in a non-viable physiological condition. *J Anat, 135*(Pt 1), 65-82.

Fortin, M., Soulhat, J., Shirazi-Adl, A., Hunziker, E. B., and Buschmann, M. D. (2000). Unconfined compression of articular cartilage: nonlinear behavior and comparison with a fibril-reinforced biphasic model. *J Biomech Eng, 122*(2), 189-195.

Glaser, C., and Putz, R. (2002). Functional anatomy of articular cartilage under compressive loading Quantitative aspects of global, local and zonal reactions of

the collagenous network with respect to the surface integrity. *Osteoarthritis Cartilage, 10*(2), 83-99.

Haut, R. C., and Little, R. W. (1972). A constitutive equation for collagen fibers. *J Biomech, 5*(5), 423-430.

Hollander, A. P., Heathfield, T. F., Webber, C., Iwata, Y., Bourne, R., Rorabeck, C., and Poole, A. R. (1994). Increased damage to type II collagen in osteoarthritic articular cartilage detected by a new immunoassay. *J Clin Invest, 93*(4), 1722-1732.

Huang, C. Y., Stankiewicz, A., Ateshian, G. A., and Mow, V. C. (2005). Anisotropy, inhomogeneity, and tension-compression nonlinearity of human glenohumeral cartilage in finite deformation. *J Biomech, 38*(4), 799-809.

Julkunen, P., Kiviranta, P., Wilson, W., Jurvelin, J. S., and Korhonen, R. K. (2007). Characterization of articular cartilage by combining microscopic analysis with a fibril-reinforced finite-element model. *J Biomech, 40*(8), 1862-1870.

Kaab, M. J., Gwynn, I. A., and Notzli, H. P. (1998). Collagen fibre arrangement in the tibial plateau articular cartilage of man and other mammalian species. *J Anat, 193 (Pt 1)*, 23-34.

Kaab, M. J., Ito, K., Clark, J. M., and Notzli, H. P. (1998). Deformation of articular cartilage collagen structure under static and cyclic loading. *J Orthop Res, 16*(6), 743-751.

Kempson, G. E., Muir, H., Pollard, C., and Tuke, M. (1973). The tensile properties of the cartilage of human femoral condyles related to the content of collagen and glycosaminoglycans. *Biochim Biophys Acta, 297*(2), 456-472.

Laasanen, M. S., Toyras, J., Korhonen, R. K., Rieppo, J., Saarakkala, S., Nieminen, M. T., Hirvonen, J., and Jurvelin, J. S. (2003). Biomechanical properties of knee articular cartilage. *Biorheology, 40*(1-3), 133-140.

Lai, W. M., Mow, V. C., and Roth, V. (1981). Effects of nonlinear strain-dependent permeability and rate of compression on the stress behavior of articular cartilage. *J Biomech Eng, 103*(2), 61-66.

Lane, J. M., and Weiss, C. (1975). Review of articular cartilage collagen research. *Arthritis Rheum, 18*(6), 553-562.

Li, L. P., Buschmann, M. D., and Shirazi-Adl, A. (2003). Strain-rate dependent stiffness of articular cartilage in unconfined compression. *J Biomech Eng, 125*(2), 161-168.

Li, L. P., Soulhat, J., Buschmann, M. D., and Shirazi-Adl, A. (1999). Nonlinear analysis of cartilage in unconfined ramp compression using a fibril reinforced poroelastic model. *Clin Biomech, 14*(9), 673-682.

Maroudas, A. (1970). Distribution and diffusion of solutes in articular cartilage. *Biophys J, 10*(5), 365-379.

Meachim, G., and Bentley, G. (1978). Horizontal splitting in patellar articular cartilage. *Arthritis Rheum, 21*(6), 669-674.

Mente, P. L., and Lewis, J. L. (1994). Elastic modulus of calcified cartilage is an order of magnitude less than that of subchondral bone. *J Orthop Res, 12*(5), 637-647.

Minns, R. J., and Steven, F. S. (1977). The collagen fibril organization in human articular cartilage. *J Anat, 123*(Pt 2), 437-457.

Morgan, F. R. (1960). Mechanical properties of collagen and leather fibres. *American Leather Chemists Association Journal, 55*(1), 4-23.

Mow, V. C., and Guo, X. E. (2002). Mechano-electrochemical properties of articular cartilage: their inhomogeneities and anisotropies. *Annu Rev Biomed Eng, 4*, 175-209.

Notzli, H., and Clark, J. (1997). Deformation of loaded articular cartilage prepared for scanning electron microscopy with rapid freezing and freeze-substitution fixation. *J Orthop Res, 15*(1), 76-86.

Oloyede, A., Flachsmann, R., and Broom, N. D. (1992). The dramatic influence of loading velocity on the compressive response of articular cartilage. *Connect Tissue Res, 27*(4), 211-224.

Redler, I., Mow, V. C., Zimny, M. L., and Mansell, J. (1975). The ultrastructure and biomechanical significance of the tidemark of articular cartilage. *Clin Orthop Relat Res*(112), 357-362.

Sathasivam, S., and Walker, P. S. (1997). A computer model with surface friction for the prediction of total knee kinematics. *J Biomech, 30*(2), 177-184.

Schinagl, R. M., Gurskis, D., Chen, A. C., and Sah, R. L. (1997). Depth-dependent confined compression modulus of full-thickness bovine articular cartilage. *J Orthop Res, 15*(4), 499-506.

Shirazi-Adl, S. A., Shrivastava, S. C., and Ahmed, A. M. (1984). Stress analysis of the lumbar disc-body unit in compression. A three-dimensional nonlinear finite element study. *Spine, 9*(2), 120-134.

Shirazi, R., and Shirazi-Adl, A. (2005). Analysis of articular cartilage as a composite using nonlinear membrane elements for collagen fibrils. *Med Eng Phys, 27*(10), 827-835.

Soulhat, J., Buschmann, M. D., and Shirazi-Adl, A. (1999). A fibril-network-reinforced biphasic model of cartilage in unconfined compression. *J Biomech Eng, 121*(3), 340-347.

Thambyah, A., and Broom, N. (2006). Micro-anatomical response of cartilage-on-bone to compression: mechanisms of deformation within and beyond the directly loaded matrix. *J Anat, 209*(5), 611-622.

Venn, M., and Maroudas, A. (1977). Chemical composition and swelling of normal and osteoarthrotic femoral head cartilage. I. Chemical composition. *Ann Rheum Dis, 36*(2), 121-129.

Wilson, W., van Burken, C., van Donkelaar, C., Buma, P., van Rietbergen, B., and Huiskes, R. (2006). Causes of mechanically induced collagen damage in articular cartilage. *J Orthop Res, 24*(2), 220-228.

Wilson, W., van Donkelaar, C. C., van Rietbergen, B., Ito, K., and Huiskes, R. (2004). Stresses in the local collagen network of articular cartilage: a poroviscoelastic fibril-reinforced finite element study. *J Biomech, 37*(3), 357-366.

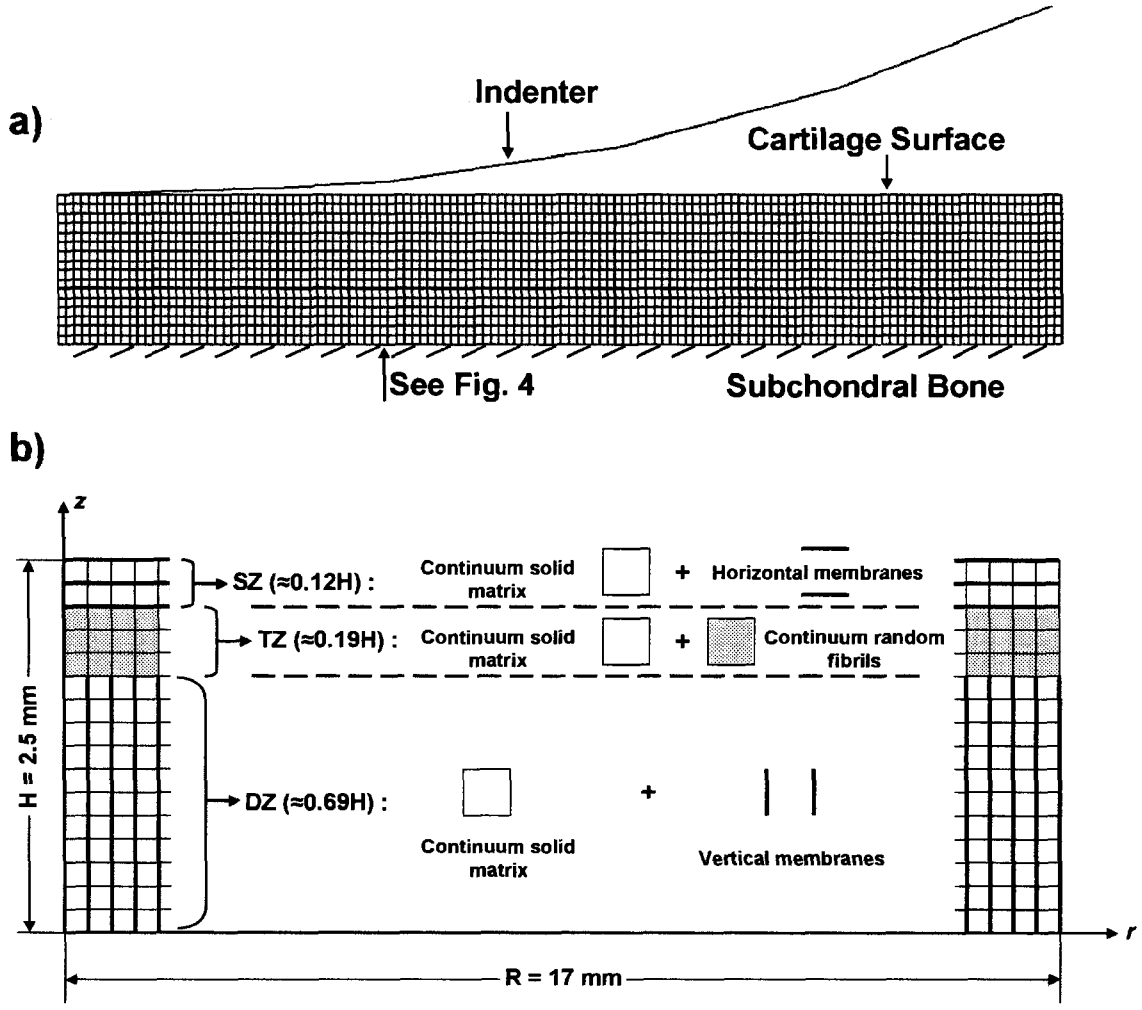

Figure 3. 1 a) Axisymmetric model of the articular cartilage along with nonporous rigid indenter b) Detailed finite element mesh showing the distinct structures representing solid matrix and collagen fibril networks in the superficial (SZ), transitional (TZ) and deep (DZ) zones.

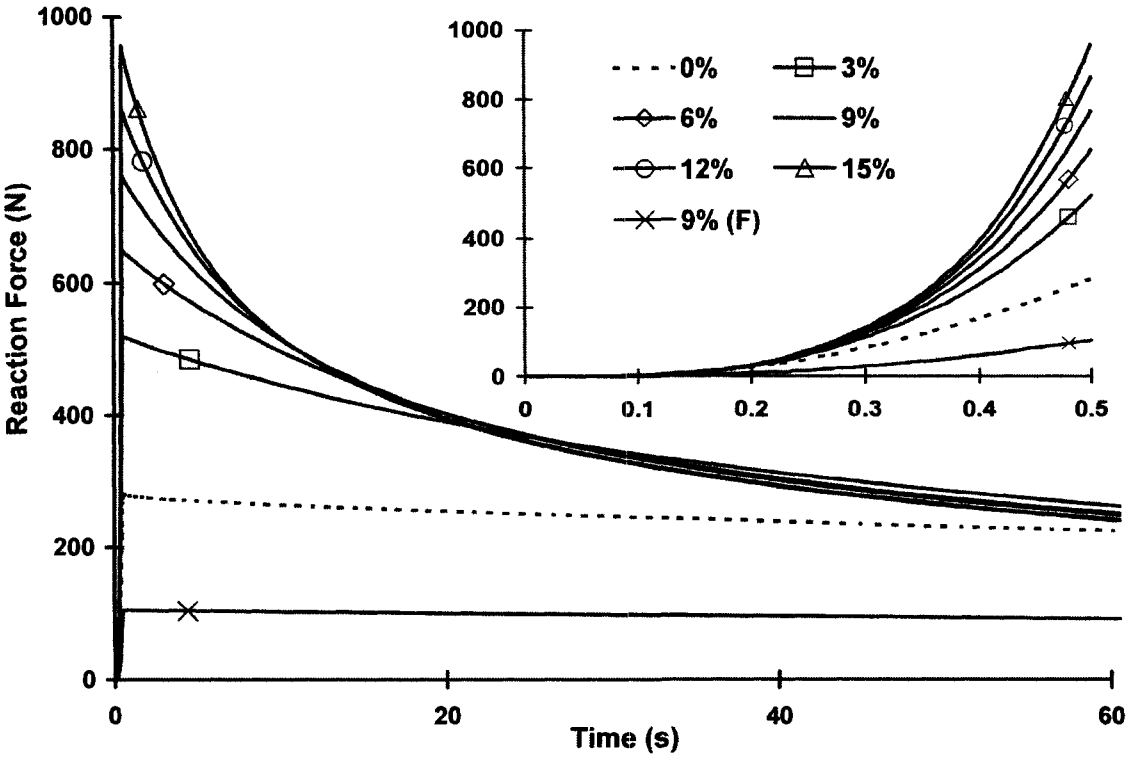

Figure 3. 2 Predicted temporal variation of the axial reaction force in the relaxation model for various vertical fibril volume fractions of 0, 3, 6, 9, 12 and 15%. The nominal strain of 20% at the centre is reached in 0.5s period. Results for the case with sliding boundary condition at the bottom is also shown (9% (F)). At equilibrium (not shown) the reaction force diminishes to 14.5 N in all cases. The transient time is magnified in the inset.

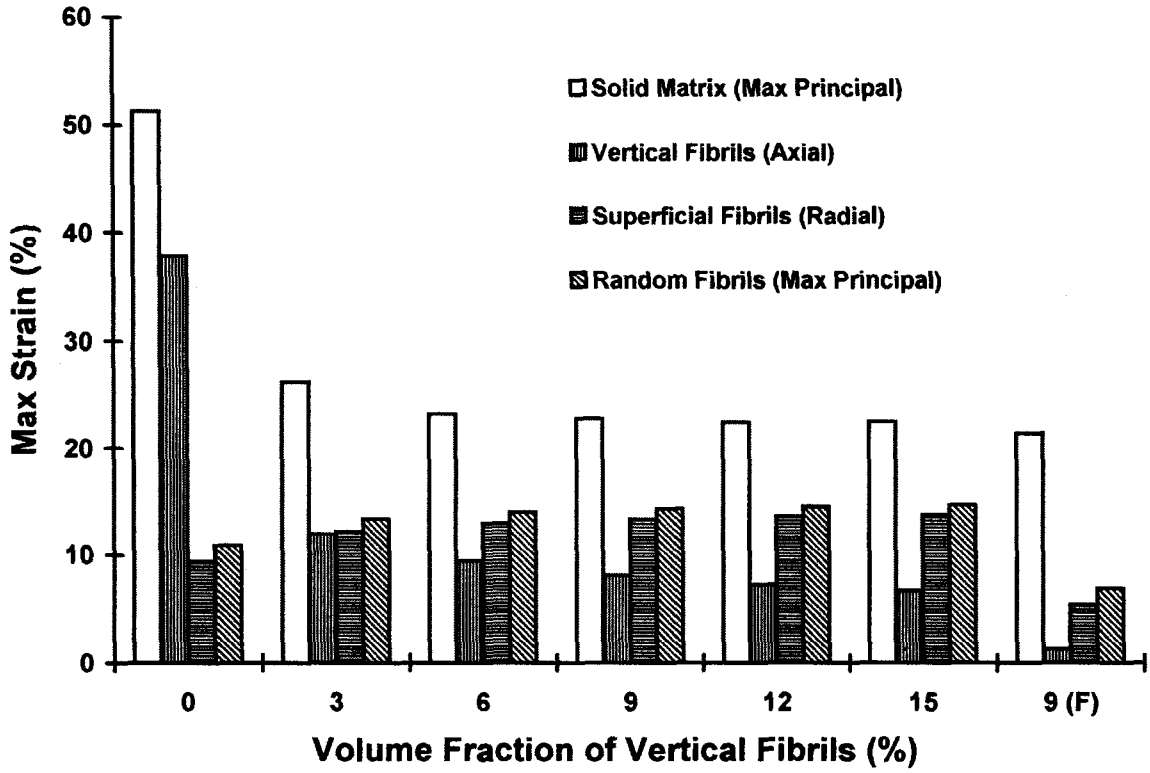

Figure 3. 3 Maximum strains in the solid matrix and collagen fibril networks at transient (t=0.5 s) in the relaxation model given for various vertical volume fraction values and the case with free sliding at the base.

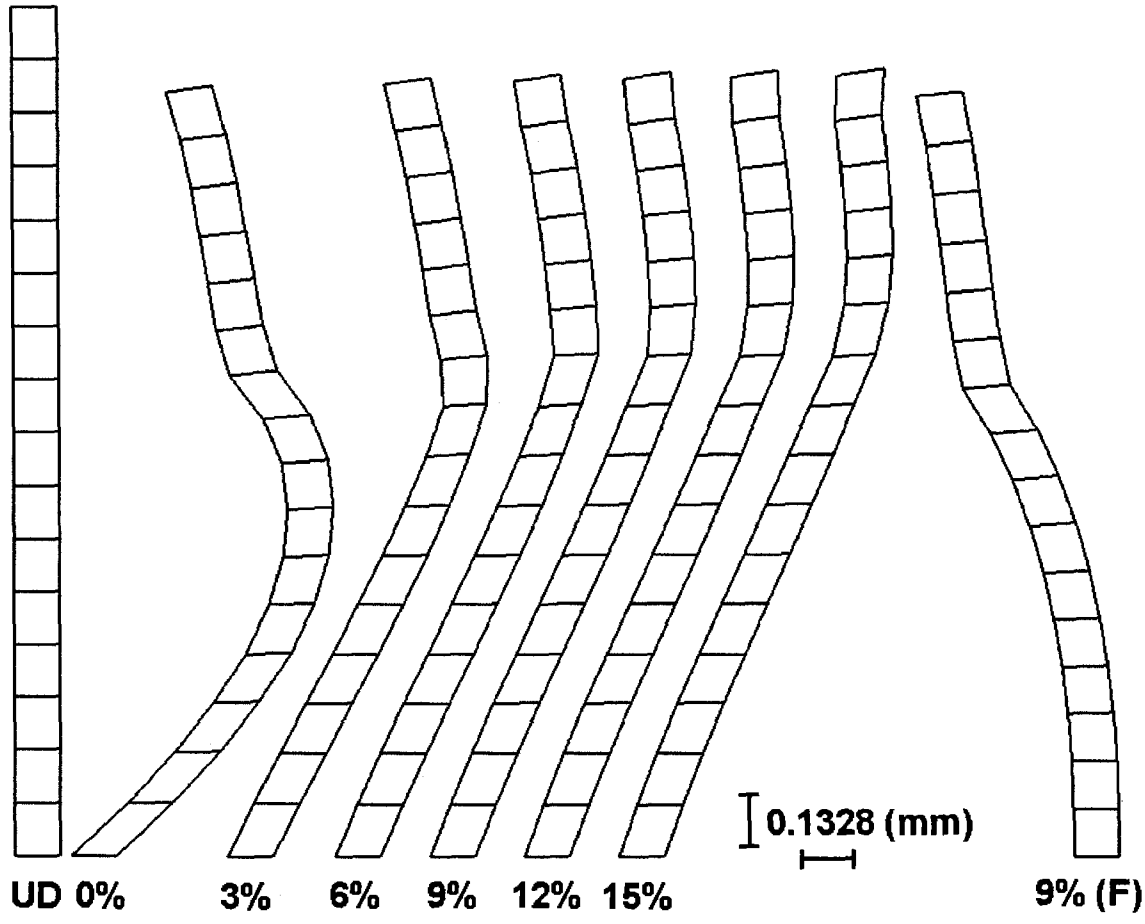

Figure 3. 4 Undeformed (UD) and deformed shapes at the transient in the relaxation model for a column of elements located initially at one-third of the outer radius from the axis of symmetry (as explicitly indicated in Fig. 3.1) given for different vertical fibrils volume fractions (0-15%). 9% (F) indicates the case with sliding boundary condition at the bottom. The scale is also shown.

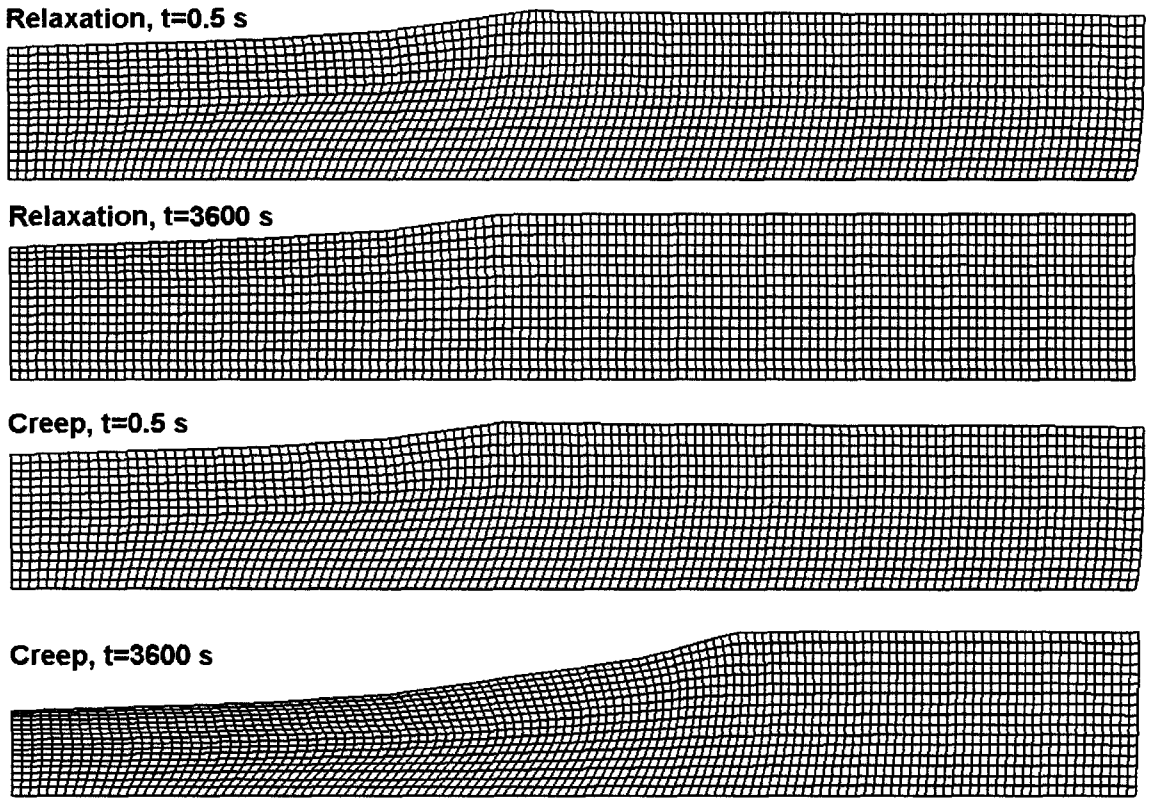

Figure 3. 5 Deformed meshes of the reference model with 9% volume content for the vertical fibrils. (a) Relaxation model at transient t=0.5s, (b) Relaxation model at t=3600 s, (c) Creep at transient t=0.5 s and (d) Creep at t=3600 s.

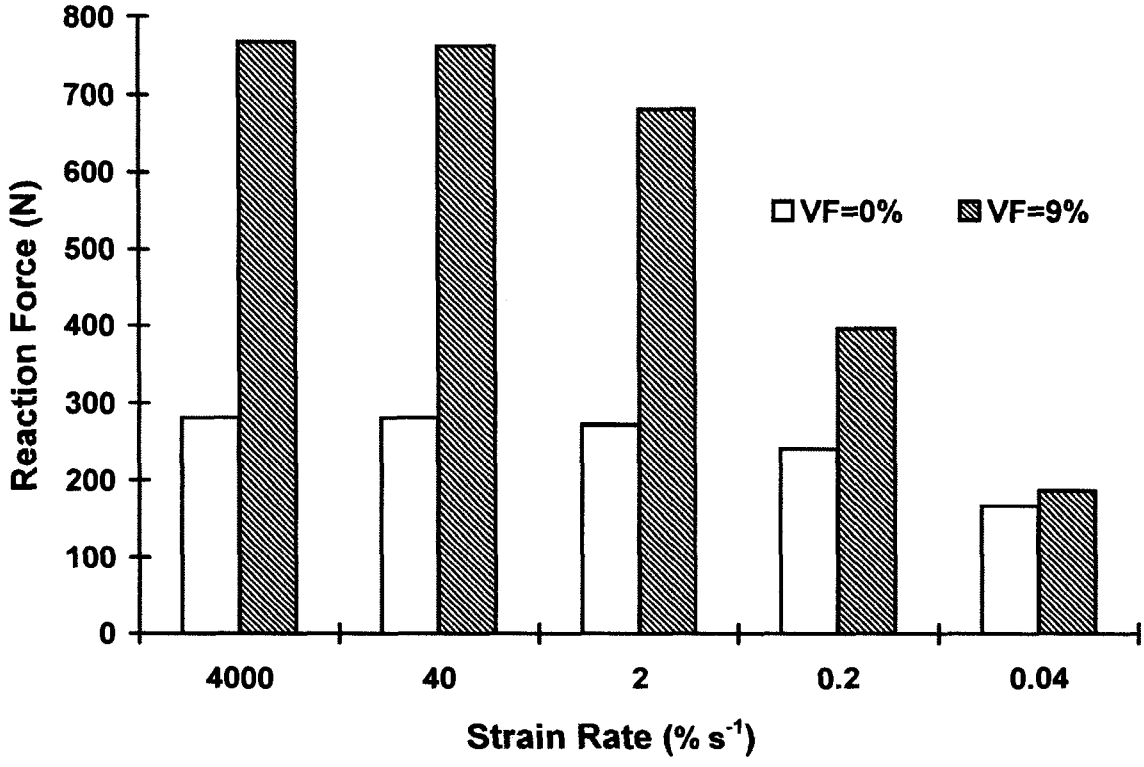

Figure 3. 6 Variation of the reaction force at transient in the relaxation model for various strain rates and two different vertical fibrils volume fractions of 0 (none) and 9%.

Chapter four

Article III: Role of cartilage collagen fibrils networks in knee joint biomechanics under compression

R. Shirazi, A. Shirazi-Adl and *M. Hurtig

Division of Applied Mechanics, Department of Mechanical Engineering
École Polytechnique, Montréal, Québec, Canada
* Department of Clinical Studies, Ontario Veterinary College, University of Guelph, Guelph, Ontario, Canada

Article published in
Journal of Biomechanics
(In press)

Keywords: Knee joint, Cartilage, Meniscus, Finite element method, Collagen fibrils

4.1 Abstract

Collagen fibrils networks in knee cartilage and menisci change in content and structure from a region to another. While resisting tension, they influence global joint response as well as local strains particularly at short-term periods. To investigate the role of fibrils networks in knee joint mechanics and in particular cartilage response, a novel model of the knee joint is developed that incorporates the cartilage and meniscus fibrils networks as well as depth-dependent properties in cartilage. The joint response under up to 2000 N compression is investigated for conditions simulating the absence in cartilage of deep fibrils normal to subchondral bone or superficial fibrils parallel to surface as well as localized split of cartilage at subchondral junction or localized damage to superficial fibrils at loaded areas. Deep vertical fibrils network in cartilage play a crucial role in stiffening (by 10%) global response and protecting cartilage by reducing large strains (from maximum of 102% to 38%), in particular at subchondral junction. Superficial horizontal fibrils protect the tissue mainly from excessive strains at superficial layers (from 27% to 8%). Local cartilage split at base disrupts the normal function of vertical fibrils at the affected areas resulting in higher strains.

Deep fibrils, and to a lesser extent superficial fibrils, play dominant mechanical roles in cartilage response under transient compression. Any treatment modality attempting to repair or regenerate cartilage defects involving partial or full thickness osteochondral grafts should account for the crucial role of collagen fibrils networks and the demanding mechanical environment of the tissue.

4.2 Introduction

Articular cartilage and meniscus of knee joints consist mainly of networks of collagen fibrils that embed water and a nonfibrillar matrix. Collagen fibrils networks in these tissues contribute to joint mechanics directly by resisting tensile stresses and indirectly by augmenting the pore fluid pressure especially at higher, more physiological, loading rates. The drastic increase in fluid pressurization in turn stiffens transient response under compression (Cohen et al., 1998; Li et al., 2003). The very low permeability causes near incompressibility during rather fast physiological loading cycles (Oloyede et al., 1992) in daily activities like walking, running and stairs ascent/descent.

The collagen fibrils structure, content, and arrangement vary not only between articular cartilage and meniscus but also in each tissue spatially along the depth (Aspden et al., 1985; Kaab et al., 1998). In cartilage, at the superficial zone, fibrils are horizontally oriented parallel to the articular surface (Minns & Steven, 1977) whereas they become rather random in the transitional zone (Broom & Marra, 1986) and finally turn perpendicular to the bone-cartilage interface in the deep zone (Kaab et al., 1998; Minns & Steven, 1977) to anchor the tissue firmly to the subchondral bone (Lane & Weiss, 1975). Hereafter, these fibrils networks are referred to as horizontal, random and vertical, respectively. In meniscus, on the other hand, while the collagen fibrils at exterior surfaces show no major preferred orientation, they are nevertheless circumferentially oriented in the bulk of the tissue (Aspden et al., 1985; Petersen & Tillmann, 1998). In addition, radial tie fibres are present that increase the tissue tensile resistance (Skaggs et al., 1994).

In earlier computational investigations of articular cartilage, fibril-reinforced composite models were introduced and validated that represented the constituents as distinct elements each playing a mechanical role for which it is optimally structured (Li

et al., 1999; Shirazi & Shirazi-Adl, 2005). Such composite models have also been employed in recent model studies on mechanics of cartilage specimens (Julkunen et al., 2007; Wilson et al., 2004). The important role of vertical fibrils, and to a lesser extent of horizontal fibrils, in cartilage mechanics was recently demonstrated by an axisymmetric model in creep and relaxation indentation loadings (Shirazi & Shirazi-Adl, 2008). The knee joint model studies, however, have failed to incorporate the composite structure of these tissues.

The objective of this study was, hence, set to initially incorporate the detailed nonhomogeneous fibrils network structure of the articular cartilage and menisci based on our earlier studies (Shirazi & Shirazi-Adl, 2005, 2008) into our existing knee model (Mesfar & Shirazi-Adl, 2006b) developing thus a novel model of the entire joint. A joint model with such detailed representation of fibrils networks constitutes an original development in the literature. The transient (i.e., short-term) response of the passive knee joint was subsequently investigated under axial compression forces up to 2000 N with special focus on the mechanical role of fibrils networks. We hypothesize that the deep vertical fibrils network and to a lesser extent superficial fibrils network play important roles in support and protection of articular cartilage and that damages to these networks, especially the former, would perturb the joint mechanics and place the tissue at higher risk of injury and long-term degeneration.

4.3 Method

4.3.1 Finite Element Model

The mesh of an existing validated 3-D model of the human knee joint (Bendjaballah et al., 1995; Mesfar & Shirazi-Adl, 2006a, 2006b) was modified by an extensive refinement of articular cartilage and menisci. These refinements allowed for the incorporation of fibrils networks at different regions along with depth-dependent variation in cartilage properties (Fig. 4.1). The subchondral bone was taken rigid due to its much greater stiffness compared to joint soft tissues (Mente & Lewis, 1994); an

assumption that negligibly influences predictions (Donahue et al., 2002). The joint ligaments; i.e. anterior/posterior cruciate (ACL/PCL) and medial/lateral collateral (MCL/LCL) ligaments, were included with nonlinear material properties and initial pre-strains (Mesfar & Shirazi-Adl, 2006a, 2006b). The surface to surface contact algorithm was used that yields accurate results by considering entire surfaces.

The cartilage non-fibrillar matrix was modelled by incompressible isotropic hyperelastic solid with depth-dependent properties whereas fibrils networks were simulated either by membrane or continuum elements (Fig. 4.1). In superficial zones of femoral and tibial cartilage layers as well as bounding surfaces of menisci, membrane elements were used to represent homogeneous in-plane distribution of fibrils with random orientations (Fig. 4.1). Despite such isotropic distribution, however, a direction-dependent response prevails due to the strain-dependency in fibrils material properties and anisotropy in strain field (Shirazi & Shirazi-Adl, 2005). The in-plane stresses in material principal axes were evaluated using the uniaxial nonlinear stress-strain curves for collagen fibrils; type I in menisci (Haut & Little, 1972; Morgan, 1960) and type II in cartilage with the latter assumed as 70% of the former (Shirazi-Adl et al., 1984). Equal principal strains would generate an isotropic material while negative principal strains result in zero principal stresses (i.e., tension only membranes). In the transitional zone with random fibrils (i.e., no dominant orientations), continuum brick elements that take the principal strain directions as the material principal axes represent collagen fibrils (Fig. 4.1). In the deep zone, however, vertical fibrils were modelled with vertical membrane elements similar to horizontal superficial ones except in offering resistance only in local fibrils directions (Fig. 4.1).

In the bulk region of each meniscus in between peripheral surfaces, collagen fibrils that are dominant in the circumferential direction were represented by membrane elements with local material principal axes defined in orthogonal circumferential and

radial directions. The formulation of fibrils networks was introduced in the ABAQUS finite element commercial program (Simulia Inc., Providence, RI).

4.3.2 Material Properties

Thickness of membrane elements in different regions of cartilage and menisci was computed based on fibrils volume fraction in each zone. In cartilage, the equivalent collagen fibrils content at the superficial zone was estimated based on reported tissue properties in tension (Kempson et al., 1968; Kempson et al., 1973; Roth & Mow, 1980; Woo et al., 1976) and type II collagen stress-strain curve (Shirazi & Shirazi-Adl, 2005). A total volume fraction of 15% was estimated in the superficial zone in agreement with the mean value of 14% reported for its wet weight (Hollander et al., 1994). Volume fractions of 18% in the transitional zone and 21% in the deep zone were subsequently taken in accordance with the reported increases in collagen content along the depth (Bi et al., 2006; Julkunen et al., 2008). Thicknesses of the superficial, transitional and deep zones were, respectively, 15, 22.5, and 62.5% of the tissue thickness (Bi et al., 2006).

Similarly, in menisci, the equivalent collagen fibrils content was estimated based on the reported tissue tensile properties in the middle bulk as well as peripheral sides (Proctor et al., 1989). The equivalent content of radial tie fibres was also estimated (Skaggs et al., 1994). Overall, 14% in the circumferential direction and 2.5% in the radial direction of bulk region along with 12% in the outer surfaces were taken in agreement with reported overall ~18% collagen content (Ghosh & Taylor, 1987; Peters & Smillie, 1972).

To study short-term (transient) biphasic response of the joint, en equivalent elastic response was sought by using equilibrium modulus of the tissue and Poisson's ratio of 0.5 (see discussion). The drained (equilibrium) modulus of solid matrix in articular cartilage was considered depth-dependent increasing from 0.3 to 0.5, 0.8 and 1.2 MPa when moving from articular surface to lowermost layer at the subchondral bone, respectively (Schinagl et al., 1997). The Ogden strain energy function was used

for all hyperelastic materials. The modulus for incompressible matrix of menisci was initially chosen to be 0.35 MPa (Joshi et al., 1995); due to slow convergence rates, however, this incompressible behaviour was replaced by a compressible one with a Young's modulus of 12 MPa and Poisson's ratio of 0.45 as used in our earlier knee joint model studies. These material properties resulted in similar global displacements and stresses/strains in different components for compressible and incompressible models of menisci under compression forces up to 800 N as the maximum force reached in the latter model.

4.3.3 Loading and Boundary Conditions

The knee joint passive response was studied at full extension under compression forces up to 2000 N. In subsequent parametric cases, however, due to convergence difficulties, lower force of 1800 N was considered. Apart from the flexion-extension degree-of-freedom that was fixed, the joint was left fully unconstrained under the applied compression force; the femur was fixed while the tibia was left free. Prior to the application of axial compression, the joint equilibrium at full extension was initially sought under pre-strains in ligaments.

4.3.4 Parametric Cases Studied

Initially, the effect of constraint on the coupled internal-external rotation on joint response was studied. To examine the roles of deep vertical and superficial horizontal fibrils, subsequent analyses were carried out in which volume fraction content of either of these fibrils networks in both femoral and tibial cartilage layers was diminished to nil. In additional cases to evaluate the role of localized cartilage split at the subchondral base, a region at the tibial cartilage-bone junction (~25%, i.e. 202.8 mm^2, of the lateral compartmental surface under the loaded area, Fig. 4.7) was detached resulting in free sliding (separation with no penetration) at the cartilage-bone interface. Finally, the effect of localized disruption in superficial collagen fibrils on joint response was studied by removing the superficial collagen fibrils network on the lateral plateau at an area of ~202.8 mm^2 under loaded areas (see Fig. 4.7).

4.4 Results

Load-deflection in the axial direction indicates a nonlinear stiffening response that increases as the internal-external rotation is constrained but decreases with removal of vertical fibrils network (Fig. 4.2). Localized split of tibial cartilage at subchondral base also softens the response, though to a lesser degree. Localized and total absences of superficial horizontal fibrils, on the other hand, do not influence the response. Total forces in ACL, MCL and LCL ligaments under 2000/1800 N compression in the reference intact case reach 166/153 N, 27/26 N and 37/39 N, respectively with the PCL remaining slack and ACL force carried entirely via its posterolateral bundle. Under these loads and fixed coupled internal/external rotation, ACL force increases to 241/214 N whereas LCL and MCL forces disappear. Removal of vertical fibrils, on the other hand, diminishes ACL force to 128 N under 1800 N compression. Changes in ligament forces were less noticeable under other cases studied.

For the reference intact model at 2000 N, peak contact and pore pressures occur in uncovered cartilage at the lateral tibial plateau (Figs. 4.3a, b). Underneath the loaded areas, the deep vertical collagen fibrils show the least strains where in contrast the superficial fibrils are most strained (Fig. 4.3). Vertical fibrils experience larger strains away from the loaded areas (Figs. 4.3c, d). Tensile principal strain in the cartilage matrix increases from the articular surface to the subchondral junction where it reaches its peak of 42.5% in the lateral tibial plateau and 24.6% in the femur at both condyles (Figs. 4.3g, h and 4.4). Contact pressures on the menisci reach maximums of 3.52 MPa on the upper surface (meniscofemoral articulation) and 3.43 MPa on the lower surface (meniscotibial articulation), both on the lateral meniscus (Fig. 4.5). Large tensile strains are computed in menisci at inner regions close to horns reaching maximum of 31.3% at medial side (Fig. 4.5). Radial strain in menisci remains less than 3.5% at 1800 N in all cases.

Under 1800 N compression, principal tensile strain in the solid matrix of cartilage substantially increases everywhere when vertical fibrils are removed (Fig. 4.6).

Likewise, maximum tensile strain in the direction of vertical fibrils themselves substantially increases. The maximum tensile strains at subchondral junction also increase, though to a lesser extent, when cartilage attachment to the subchondral bone is locally disrupted (Fig. 4.6). Localized or total absence of superficial fibrils has much less effects on these matrix strains. They, however, increase the tensile strains within articulating surfaces of cartilage (Fig. 4.7). Removal of vertical fibrils also increases strains in superficial fibrils membranes (Fig. 4.7). Restraint on coupled internal-external rotation diminishes maximum tensile strains in cartilage and meniscus matrices from 37.8% and 28.4% respectively to 33.2% and 15.9%. Maximum tensile strain in meniscus matrix, in contrast to cartilage matrix, only negligibly (<1.3%) alters when comparing the reference intact case to other cases studied.

Under 1800 N compression force, the lateral compartment transfers a larger portion of load than the medial one (Fig. 4.8). The relative load-bearing share of menisci (i.e., covered areas) is much greater in the lateral plateau. The contribution of cartilage versus meniscus in carrying the applied force alters slightly in different cases. In the lateral tibial plateau, the uncovered (tibiofemoral) contact area is about half the covered (meniscotibial) contact area. In the medial side, the uncovered area is also smaller than the covered one. The mean contact pressure in the reference case under 2000 N reaches 1.74, 1.39 and 2.93 MPa at the meniscofemoral, meniscotibial and uncovered tibiofemoral contact areas at the lateral articulation, respectively, whereas corresponding values for the medial side reach 0.91, 0.85 and 1.93 MPa.

4.5 Discussion

An earlier validated model of the knee joint (Bendjaballah et al., 1995; Mesfar & Shirazi-Adl, 2006a, 2006b) was substantially refined to allow for the incorporation of detailed collagen fibrils networks in articular cartilage and menisci as well as the depth-dependent properties in cartilage. The role of deep vertical and superficial horizontal collagen fibrils networks in articular cartilage on biomechanics of the entire knee joint

was subsequently investigated for the first time under axial compression forces up to 2000 N at full extension. Predictions confirmed the hypothesis that deep vertical and horizontal superficial (though to a much lesser extent) collagen fibrils networks stiffen the cartilage tissue while protecting it from excessive strains and distortions under physiological compression loads at transient periods. Disruptions in these networks (particularly in the vertical fibrils) would hence place the tissue at greater risk of injury and degeneration. The simulated perturbations in cartilage had much smaller effects on the menisci.

In accordance with earlier (Brown & Singerman, 1986) and recent (Ateshian et al., 2007) investigations, the transient response of cartilage and meniscus under higher strain rates in physiological activities can accurately be captured either by a biphasic analysis or equivalently by an incompressible elastic analysis using equilibrium modulus. Examining this equivalency as a function of Poisson's ratio using our earlier non-homogeneous axisymmetric model of cartilage (Shirazi & Shirazi-Adl, 2008), indentation results at 20% strain in 0.5 s demonstrated a significant sensitivity in transient reaction force (Fig. 4.9). It appears, hence, that Poisson's ratios in the range of 0.4999-0.5 should be considered in incompressible elastic models if equivalent transient results are to be obtained. In comparison, the model demonstrated less sensitivity to variations in equilibrium modulus of solid matrix. Since loading cycles of daily activities like walking and running last for only a fraction of second, an incompressible elastic model can alternatively be employed with no loss of accuracy to compute the transient response. In this case the hydrostatic pressure in the elastic model represents the transient pore pressure in its equivalent poroelastic model. An equivalent compressible elastic material can also be employed in which case greater equilibrium modulus should be used depending on the Poisson's ratio considered.

4.5.1 Comparison with Measurements

Constraint on the internal-external rotation stiffened the overall primary response (Fig. 4.2) in agreement with model studies (Bendjaballah et al., 1995). The axial deflection agreed with measurements (Kurosawa et al., 1980; Walker & Erkman, 1975) performed under uniaxial displacement, a boundary condition similar to the case with fixed internal-external rotation.

In agreement with predictions (Bendjaballah et al., 1995) and measurements (Ahmed & Burke, 1983; Walker & Erkman, 1975), relative load-bearing contribution of menisci decreased with compression. In measurement studies (Ahmed & Burke, 1983) under 445 N and 1335 N, the compartmental portion of lateral meniscus reached 82±10% and 77±7% whereas that of medial meniscus was lower at 69±17% and 62±12%, respectively. The corresponding predictions were 54% and 51% for the lateral meniscus and 45% and 39% for the medial meniscus. Moreover, predicted values of 50% and 39% for respectively lateral and medial menisci at 1400 N, though less than measured values of 81% and 77% (Seedhom & Hargreaves, 1979), compared with reported value of ~45% averaged over both compartments of 16 specimens under similar loads (Shrive et al., 1978). The average circumferential strain of 2.40±1.61% in the outer surface of medial meniscus measured in vitro under three times body weight at 0° and 30° flexion angles (Jones et al., 1996) compared with ~1.5% predicted under 2000 N at full extension. The predicted contact areas/pressures at various load levels fell also within reported measurements (Table 4.1).

4.5.2 Implications

Articular cartilage experienced much greater distortions at bone-cartilage junction (Fig. 4.4) where horizontal split fractures occur in daily activities (Meachim & Bentley, 1978) and impact loads (Atkinson & Haut, 1995; Vener et al., 1992). Larger strains at subchondral junction are likely due to the existing stiffness gradient (Radin & Rose, 1986). Despite a moderate (~10%) softening effect on overall response, removal

of deep vertical fibrils substantially increased maximum cartilage tensile/shear strains especially at subchondral junction (Fig. 4.6) where large strains already existed. The current model study, hence, highlights the primary role of vertical fibrils network in stiffening articular cartilage while protecting it from excessive strains and distortions. Unlike the peak compressive strains, the maximum shear and tensile strains at deeper cartilage layers and in vertical fibrils themselves occur away from the loaded areas. Prediction of crimped fibrils underneath the loaded areas is corroborated by experimental studies (Broom & Poole, 1982; Glaser & Putz, 2002).

Foregoing mechanical role of vertical fibrils further accentuate under larger compression loads expected in running, high impacts and more strenuous activities. Our preliminary results not reported here (with lower vertical fibrils content of 9%) as well as earlier works (Shirazi & Shirazi-Adl, 2008) also demonstrate the protective role of vertical fibrils even at volume fractions much smaller than 21% considered in this study. Absence of deep vertical fibrils also increases the tensile strain in superficial horizontal fibrils. In comparison, removal of superficial horizontal fibrils network play a less significant role in joint stiffness and cartilage strains. This appears to agree with the observation of lack of progression of tissue injury in presence of superficial defects (Ghadially et al., 1977).

The importance of the integrity of cartilage anchorage at base in augmenting the tissue stability and load-bearing (Keinan-Adamsky et al., 2005) as well as in initiation of joint failure and osteoarthritis (Atkinson & Haut, 1995; Vener et al., 1992) has been recognized. Local damages at the subchondral junction could potentially precede degenerative changes in overlying cartilage (Atkinson & Haut, 1995; Keinan-Adamsky et al., 2005; Meachim & Bentley, 1978; Radin & Rose, 1986). Apart from bone bruises at base (Henderson & La Valette, 2005; Tandogan et al., 2004), surface cartilage defects have also been reported (Hollander et al., 1995; Vande Berg et al., 2002). In this study, the effect of two distinct localized damages in tibial cartilage at loaded areas were

investigated; the tissue was either detached at the subchondral junction or weakened at the surface by removing the superficial fibrils. The foregoing model of localized detachment at base cannot adequately simulate subchondral failures due to associated compromise in the underlying bone that would further increase distortions in overlying cartilage. The base split compared to surface damage had much greater effect in increasing maximum tensile strain in cartilage matrix of the affected plateau.

In conclusion, vertical fibrils play a crucial role in stiffening and protecting articular cartilage from large tensile/shear strains, in particular at the subchondral junction where peak strains occur. Superficial horizontal fibrils, on the other hand, protect the tissue mainly from excessive strains at superficial layers. Local detachment of cartilage at base disrupts the function of vertical fibrils at the affected areas resulting in higher strains in cartilage. Any treatment modality attempting to repair or regenerate cartilage defects involving partial or full thickness osteochondral grafts should account for the crucial role of collagen fibrils networks and the demanding mechanical environment of the tissue. This work also emphasizes the importance in cartilage mechanics of realistic representation of fibrils arrangements that may alter depending on age and location on articular cartilage (Kaab et al., 1998; Xia et al., 2003).

4.6 Conflict of Interest Statement

None.

4.7 Acknowledgment

This research work is supported by grants from the Canadian Institute of Health Research (CIHR) and the National Sciences and Engineering Research Council of Canada (NSERC).

4.8 References

Ahmed, A. M., and Burke, D. L. (1983). In-vitro measurement of static pressure distribution in synovial joints--Part I: Tibial surface of the knee. *J Biomech Eng, 105*(3), 216-225.

Aspden, R. M., Yarker, Y. E., and Hukins, D. W. (1985). Collagen orientations in the meniscus of the knee joint. *J Anat, 140 (Pt 3)*, 371-380.

Ateshian, G. A., Ellis, B. J., and Weiss, J. A. (2007). Equivalence between short-time biphasic and incompressible elastic material responses. *J Biomech Eng, 129*(3), 405-412.

Atkinson, P. J., and Haut, R. C. (1995). Subfracture insult to the human cadaver patellofemoral joint produces occult injury. *J Orthop Res, 13*(6), 936-944.

Bendjaballah, M. Z., Shirazi-Adl, A., and Zukor, D. J. (1995). Biomechanics of the human knee joint in compression: reconstruction, mesh generation and finite element analysis. *The Knee, 2*(2), 69-79.

Bi, X., Yang, X., Bostrom, M. P., and Camacho, N. P. (2006). Fourier transform infrared imaging spectroscopy investigations in the pathogenesis and repair of cartilage. *Biochim Biophys Acta, 1758*(7), 934-941.

Broom, N. D., and Marra, D. L. (1986). Ultrastructural evidence for fibril-to-fibril associations in articular cartilage and their functional implication. *J Anat, 146*, 185-200.

Broom, N. D., and Poole, C. A. (1982). A functional-morphological study of the tidemark region of articular cartilage maintained in a non-viable physiological condition. *J Anat, 135*(Pt 1), 65-82.

Brown, T. D., and Shaw, D. T. (1984). In vitro contact stress distribution on the femoral condyles. *J Orthop Res, 2*(2), 190-199.

Brown, T. D., and Singerman, R. J. (1986). Experimental determination of the linear biphasic constitutive coefficients of human fetal proximal femoral chondroepiphysis. *J Biomech, 19*(8), 597-605.

Cohen, B., Lai, W. M., and Mow, V. C. (1998). A transversely isotropic biphasic model for unconfined compression of growth plate and chondroepiphysis. *J Biomech Eng, 120*(4), 491-496.

Donahue, T. L., Hull, M. L., Rashid, M. M., and Jacobs, C. R. (2002). A finite element model of the human knee joint for the study of tibio-femoral contact. *J Biomech Eng, 124*(3), 273-280.

Fukubayashi, T., and Kurosawa, H. (1980). The contact area and pressure distribution pattern of the knee. A study of normal and osteoarthrotic knee joints. *Acta Orthop Scand, 51*(6), 871-879.

Ghadially, F. N., Thomas, I., Oryschak, A. F., and Lalonde, J. M. (1977). Long-term results of superficial defects in articular cartilage: a scanning electron-microscope study. *J Pathol, 121*(4), 213-217.

Ghosh, P., and Taylor, T. K. (1987). The knee joint meniscus. A fibrocartilage of some distinction. *Clin Orthop Relat Res*(224), 52-63.

Glaser, C., and Putz, R. (2002). Functional anatomy of articular cartilage under compressive loading Quantitative aspects of global, local and zonal reactions of the collagenous network with respect to the surface integrity. *Osteoarthritis Cartilage, 10*(2), 83-99.

Haut, R. C., and Little, R. W. (1972). A constitutive equation for collagen fibers. *J Biomech, 5*(5), 423-430.

Henderson, I. J., and La Valette, D. P. (2005). Subchondral bone overgrowth in the presence of full-thickness cartilage defects in the knee. *Knee, 12*(6), 435-440.

Hollander, A. P., Heathfield, T. F., Webber, C., Iwata, Y., Bourne, R., Rorabeck, C., and Poole, A. R. (1994). Increased damage to type II collagen in osteoarthritic articular cartilage detected by a new immunoassay. *J Clin Invest, 93*(4), 1722-1732.

Hollander, A. P., Pidoux, I., Reiner, A., Rorabeck, C., Bourne, R., and Poole, A. R. (1995). Damage to type II collagen in aging and osteoarthritis starts at the

articular surface, originates around chondrocytes, and extends into the cartilage with progressive degeneration. *J Clin Invest, 96*(6), 2859-2869.

Huang, A., Hull, M. L., and Howell, S. M. (2003). The level of compressive load affects conclusions from statistical analyses to determine whether a lateral meniscal autograft restores tibial contact pressure to normal: a study in human cadaveric knees. *J Orthop Res, 21*(3), 459-464.

Inaba, H. I., Arai, M. A., and Watanabe, W. W. (1990). Influence of the varus-valgus instability on the contact of the femoro-tibial joint. *Proc Inst Mech Eng [H], 204*(1), 61-64.

Jones, R. S., Keene, G. C., Learmonth, D. J., Bickerstaff, D., Nawana, N. S., Costi, J. J., and Pearcy, M. J. (1996). Direct measurement of hoop strains in the intact and torn human medial meniscus. *Clin Biomech (Bristol, Avon), 11*(5), 295-300.

Joshi, M. D., Suh, J. K., Marui, T., and Woo, S. L. (1995). Interspecies variation of compressive biomechanical properties of the meniscus. *J Biomed Mater Res, 29*(7), 823-828.

Julkunen, P., Kiviranta, P., Wilson, W., Jurvelin, J. S., and Korhonen, R. K. (2007). Characterization of articular cartilage by combining microscopic analysis with a fibril-reinforced finite-element model. *J Biomech, 40*(8), 1862-1870.

Julkunen, P., Wilson, W., Jurvelin, J. S., Rieppo, J., Qu, C. J., Lammi, M. J., and Korhonen, R. K. (2008). Stress-relaxation of human patellar articular cartilage in unconfined compression: Prediction of mechanical response by tissue composition and structure. *J Biomech, 41*(9), 1978-1986.

Kaab, M. J., Gwynn, I. A., and Notzli, H. P. (1998). Collagen fibre arrangement in the tibial plateau articular cartilage of man and other mammalian species. *J Anat, 193 (Pt 1)*, 23-34.

Keinan-Adamsky, K., Shinar, H., and Navon, G. (2005). The effect of detachment of the articular cartilage from its calcified zone on the cartilage microstructure, assessed by 2H-spectroscopic double quantum filtered MRI. *J Orthop Res, 23*(1), 109-117.

Kempson, G. E., Freeman, M. A., and Swanson, S. A. (1968). Tensile properties of articular cartilage. *Nature, 220*(172), 1127-1128.

Kempson, G. E., Muir, H., Pollard, C., and Tuke, M. (1973). The tensile properties of the cartilage of human femoral condyles related to the content of collagen and glycosaminoglycans. *Biochim Biophys Acta, 297*(2), 456-472.

Krause, W. R., Pope, M. H., Johnson, R. J., and Wilder, D. G. (1976). Mechanical changes in the knee after meniscectomy. *J Bone Joint Surg Am, 58*(5), 599-604.

Kurosawa, H., Fukubayashi, T., and Nakajima, H. (1980). Load-bearing mode of the knee joint: physical behavior of the knee joint with or without menisci. *Clin Orthop Relat Res*(149), 283-290.

Lane, J. M., and Weiss, C. (1975). Review of articular cartilage collagen research. *Arthritis Rheum, 18*(6), 553-562.

Li, L. P., Buschmann, M. D., and Shirazi-Adl, A. (2003). Strain-rate dependent stiffness of articular cartilage in unconfined compression. *J Biomech Eng, 125*(2), 161-168.

Li, L. P., Soulhat, J., Buschmann, M. D., and Shirazi-Adl, A. (1999). Nonlinear analysis of cartilage in unconfined ramp compression using a fibril reinforced poroelastic model. *Clin Biomech, 14*(9), 673-682.

Maquet, P. G., Van de Berg, A. J., and Simonet, J. C. (1975). Femorotibial weight-bearing areas. Experimental determination. *J Bone Joint Surg Am, 57*(6), 766-771.

Meachim, G., and Bentley, G. (1978). Horizontal splitting in patellar articular cartilage. *Arthritis Rheum, 21*(6), 669-674.

Mente, P. L., and Lewis, J. L. (1994). Elastic modulus of calcified cartilage is an order of magnitude less than that of subchondral bone. *J Orthop Res, 12*(5), 637-647.

Mesfar, W., and Shirazi-Adl, A. (2006a). Biomechanics of changes in ACL and PCL material properties or prestrains in flexion under muscle force-implications in ligament reconstruction. *Comput Methods Biomech Biomed Engin, 9*(4), 201-209.

Mesfar, W., and Shirazi-Adl, A. (2006b). Knee joint mechanics under quadriceps--hamstrings muscle forces are influenced by tibial restraint. *Clin Biomech (Bristol, Avon), 21*(8), 841-848.

Minns, R. J., and Steven, F. S. (1977). The collagen fibril organization in human articular cartilage. *J Anat, 123*(Pt 2), 437-457.

Morgan, F. R. (1960). Mechanical properties of collagen and leather fibres. *American Leather Chemists Association Journal, 55*(1), 4-23.

Oloyede, A., Flachsmann, R., and Broom, N. D. (1992). The dramatic influence of loading velocity on the compressive response of articular cartilage. *Connect Tissue Res, 27*(4), 211-224.

Peters, T. J., and Smillie, I. S. (1972). Studies on the chemical composition of the menisci of the knee joint with special reference to the horizontal cleavage lesion. *Clin Orthop Relat Res, 86*, 245-252.

Petersen, W., and Tillmann, B. (1998). Collagenous fibril texture of the human knee joint menisci. *Anat Embryol (Berl), 197*(4), 317-324.

Proctor, C. S., Schmidt, M. B., Whipple, R. R., Kelly, M. A., and Mow, V. C. (1989). Material properties of the normal medial bovine meniscus. *J Orthop Res, 7*(6), 771-782.

Radin, E. L., and Rose, R. M. (1986). Role of subchondral bone in the initiation and progression of cartilage damage. *Clin Orthop Relat Res*(213), 34-40.

Roth, V., and Mow, V. C. (1980). The intrinsic tensile behavior of the matrix of bovine articular cartilage and its variation with age. *J Bone Joint Surg Am, 62*(7), 1102-1117.

Schinagl, R. M., Gurskis, D., Chen, A. C., and Sah, R. L. (1997). Depth-dependent confined compression modulus of full-thickness bovine articular cartilage. *J Orthop Res, 15*(4), 499-506.

Seedhom, B. B., and Hargreaves, D. J. (1979). Transmission of the load in the knee joint with special reference to the role of the menisci. II. Experimental results, discussion and conclusions. *Engineering in Medicine, 8*(4), 220-228.

Shirazi-Adl, S. A., Shrivastava, S. C., and Ahmed, A. M. (1984). Stress analysis of the lumbar disc-body unit in compression. A three-dimensional nonlinear finite element study. *Spine, 9*(2), 120-134.

Shirazi, R., and Shirazi-Adl, A. (2005). Analysis of articular cartilage as a composite using nonlinear membrane elements for collagen fibrils. *Med Eng Phys, 27*(10), 827-835.

Shirazi, R., and Shirazi-Adl, A. (2008). Deep vertical collagen fibrils play a significant role in mechanics of articular cartilage. *J Orthop Res, 26*(5), 608-615.

Shrive, N. G., O'Connor, J. J., and Goodfellow, J. W. (1978). Load-bearing in the knee joint. *Clin Orthop Relat Res*(131), 279-287.

Skaggs, D. L., Warden, W. H., and Mow, V. C. (1994). Radial tie fibers influence the tensile properties of the bovine medial meniscus. *J Orthop Res, 12*(2), 176-185.

Tandogan, R. N., Taser, O., Kayaalp, A., Taskiran, E., Pinar, H., Alparslan, B., and Alturfan, A. (2004). Analysis of meniscal and chondral lesions accompanying anterior cruciate ligament tears: relationship with age, time from injury, and level of sport. *Knee Surg Sports Traumatol Arthrosc, 12*(4), 262-270.

Vande Berg, B. C., Lecouvet, F. E., and Malghem, J. (2002). Frequency and topography of lesions of the femoro-tibial cartilage at spiral CT arthrography of the knee: a study in patients with normal knee radiographs and without history of trauma. *Skeletal Radiol, 31*(11), 643-649.

Vener, M. J., Thompson, R. C., Jr., Lewis, J. L., and Oegema, T. R., Jr. (1992). Subchondral damage after acute transarticular loading: an in vitro model of joint injury. *J Orthop Res, 10*(6), 759-765.

Walker, P. S., and Erkman, M. J. (1975). The role of the menisci in force transmission across the knee. *Clin Orthop Relat Res*(109), 184-192.

Walker, P. S., and Hajek, J. V. (1972). The load-bearing area in the knee joint. *J Biomech, 5*(6), 581-589.

Wilson, W., van Donkelaar, C. C., van Rietbergen, B., Ito, K., and Huiskes, R. (2004). Stresses in the local collagen network of articular cartilage: a poroviscoelastic fibril-reinforced finite element study. *J Biomech, 37*(3), 357-366.

Woo, S. L., Akeson, W. H., and Jemmott, G. F. (1976). Measurements of nonhomogeneous, directional mechanical properties of articular cartilage in tension. *J Biomech, 9*(12), 785-791.

Xia, Y., Moody, J. B., Alhadlaq, H., and Hu, J. (2003). Imaging the physical and morphological properties of a multi-zone young articular cartilage at microscopic resolution. *J Magn Reson Imaging, 17*(3), 365-374.

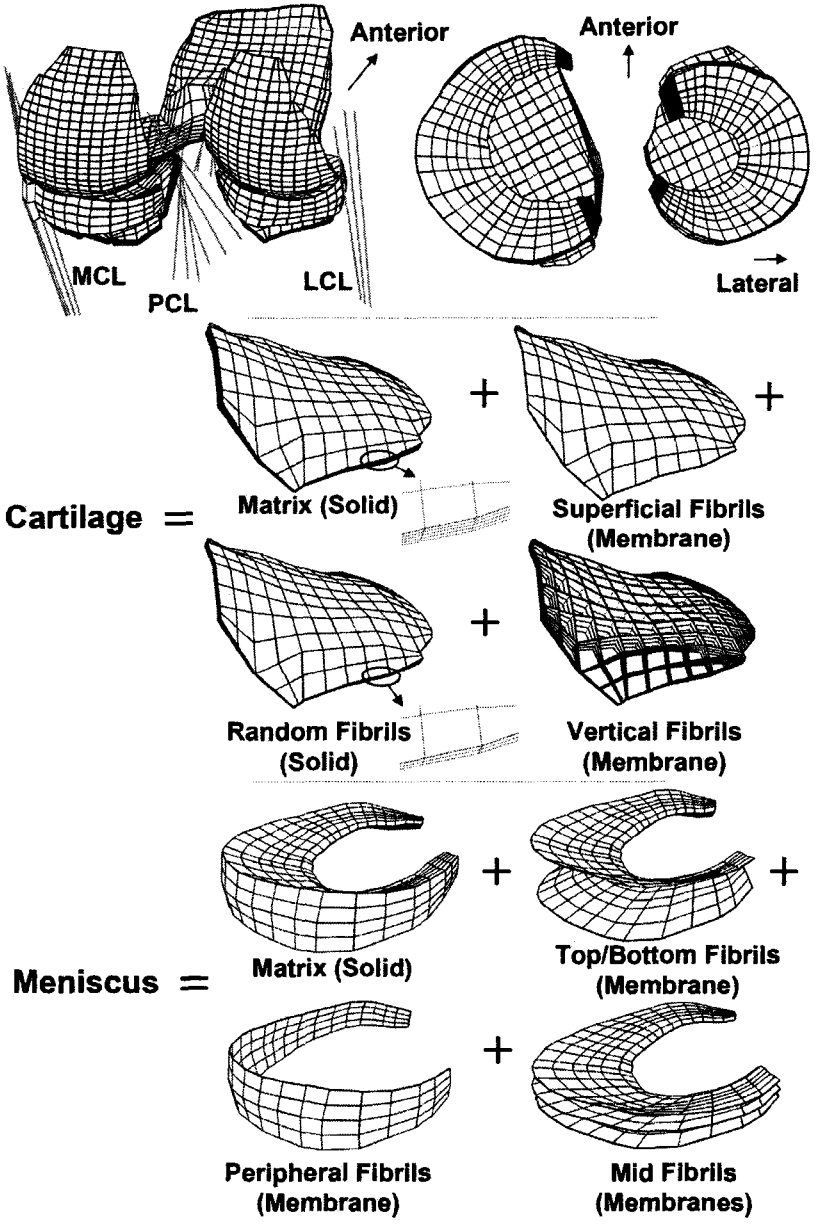

Figure 4. 1 Finite element mesh; Top left: posterior view of the knee joint with tibial and femoral cartilage layers, menisci and major ligaments. Top right: top view of menisci (horns are in grey) and tibial articular cartilage. Middle and bottom: respectively tibial lateral cartilage and medial meniscus showing distinct elements representing solid matrix along with collagen fibrils networks at different zones. Tibial medial plateau, femoral cartilage and lateral meniscus have similar structures though not shown here. Random fibrils in cartilage are distributed on the two upper layers of cartilage. Similar nonhomogeneous fibre-reinforced models of cartilage have also been used in our earlier publications (Figure 1 & 3 in Shirazi and Shirazi-Adl, 2005 and Figure 1 in Shirazi and Shirazi-Adl, 2008).

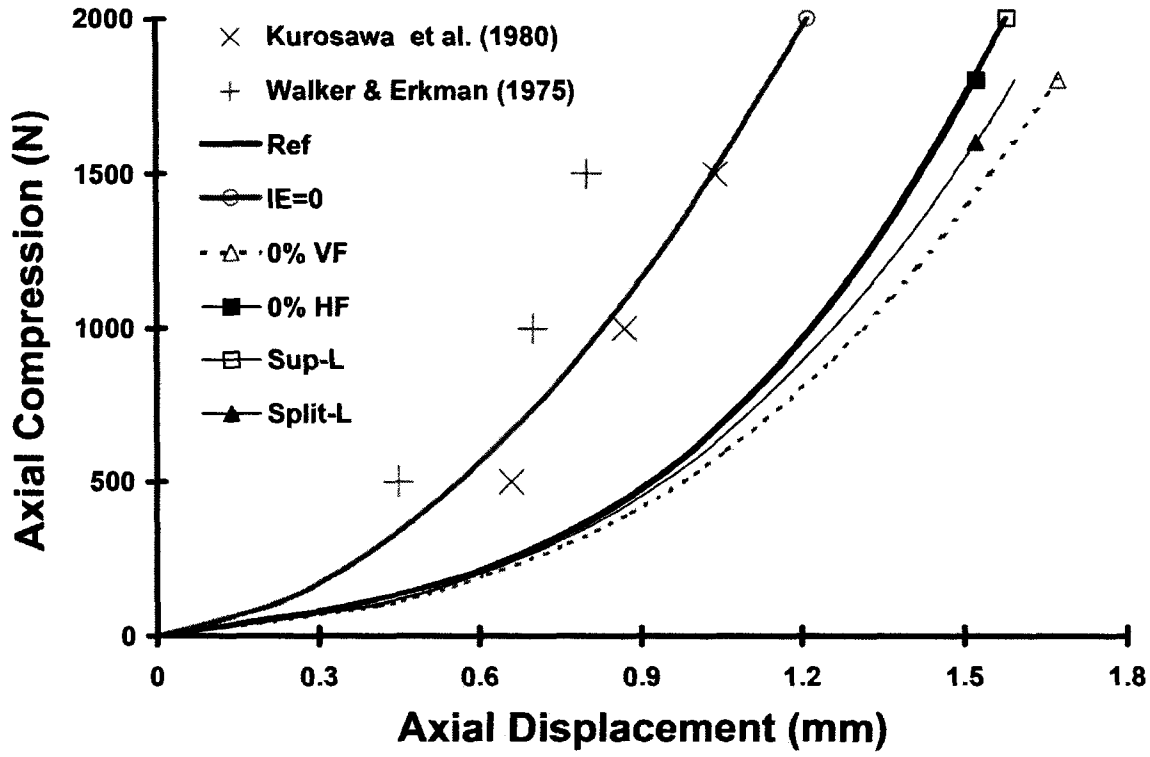

Figure 4. 2 Tibial axial displacement under axial compressive loads up to 2000 N. Ref: reference intact case. IE=0: same as reference case but with fixed tibial coupled internal-external rotation. 0% HF: superficial horizontal fibrils are absent everywhere in femoral and tibial cartilage layers. 0% VF: deep vertical fibrils are absent everywhere in femoral and tibial cartilage layers. Split-L: local lateral detachment (split) of cartilage from its underlying bone (see text and Figure 4.7 for the detachment area). Sup-L: local removal of superficial fibrils network on the tibial lateral plateau (see text and Figure 4.7). Experimental measurements under uniaxial compression loading are also shown for comparison.

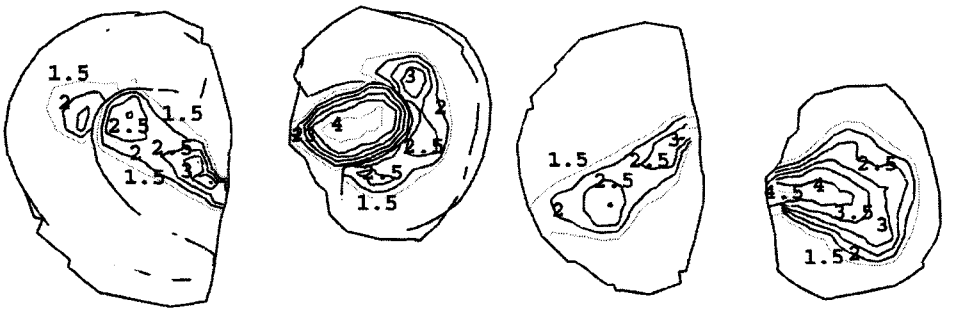

(a) (max. 4.32 MPa) **(b)** (max. 4.97MPa)

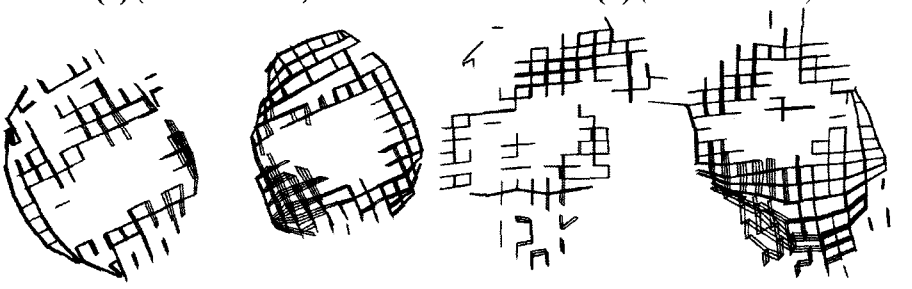

(c) (fibrils shown ≥2%, max. 8.1%) **(d)** (fibrils shown ≥2%, max. 8.6%)

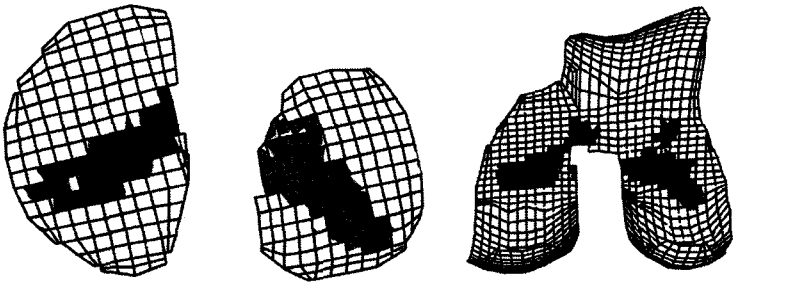

(e) (grey area ≥3%, max. 7.9%) **(f)** (grey area ≥3%, max. 9.8%)

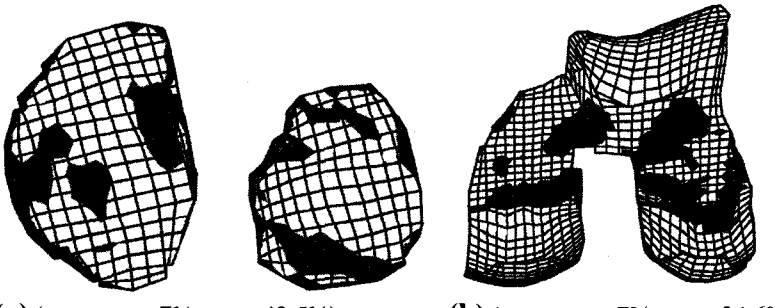

(g) (grey area ≥7%, max. 42.5%) **(h)** (grey area ≥7%, max. 24.6%)

Figure 4. 3 Predictions for the intact reference case at 2000 N compression; (a) Contact pressure on the tibial surface, (b) Pore pressure at the uppermost layer of cartilage at tibial plateaus, (c), (d) Vertical collagen fibrils elements experiencing ≥ 2% tensile strain in the tibial and femoral cartilage, respectively, (e), (f) Areas with maximum principal strain ≥ 3% in superficial fibrils network in tibial and femoral articulating surfaces, respectively, (g), (h) Maximum principal strain ≥ 7% in solid matrix at the deep lowermost layer of tibial and femoral cartilage layers, respectively.

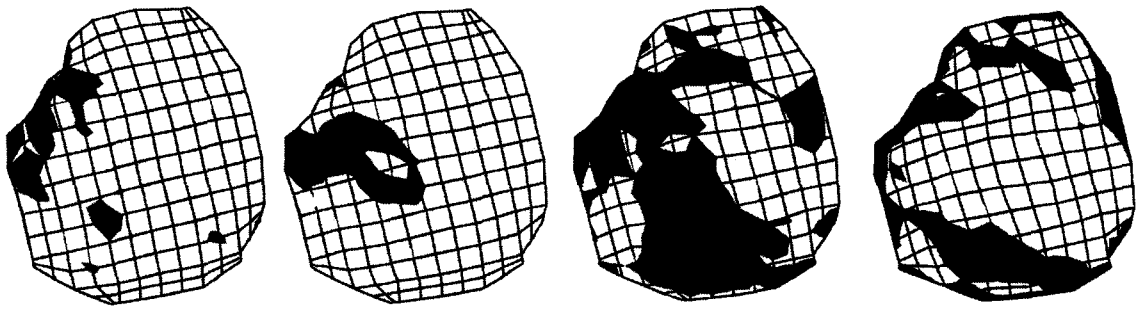

(a) (max. 21.0%) **(b)** (max. 19.5%) **(c)** (max, 35.7%) **(d)** (max, 42.5%)
(grey area ≥7%)

Figure 4. 4 Computed maximum principal strain ≥ 7% in different cartilage layers at tibial lateral plateau from superficial top (a) to deep bottom (d) under 2000 N compression in the reference case.

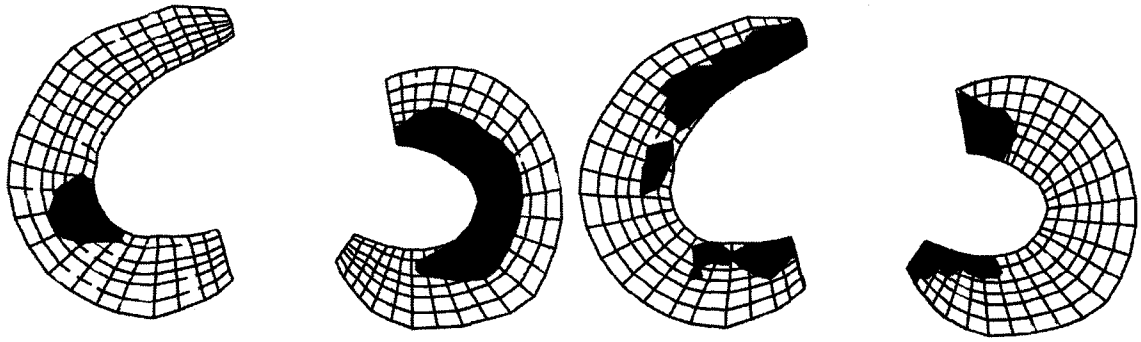

(a) (grey area ≥1.5 Mpa, max. 3.43 MPa) **(b)** (grey area ≥7%, max. 31.3%)

Figure 4. 5 Predicted (a) contact pressure at meniscotibial articulation area and (b) maximum tensile strain at lowermost layer of menisci in the reference case under 2000 N compression. Contact pressures and maximum strains are of nearly similar patterns at opposite top surface of the menisci at meniscofemoral articulation (not shown).

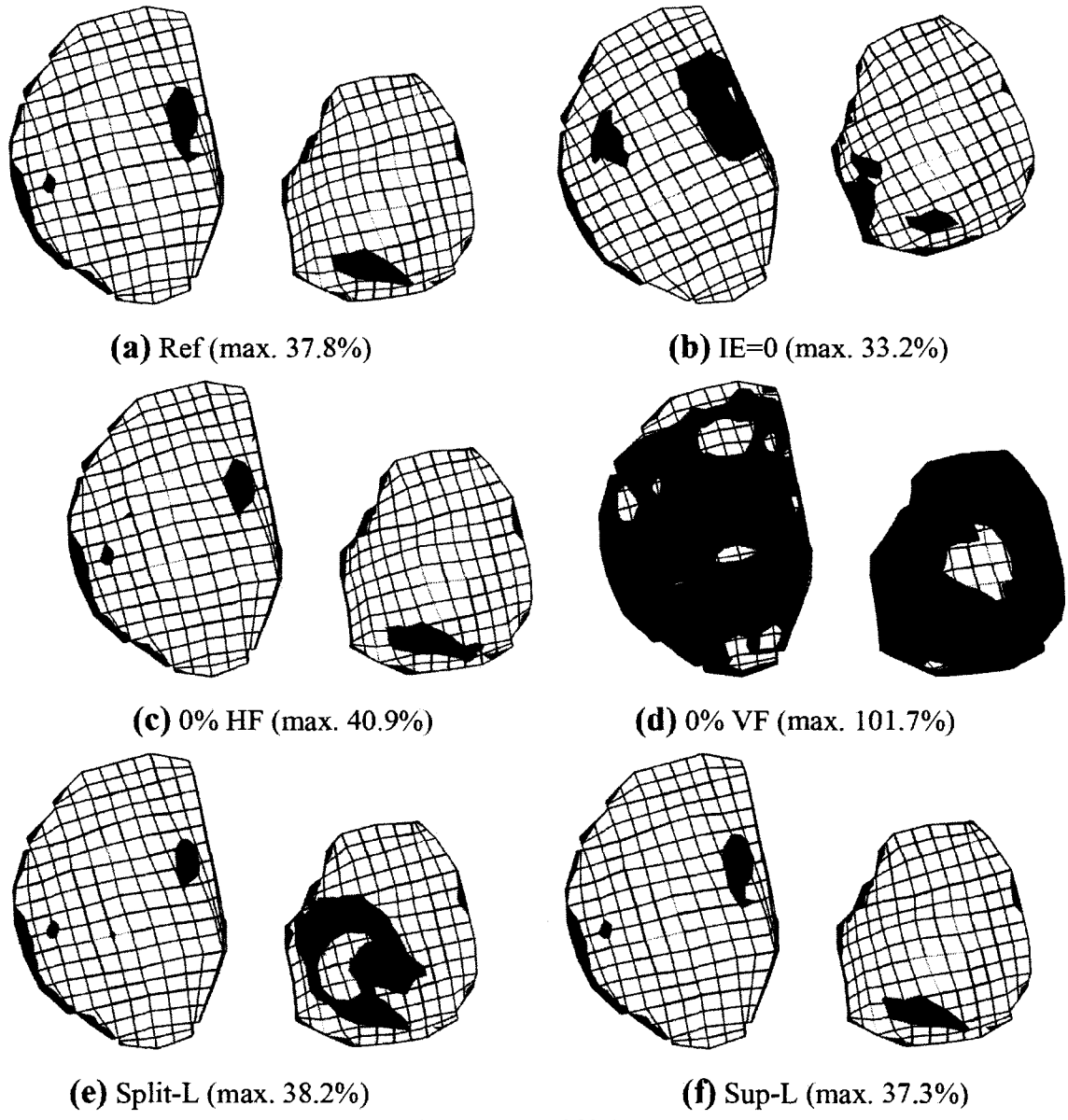

(a) Ref (max. 37.8%) **(b)** IE=0 (max. 33.2%)

(c) 0% HF (max. 40.9%) **(d)** 0% VF (max. 101.7%)

(e) Split-L (max. 38.2%) **(f)** Sup-L (max. 37.3%)

(grey area ≥10%)

Figure 4. 6 Maximum principal strain in solid matrix at the lowermost layer of tibial cartilage under 1800 N compression (grey areas indicate regions with strain ≥10%); (a) Intact reference case, (b) Coupled internal-external rotation is fixed, (c) Superficial horizontal fibrils are absent everywhere in femoral and tibial cartilage layers, (d) Deep vertical fibrils are absent everywhere in femoral and tibial cartilage layers, (e) Local lateral detachment of cartilage from its underlying bone (see text and Figure 4.7 for the detachment area), (f) Local removal of superficial fibrils network on the tibial lateral plateau (see text and Figure 4.7).

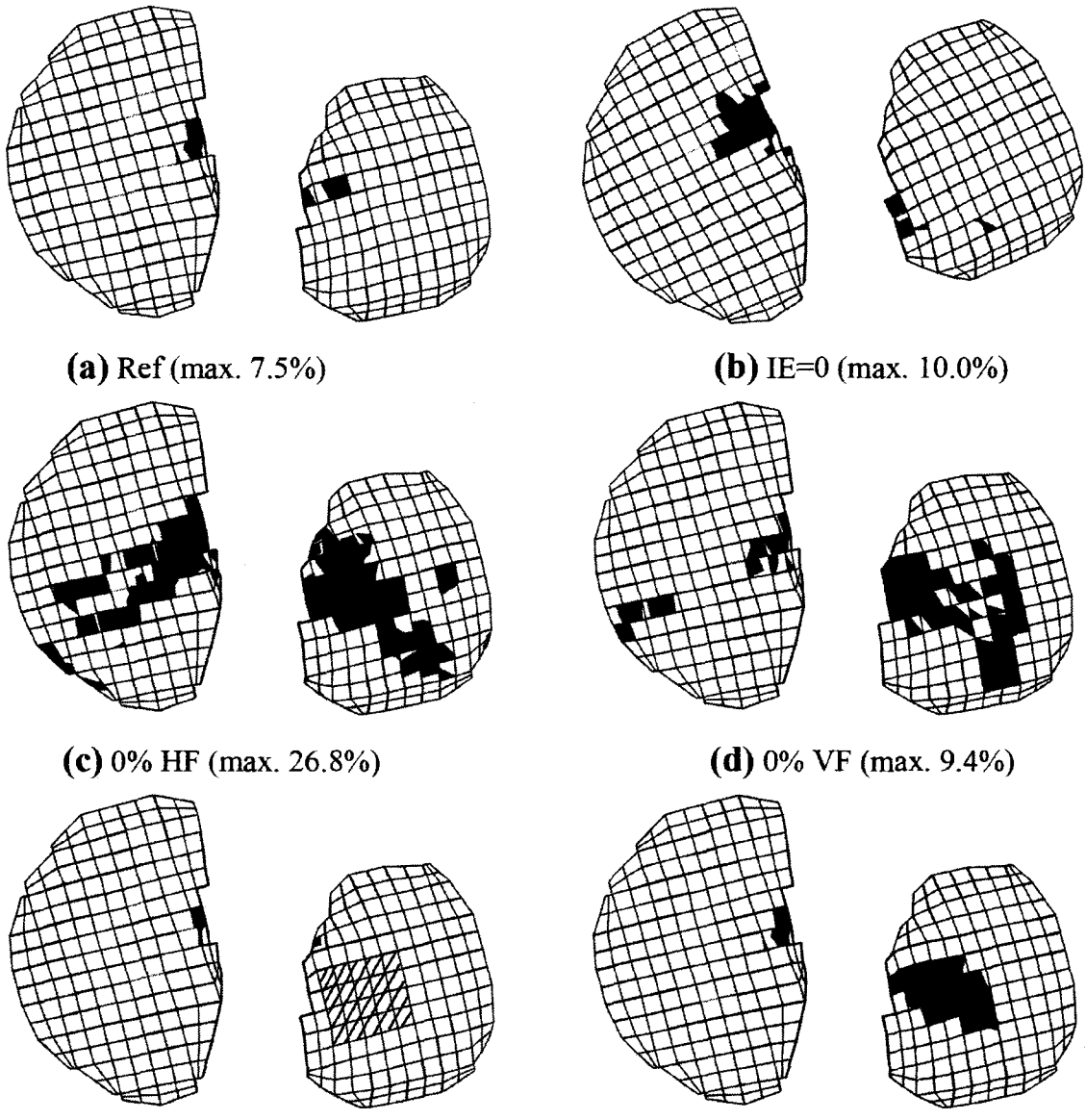

(a) Ref (max. 7.5%)

(b) IE=0 (max. 10.0%)

(c) 0% HF (max. 26.8%)

(d) 0% VF (max. 9.4%)

(e) Split-L (max. 8.4%)

(f) Sup-L (max. 12.3%)

(grey area ≥5%)

Figure 4. 7 Maximum principal strain in superficial tibial fibrils network under 1800 N compression (grey areas indicate regions with strain ≥5%); (a) Intact reference case, (b) Coupled internal-external rotation is fixed, (c) Superficial horizontal fibrils are absent everywhere in femoral and tibial cartilage layers, (d) Deep vertical fibrils are absent everywhere in femoral and tibial cartilage layers, (e) Local lateral detachment of cartilage from its underlying bone at hatched areas (see text), (f) Local removal of superficial fibrils network on the tibial lateral plateau at the same hatched areas in (e) (see text).

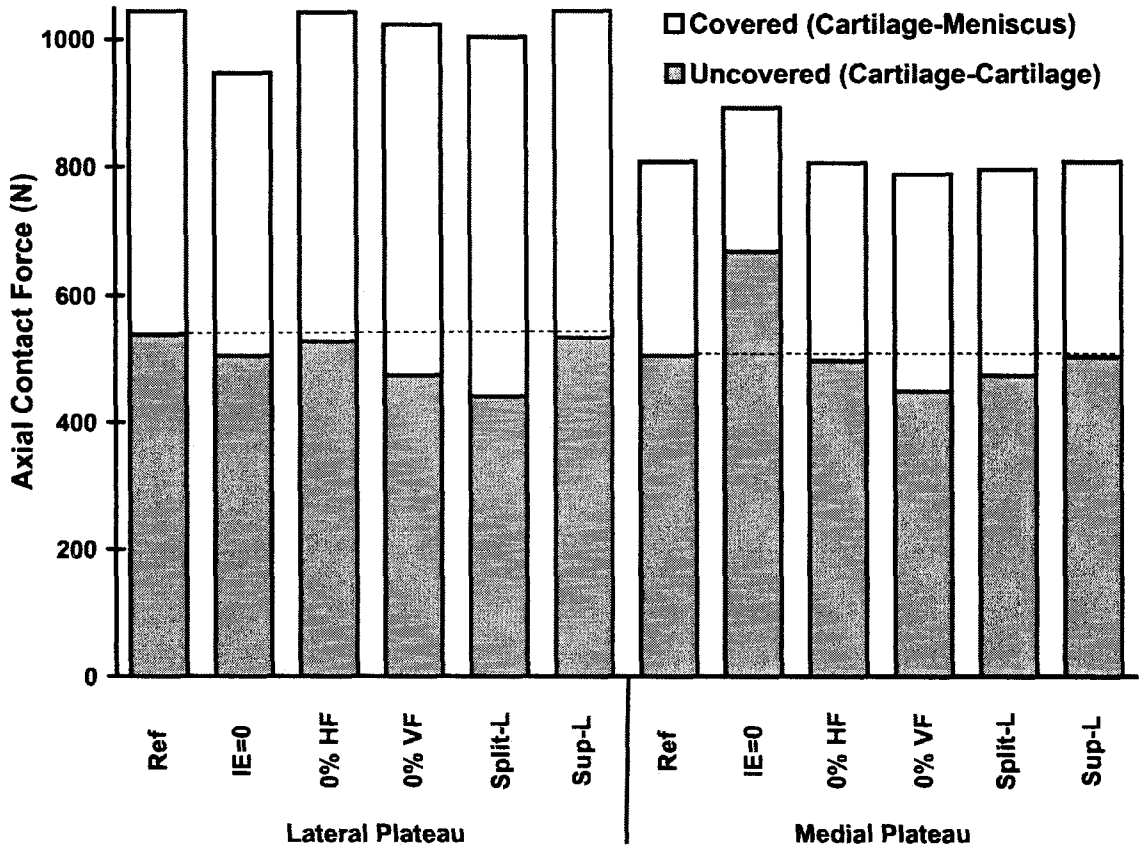

Figure 4. 8 Predicted total axial contact force at covered (menisci) and uncovered (cartilage to cartilage) areas for different cases under 1800 N compression force (see caption of Figure 4.2 for legends).

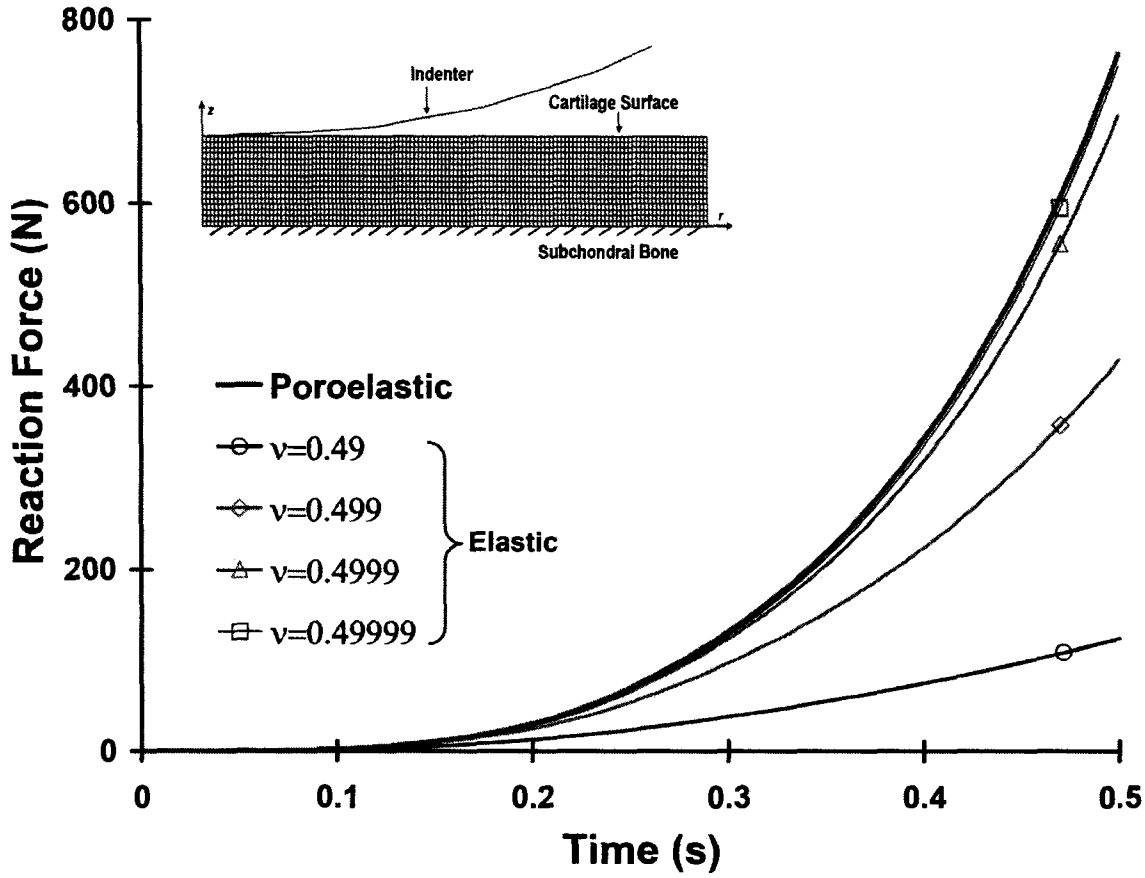

Figure 4. 9 Comparison of reaction forces in an axisymmetric model of cartilage (shown inlay) under 20% indentation at 0.5 s computed using either a poroelastic or nearly incompressible elastic material.

Table 4. 1 Comparison of predicted (reference case) and measured contact areas/pressures at different compression loads.

		Compressive Load (N) →						
Total Tibial Contact Area on Both Plateaus (mm^2)		***0***	***200***	***400***	***445***	***500***	***890***	***1000***
	Present Model Study	355	708	824	851	893	1034	1083
	Walker & Hajek 1972 †	330	-	-	-	-	-	-
	Fukubayashi & Kurosawa 1980	-	690±150	-	-	960±170	-	1150±200
	Kurosawa et al. 1980	-	750±150	-	-	1130±250	-	1300±300
	Brown & Shaw 1984	-	-	-	-	1125±180	-	1250±100
	Huang et al. 2003	-	-	235±135	-	-	-	-
	Ahmed & Burke 1983 †	-	-	-	1200	-	1650	-
	Krause et al. 1976 †	-	-	-	-	-	-	2084
		1200	***1335***	***1400***	***1500***	***1779***	***1960***	***2000***
	Present Model Study	1128	1161	1190	1214	1253	1280	1283
	Kurosawa et al. 1980	-	-	-	1410±320	-	-	-
	Brown & Shaw 1984	-	-	-	1340±100	-	-	1400±110
	Seedhom & Hargreaves 1979 †	-	-	1162	-	-	-	-
	Huang et al. 2003	295±105	-	-	-	-	-	-
	Maquet et al. 1975 †	-	-	-	-	-	1822	-
	Ahmed & Burke 1983	-	1800	-	-	2000	-	-
Peak Contact Pressure (MPa)				***890***	***1000***	***1500***	***2000***	
	Present Model Study			2.89	2.96	3.42	4.32	
	Walker & Erkman 1975			-	3.20	2.92	-	
	Fukubayashi & Kurosawa 1980			-	~3	~4	-	
	Ahmed & Burke 1983 †			2.75	-	-	-	
	Inaba et al. 1990			1.4	1.6	2.3	2.75	
Average Contact Pressure (MPa)		***200***	***400***	***500***	***1000***	***1200***	***1400***	***1500***
	Present Model Study	0.37	0.58	0.65	1.0	1.13	1.24	1.29
	Kurosawa et al. 1980	0.27±0.06	-	0.47±0.12	0.8±0.2	-	-	1.1±0.28
	Seedhom & Hargreaves 1979 †	-	-	-	-	-	1.2	-
	Huang et al. 2003	-	1.45±0.95	-	-	2.6±0.8	-	-
	Krause et al. 1976	-	-	-	0.48±0.08	-	-	-

† Mean of measured data

Chapter five

Article IV: Analysis of partial meniscectomy and ACL reconstruction in knee joint biomechanics under combined loading

R. Shirazi, A. Shirazi-Adl

Division of Applied Mechanics, Department of Mechanical Engineering
École Polytechnique, Montréal, Québec, Canada

Article submitted to
The American Journal of Sports Medicine
(November 2008)

Keywords: Knee Joint, Meniscectomy, Anterior Cruciate Ligament, Contact Pressure, Combined Loading

5.1 Abstract

A detailed novel model of the knee joint was developed to evaluate biomechanics of the tibiofemoral joint under 200 N drawer load with and without 1500 N compression. The model incorporated nonhomogeneous and anisotropic nature of cartilage and meniscus. The effects on joint response of unilateral partial meniscectomy, changes in ACL prestrain or material properties expected in reconstruction, concurrent partial meniscectomy and ACL perturbations and finally removal of deep vertical collagen fibrils in cartilage were investigated under both single and combined loads.

Compressive preload further increases ACL strains/forces in drawer loading. Partial meniscectomy and perturbations in ACL prestrain and material properties, alone or together, substantially alter the load transfer via covered and uncovered areas of cartilage as well as contact pressure distribution on cartilage. Partial meniscectomy completely unloads the cartilage area underneath the resected region which would otherwise articulate with the meniscus. Concurrent partial mensicectomy and slacker ACL further diminishes the load via affected meniscus with two distinct unloaded regions on the cartilage underneath it. Foregoing alterations are expected to further increase in presence of greater external forces, larger meniscal resections, complete ACL rupture and damages to cartilage fibril networks. Adequate considerations of the new mechanical environment of the joint are crucial for an improved assessment of the likelihood of success in various treatment attempts.

5.2 Introduction

Axial compressive and anterior-posterior shear forces, commonly occurring in activities such as walking, running, jumping and stairs ascent/descent, are due both directly to gravity, external and inertia loads and indirectly to activation of muscles crossing the knee joint. The drawer forces at higher magnitudes can cause excessive strains in joint ligaments such as the anterior cruciate ligament, ACL, which is known as a primary restraint to anterior translation of the tibia relative to the femur. Compression force has been reported to reduce total anterior-posterior laxity (Hsieh & Walker, 1976; G. Li et al., 1998; Markolf et al., 1981; Torzilli et al., 1994) and to protect the ACL (Markolf et al., 1990) or on the contrary to cause higher ACL strains (Fleming et al., 2001; G. Li et al., 1998; Torzilli et al., 1994).

Injuries or alterations to the ACL and menisci would influence overall joint response as well as mechanical role of remaining components with the likelihood to exacerbate the joint condition causing recurrent injuries and further damages. Existing ACL reconstruction techniques use different ligament pretension/prestrain levels and replacement materials such as bone-patellar-tendon-bone and hamstrings grafts with much stiffer material properties (Butler et al., 1986). The graft material/pretension have been recognized as primary variables that could influence the outcome of reconstruction attempts. Meniscal tears are also commonly observed along with ACL ruptures (Indelicato & Bittar, 1985) as the risk of meniscus failure increases in ACL deficient knees (Noyes et al., 1980). Due to the dramatic adverse effect of total meniscectomy on load distribution and development of joint osteoarthritis, partial meniscectomies are performed with the resection of the torn tissues. Concurrent ACL and meniscus ruptures are treated by ACL reconstruction and partial meniscectomy. Incidence of osteoarthritis in mid- and long-term outcome studies of ACL reconstruction (van der Hart et al., 2008) and partial meniscectomy (Rangger et al., 1995) has nevertheless persisted.

Although earlier axisymmetric model studies of articular cartilage specimens have accounted for the detailed fibril-reinforced structure of the tissue (Julkunen et al., 2008; L. P. Li et al., 1999; Shirazi & Shirazi-Adl, 2005), the knee joint model studies, however, have failed to incorporate the realistic composite nature of cartilage. This study aimed initially to incorporate the detailed nonhomogeneous fibrils network structure of the articular cartilage and menisci (Shirazi & Shirazi-Adl, 2005, 2008) into our existing model of the human knee joint (Mesfar & Shirazi-Adl, 2006) developing thus a novel model of the entire tibiofemoral joint. Such complex model appears as an appropriate computational tool to study biomechanics of the knee joint under physiological compression and drawer loads, acting alone or combined.

The effects of partial medial and lateral meniscectomies, alterations in ACL prestrain and material properties, combined ACL-reconstruction and lateral meniscectomy, and removal of deep vertical fibrils network in articular cartilage on the response of the entire tibiofemoral joint as compared to the reference intact case were subsequently investigated. To do so, the joint response in both intact and altered conditions under single as well as combined drawer and compression forces is investigated. Attention is focused on the effect of various loads and joint perturbations on the cartilage strains/stresses, contact loads and ACL forces. These studies should improve our understanding of likely short-term effects of foregoing ACL and mensical treatment modalities on joint biomechanics.

5.3 Method

5.3.1 Finite Element Model

Being highly nonlinear and anisotropic, articular cartilage and meniscus consist mainly of networks of collagen fibrils that embed water and a nonfibrillar matrix. The collagen fibrils structure, content, and arrangement vary not only between articular cartilage and meniscus but also in each tissue along the depth (Aspden & Hukins, 1981; Kaab et al., 1998). In cartilage, at the superficial zone, fibrils are horizontally oriented

parallel to the articular surface (Minns & Steven, 1977) whereas they become rather random in the transitional zone (Broom & Marra, 1986) and finally turn perpendicular in the deep zone to anchor the tissue firmly to the subchondral bone (Minns & Steven, 1977). In meniscus, while the collagen fibrils at exterior surfaces show no major preferred orientation, they are nevertheless circumferentially oriented in the bulk of the tissue (Aspden et al., 1985). In addition, radial tie fibres are present that increase the tissue tensile resistance (Skaggs et al., 1994).

An extensive refinement at articular cartilage and menisci regions of an existing validated 3-D model of the human knee joint (Mesfar & Shirazi-Adl, 2006) allowed for the incorporation of fibrils networks at different regions along with depth-dependent variation in cartilage properties (Fig. 5.1). The joint ligaments; i.e. anterior/posterior cruciate (ACL/PCL) and medial/lateral collateral (MCL/LCL) ligaments, were included with appropriate nonlinear material properties and initial pre-strains (Mesfar & Shirazi-Adl, 2006). Anterior and posterior horns of the lateral and medial menisci were represented by extension of each meniscus at both ends via two layers of brick and membrane elements as shown in Fig. 5.1.

The cartilage non-fibrillar matrix was modelled by incompressible isotropic hyperelastic solid with depth-dependent properties whereas fibrils networks were simulated either by membrane or continuum elements (Fig. 5.1). In superficial zones of femoral and tibial cartilage layers as well as bounding surfaces of menisci, the collagen fibrils were uniformly distributed in the plane of membrane elements (Fig. 5.1). The in-plane stresses in material principal axes were evaluated using the uniaxial nonlinear stress-strain curves for collagen fibrils; type I in menisci (Haut & Little, 1972) and type II in cartilage with the latter assumed as 70% of the former. Equal principal strains would generate an isotropic material while negative principal strains result in zero principal stresses (i.e., tension only membranes). In the transitional zone with random fibrils (i.e., no dominant orientations), continuum brick elements represent collagen

fibrils (Fig. 5.1). In the deep zone, however, vertical fibrils were modelled with vertical membrane elements similar to horizontal superficial ones except in offering resistance only in local fibrils directions (Fig. 5.1).

In the bulk region of each meniscus in between peripheral surfaces, collagen fibrils that are dominant in the circumferential direction were represented by membrane elements with local material principal axes defined in orthogonal circumferential and radial directions. The formulation of fibrils networks was introduced in the ABAQUS finite element commercial program (Simulia Inc., Providence, RI).

5.3.2 Material Properties

Thickness of membrane elements in different regions of cartilage and menisci was computed based on the fibrils volume fraction in each zone. In cartilage, the equivalent collagen fibrils content at the superficial zone was estimated based on reported tissue properties in tension (Kempson et al., 1973) and type II collagen stress-strain curve (Shirazi & Shirazi-Adl, 2005). A total volume fraction of 15% was estimated in the superficial zone in agreement with the mean value of 14% reported for its wet weight (Hollander et al., 1994). Volume fractions of 18% in the transitional zone and 21% in the deep zone were subsequently taken in accordance with the reported increases in collagen content along the depth (Bi et al., 2006; Julkunen et al., 2008). Thicknesses of the superficial, transitional and deep zones were, respectively, 15, 22.5, and 62.5% of the tissue thickness (Bi et al., 2006).

Similarly, in menisci, the equivalent collagen fibrils content was estimated based on the reported tissue tensile properties in mid-bulk as well as peripheral sides (Proctor et al., 1989). The equivalent content of radial tie fibres was also estimated (Skaggs et al., 1994). Overall, 14% in the circumferential direction and 2.5% in the radial direction of bulk region along with 12% in the outer surfaces were taken in agreement with reported overall ~18% collagen content (Peters & Smillie, 1971).

To study short-term (transient) biphasic response of the joint, en equivalent elastic response was sought by using equilibrium modulus of the tissue (Ateshian et al., 2007) and Poisson's ratio of 0.5. The drained (equilibrium) modulus of solid matrix in articular cartilage was considered depth-dependent increasing from 0.3 to 0.5, 0.8 and 1.2 MPa from articular surface to lowermost layer at the subchondral bone, respectively (Schinagl et al., 1997). The modulus for incompressible matrix of menisci was initially chosen to be 0.35 MPa; (Joshi et al., 1995) due to slow convergence rates, however, this incompressible behaviour was replaced by an equivalent compressible one with a Young's modulus of 12 MPa and Poisson's ratio of 0.45 as used in our earlier knee joint model studies. These material properties resulted in almost the same global displacements and stresses/strains in different components in both models with compressible or incompressible menisci under compression forces up to 800 N as the maximum force reached in the latter case.

5.3.3 Loading and Boundary Conditions

The knee joint passive response was studied at full extension under a femoral posterior drawer force up to 200 N acting alone or in presence of a 1500 N compression preload. For an unconstrained response while avoiding the adverse effect of load positioning on joint kinematics (Rudy et al., 2000), the femur was left free in three translations while fixed in all three rotations. A posterior drawer force of 200 N was applied onto the femur with and without a 1500 N compression preload. For the tibia, on the other hand, internal-external and varus-valgus rotations were left free while constraining flexion-extension and three translations. An equivalent reversed unconstrained set of boundary conditions was also examined, i.e. free rotations on the femur while loading the tibia with free translations, a different boundary condition that yielded almost the same results. Prior to the application of loads, the joint equilibrium at full extension was initially sought under pre-strains in ligaments.

5.3.4 Parametric Studies

To examine the likely effects on response of changes in material properties/prestrain in the ACL, ACL material properties was replaced by that of patellar tendon (Butler et al., 1986) or prestrains in both anteromedial and posterolateral bundles of the ACL were changed by +4% or -4% in strains, i.e. initial values of 1% and 8% respectively altered to either 5% and 12% (tauter case) or -3% and 4% (slacker case). Moreover, to evaluate the role of partial meniscectomy on joint response, an internal part at posterior-central regions of either lateral or medial meniscus was resected (see Fig. 5.1). Concurrent ACL perturbations and lateral meniscectomy was also studied. Finally, to examine the mechanical role of deep cartilage vertical fibrils, analyses were carried out in which volume fraction content of these fibrils networks in both femoral and tibial cartilage layers was diminished from 21% in the reference case to nil.

5.4 Results

In the reference intact joint, the femoral primary translation demonstrated a nonlinear stiffening behavior under femoral posterior drawer alone that turned linear and much stiffer in presence of compression (Fig. 5.2). These femoral translations are relative to initial values of 4.5mm in posterior direction under 1500 N compression and 3.6mm in anterior direction under no load with ligament prestrains. In the reference intact case, large ACL force was computed under femoral posterior drawer that further increased by 30% with compression preload (Fig. 5.3). The posterolateral bundle was solely loaded with the anteromedial bundle remaining slack.

In the intact case, mean contact pressures under drawer alone were much smaller compared to those under compression especially on the lateral compartment. In combined loading, addition of drawer to compression preload resulted in an increase of ~10% in mean pressure on all contact surfaces whereas contact areas remained nearly unchanged. Contact areas were much higher under pure compression when compared to drawer alone.

Increasing ACL prestrain by 4% strain or replacing it with a stiffer material increased ACL force in both single and combined loads (Fig. 5.3). In contrast, decreasing ACL prestrain by 4% strain or removing deep vertical fibrils in cartilage layers diminished ACL force drastically by 31% and 38% under combined load, respectively. These latter drops were much less under drawer alone especially in the case with no vertical fibrils; role of vertical fibrils was more pronounced in presence of axial compression. Lateral or medial meniscectomy influenced only negligibly (<3%) ACL force under drawer alone or combined with compression (Fig. 5.3).

Partial meniscectomy altered the load distribution pattern on the tibial plateaus and femoral condyles by shifting the applied compression away from the meniscus (covered region) onto the cartilage at uncovered regions, in particular on the side of resection (Figs. 5.4 and 5.5). After meniscectomy (Fig. 5.5 b,c) and contrary to the intact case (Fig. 5.5a), no contact was detected at areas under meniscal resection while the peak contact stress increased by ~5%. Stiffer material properties or greater initial strain in the ACL increased the total load and the portion transferred via the uncovered cartilage areas (Fig. 5.4). On the contrary, slacker ACL decreased contact loads on both covered and uncovered areas of the lateral plateau (Fig. 5.4) and unloaded an area at anterior-central region of lateral meniscus (Fig. 5.6d). Absence of vertical fibrils diminished the total load by decreasing the uncovered contribution.

Changes in ACL prestrain further altered the state of stress distribution after meniscectomy. A slacker ACL in the joint with partial lateral mensicectomy decreased the load on both covered and uncovered areas of the lateral plateau (Fig. 5.4) and caused a second unloaded area below lateral meniscus on the anterior-central region away from the resected area (Fig. 5.6d). On the contrary, a tenser ACL increased the load transferred via the uncovered areas at cartilage-cartilage contact on both plateaus (Fig. 5.4).

5.5 Discussion

A validated model of the knee joint (Mesfar & Shirazi-Adl, 2006) was substantially refined to allow for the incorporation of detailed collagen fibrils networks in articular cartilage and menisci as well as the depth-dependent properties in cartilage. This novel model of the joint was then employed as an appropriate computational tool to study biomechanics of the tibiofemoral joint under drawer force alone or combined with compression. Cases with changes in ACL prestrain or its material properties, with partial unilateral (lateral or medial) meniscectomy, with concurrent alterations in ACL prestrain plus partial lateral meniscectomy and finally with deep vertical collagen fibrils removed were investigated under single and combined loads. In accordance with recent investigations (Ateshian et al., 2007), the transient response of cartilage and meniscus under higher strain rates in physiological activities can accurately be captured either by a biphasic analysis or equivalently by an incompressible elastic analysis using equilibrium modulus. We have also confirmed this equivalency as a function of the Poisson's ratio using our earlier non-homogeneous axisymmetric model of cartilage (Shirazi et al., 2008).

The mean anterior tibial laxities in between 2.8 mm to 6.7 mm are reported under 100 N anterior tibial force at full extension (Markolf et al., 1981; Rudy et al., 2000) that compare with our posterior femoral laxity of 3.6 mm under 100 N posterior femoral force. Current predictions under larger drawer forces are also in agreement with measurements (Markolf et al., 1981). The posterior translation of the femur relative to the tibia under compression is due to the posterior slope of the tibia (Torzilli et al., 1994) and agrees with observation of anterior tibial displacement relative to the femur (Markolf et al., 1981; Torzilli et al., 1994). The relative magnitude and variation of femoral primary translation under drawer force with compression (Fig. 5.2) are also in agreement with measurements (Hsieh & Walker, 1976; G. Li et al., 1998; Markolf et al., 1981; Torzilli et al., 1994). Overall, predicted results on contact forces and areas under

axial compression are also in general agreement with measurements (Kurosawa et al., 1980).

The computed force of 170 N in ACL is in good agreement with measured values of 75-162 N reported under ~100 N drawer at full extension (Markolf et al., 1995; Takai et al., 1993). Compression preload further increases ACL force under drawer (Fig. 5.3) from ~1.6 times, in agreement with 150% in measurements (Markolf et al., 1995), to more than two-fold that of applied drawer force. Prediction of the marked increase in ACL force in presence of compression preload corroborates earlier findings (Fleming et al., 2001; G. Li et al., 1998; Torzilli et al., 1994) but contradicts others suggesting the notion that compression preload in drawer protects the ACL from damage (Markolf et al., 1990). Our predictions therefore advocate rehabilitation and training strategies that avoid large axial compression preloads at near full extension on the joint subject to drawer forces.

Perturbations in prestrains/material properties of the ACL expected following reconstruction influences the redistribution of contact forces on covered and uncovered areas (Fig. 5.4). Replacement of a ruptured ACL by a patellar tendon graft with higher stiffness appears to have similar mechanical effect on the joint response as an increase of ~4% in ACL prestrain, a finding in agreement with our earlier studies of the knee joint under quadriceps activation (Mesfar & Shirazi-Adl, 2006). On the contrary, a decrease of 4% in ACL prestrain appears to somewhat simulate a case with partial ACL damage. In this case with slacker ACL, the contact pressure pattern on the lateral plateau (Fig. 5.6d) demonstrates an unloaded region of cartilage underneath meniscus. This unloading phenomenon would likely intensify had a complete ACL rupture been simulated in this study. Such alterations in joint load redistribution (i.e., contact forces and pressure) following ACL reconstruction or ACL rupture could hence contribute to the development of OA (van der Hart et al., 2008). It should be noted that the limited cases studied in the current work in which ACL initial strain (or stress) and material properties

were each altered from those in the reference intact case cannot be considered as a comprehensive simulation of all reconstruction attempts. Various reconstruction techniques, graft insertion sites as well as initial strains/forces set at different joint angles with changes expected therein with time after operation influence ligament forces and joint response.

While under loads considered in this study partial meniscectomy does not noticeably influence ACL forces, it does however substantially alter contact stress distribution on the articular cartilage. Partial meniscectomy shifts the transfer of applied compression away from the resected meniscus onto the nearby cartilage while completely unloading previously covered femoral/tibial cartilage areas that otherwise would articulate with the meniscus (Fig. 5.5). In addition, the peak pressure on nearby uncovered cartilage increases by ~5%. When partial lateral meniscectomy is combined with a 4% increase in ACL prestrain (a tenser ACL), contact load/pressure further increases on the nearby cartilage at uncovered areas. A concurrent 4% decrease in ACL prestrain (slacker ACL), however, diminishes the load via lateral meniscus to its minimum among all cases considered in this study (Fig. 5.4) and creates an additional unloaded area on the cartilage covered by the lateral meniscus (Fig. 5.6f). Absence of the ACL in ACL-deficient joints, not simulated in this work, would further intensify the above alterations in pattern of stress distribution away from that expected in intact reference case. Such changes in contact stresses on the joint cartilage that are expected to further accentuate under larger loads than those considered in this work adversely affect the cartilage function and health likely leading in long-term to OA (Rangger et al., 1995; van der Hart et al., 2008).

Deep cartilage vertical fibrils were found in our earlier studies (Shirazi & Shirazi-Adl, 2008; Shirazi et al., 2008) to protect cartilage by substantially increasing tissue stiffness while diminishing excessive deformations. In the present study, absence of this fibril network diminished the total contact load by mainly unloading the

uncovered cartilage at the lateral plateau. The peak contact pressure at uncovered area of lateral plateau dramatically decreased from ~4 MPa in the intact case to ~3 MPa as these fibrils disappeared. Damages to this network, either locally or throughout the joint, increases maximum strains but decreases peak contact pressures thereby influencing cartilage mechanical environment.

In conclusion, both partial meniscectomies and perturbations in ACL material properties/ prestrains alter load redistribution and contact stresses on cartilage layers especially on the lateral plateau. Partial meniscectomy concurrent with ACL damage could further alter the contact pressures by substantially reducing load via resected meniscus and unloading areas of covered cartilage that would otherwise be in contact with meniscus. Foregoing alterations further intensify in the event of greater external forces, larger meniscal resections, ACL deficiency and damages to cartilage fibril networks. Adequate considerations of the new mechanical environment of the joint are crucial for an improved assessment of the likelihood of success in treatment attempts to avert further joint disorders.

5.6 Acknowledgement

This work is supported by grants from the Canadian Institute of Health Research (CIHR) and the National Sciences and Engineering Research Council of Canada (NSERC).

5.7 References

Aspden, R. M., and Hukins, D. W. (1981). Collagen organization in articular cartilage, determined by X-ray diffraction, and its relationship to tissue function. *Proc R Soc Lond B Biol Sci, 212*(1188), 299-304.

Aspden, R. M., Yarker, Y. E., and Hukins, D. W. (1985). Collagen orientations in the meniscus of the knee joint. *J Anat, 140 (Pt 3)*, 371-380.

Ateshian, G. A., Ellis, B. J., and Weiss, J. A. (2007). Equivalence between short-time biphasic and incompressible elastic material responses. *J Biomech Eng, 129*(3), 405-412.

Bi, X., Yang, X., Bostrom, M. P., and Camacho, N. P. (2006). Fourier transform infrared imaging spectroscopy investigations in the pathogenesis and repair of cartilage. *Biochim Biophys Acta, 1758*(7), 934-941.

Broom, N. D., and Marra, D. L. (1986). Ultrastructural evidence for fibril-to-fibril associations in articular cartilage and their functional implication. *J Anat, 146*, 185-200.

Butler, D. L., Kay, M. D., and Stouffer, D. C. (1986). Comparison of material properties in fascicle-bone units from human patellar tendon and knee ligaments. *J Biomech, 19*(6), 425-432.

Fleming, B. C., Renstrom, P. A., Beynnon, B. D., Engstrom, B., Peura, G. D., Badger, G. J., and Johnson, R. J. (2001). The effect of weightbearing and external loading on anterior cruciate ligament strain. *J Biomech, 34*(2), 163-170.

Haut, R. C., and Little, R. W. (1972). A constitutive equation for collagen fibers. *J Biomech, 5*(5), 423-430.

Hollander, A. P., Heathfield, T. F., Webber, C., Iwata, Y., Bourne, R., Rorabeck, C., and Poole, A. R. (1994). Increased damage to type II collagen in osteoarthritic articular cartilage detected by a new immunoassay. *J Clin Invest, 93*(4), 1722-1732.

Hsieh, H. H., and Walker, P. S. (1976). Stabilizing mechanisms of the loaded and unloaded knee joint. *J Bone Joint Surg Am, 58*(1), 87-93.

Indelicato, P. A., and Bittar, E. S. (1985). A perspective of lesions associated with ACL insufficiency of the knee. A review of 100 cases. *Clin Orthop Relat Res*(198), 77-80.

Joshi, M. D., Suh, J. K., Marui, T., and Woo, S. L. (1995). Interspecies variation of compressive biomechanical properties of the meniscus. *J Biomed Mater Res, 29*(7), 823-828.

Julkunen, P., Wilson, W., Jurvelin, J. S., Rieppo, J., Qu, C. J., Lammi, M. J., and Korhonen, R. K. (2008). Stress-relaxation of human patellar articular cartilage in unconfined compression: Prediction of mechanical response by tissue composition and structure. *J Biomech, 41*(9), 1978-1986.

Kaab, M. J., Gwynn, I. A., and Notzli, H. P. (1998). Collagen fibre arrangement in the tibial plateau articular cartilage of man and other mammalian species. *J Anat, 193 (Pt 1)*, 23-34.

Kempson, G. E., Muir, H., Pollard, C., and Tuke, M. (1973). The tensile properties of the cartilage of human femoral condyles related to the content of collagen and glycosaminoglycans. *Biochim Biophys Acta, 297*(2), 456-472.

Kurosawa, H., Fukubayashi, T., and Nakajima, H. (1980). Load-bearing mode of the knee joint: physical behavior of the knee joint with or without menisci. *Clin Orthop Relat Res*(149), 283-290.

Li, G., Rudy, T. W., Allen, C., Sakane, M., and Woo, S. L. (1998). Effect of combined axial compressive and anterior tibial loads on in situ forces in the anterior cruciate ligament: a porcine study. *J Orthop Res, 16*(1), 122-127.

Li, L. P., Soulhat, J., Buschmann, M. D., and Shirazi-Adl, A. (1999). Nonlinear analysis of cartilage in unconfined ramp compression using a fibril reinforced poroelastic model. *Clin Biomech, 14*(9), 673-682.

Markolf, K. L., Bargar, W. L., Shoemaker, S. C., and Amstutz, H. C. (1981). The role of joint load in knee stability. *J Bone Joint Surg Am, 63*(4), 570-585.

Markolf, K. L., Burchfield, D. M., Shapiro, M. M., Shepard, M. F., Finerman, G. A., and Slauterbeck, J. L. (1995). Combined knee loading states that generate high anterior cruciate ligament forces. *J Orthop Res, 13*(6), 930-935.

Markolf, K. L., Gorek, J. F., Kabo, J. M., and Shapiro, M. S. (1990). Direct measurement of resultant forces in the anterior cruciate ligament. An in vitro study performed with a new experimental technique. *J Bone Joint Surg Am, 72*(4), 557-567.

Mesfar, W., and Shirazi-Adl, A. (2006). Biomechanics of changes in ACL and PCL material properties or prestrains in flexion under muscle force-implications in ligament reconstruction. *Comput Methods Biomech Biomed Engin, 9*(4), 201-209.

Minns, R. J., and Steven, F. S. (1977). The collagen fibril organization in human articular cartilage. *J Anat, 123*(Pt 2), 437-457.

Noyes, F. R., Bassett, R. W., Grood, E. S., and Butler, D. L. (1980). Arthroscopy in acute traumatic hemarthrosis of the knee. Incidence of anterior cruciate tears and other injuries. *J Bone Joint Surg Am, 62*(5), 687-695.

Peters, T. J., and Smillie, I. S. (1971). Studies on chemical composition of menisci from the human knee-joint. *Proc R Soc Med, 64*(3), 261-262.

Proctor, C. S., Schmidt, M. B., Whipple, R. R., Kelly, M. A., and Mow, V. C. (1989). Material properties of the normal medial bovine meniscus. *J Orthop Res, 7*(6), 771-782.

Rangger, C., Klestil, T., Gloetzer, W., Kemmler, G., and Benedetto, K. P. (1995). Osteoarthritis after arthroscopic partial meniscectomy. *Am J Sports Med, 23*(2), 240-244.

Rudy, T. W., Sakane, M., Debski, R. E., and Woo, S. L. (2000). The effect of the point of application of anterior tibial loads on human knee kinematics. *J Biomech, 33*(9), 1147-1152.

Schinagl, R. M., Gurskis, D., Chen, A. C., and Sah, R. L. (1997). Depth-dependent confined compression modulus of full-thickness bovine articular cartilage. *J Orthop Res, 15*(4), 499-506.

Shirazi, R., and Shirazi-Adl, A. (2005). Analysis of articular cartilage as a composite using nonlinear membrane elements for collagen fibrils. *Med Eng Phys, 27*(10), 827-835.

Shirazi, R., and Shirazi-Adl, A. (2008). Deep vertical collagen fibrils play a significant role in mechanics of articular cartilage. *J Orthop Res, 26*(5), 608-615.

Shirazi, R., Shirazi-Adl, A., and Hurtig, M. (2008). Role of cartilage collagen fibrils networks in knee joint biomechanics under compression. *Accepted for Publication in J Biomech.*

Skaggs, D. L., Warden, W. H., and Mow, V. C. (1994). Radial tie fibers influence the tensile properties of the bovine medial meniscus. *J Orthop Res, 12*(2), 176-185.

Takai, S., Woo, S. L., Livesay, G. A., Adams, D. J., and Fu, F. H. (1993). Determination of the in situ loads on the human anterior cruciate ligament. *J Orthop Res, 11*(5), 686-695.

Torzilli, P. A., Deng, X., and Warren, R. F. (1994). The effect of joint-compressive load and quadriceps muscle force on knee motion in the intact and anterior cruciate ligament-sectioned knee. *Am J Sports Med, 22*(1), 105-112.

van der Hart, C. P., van den Bekerom, M. P., and Patt, T. W. (2008). The occurrence of osteoarthritis at a minimum of ten years after reconstruction of the anterior cruciate ligament. *J Orthop Surg, 3*, 24.

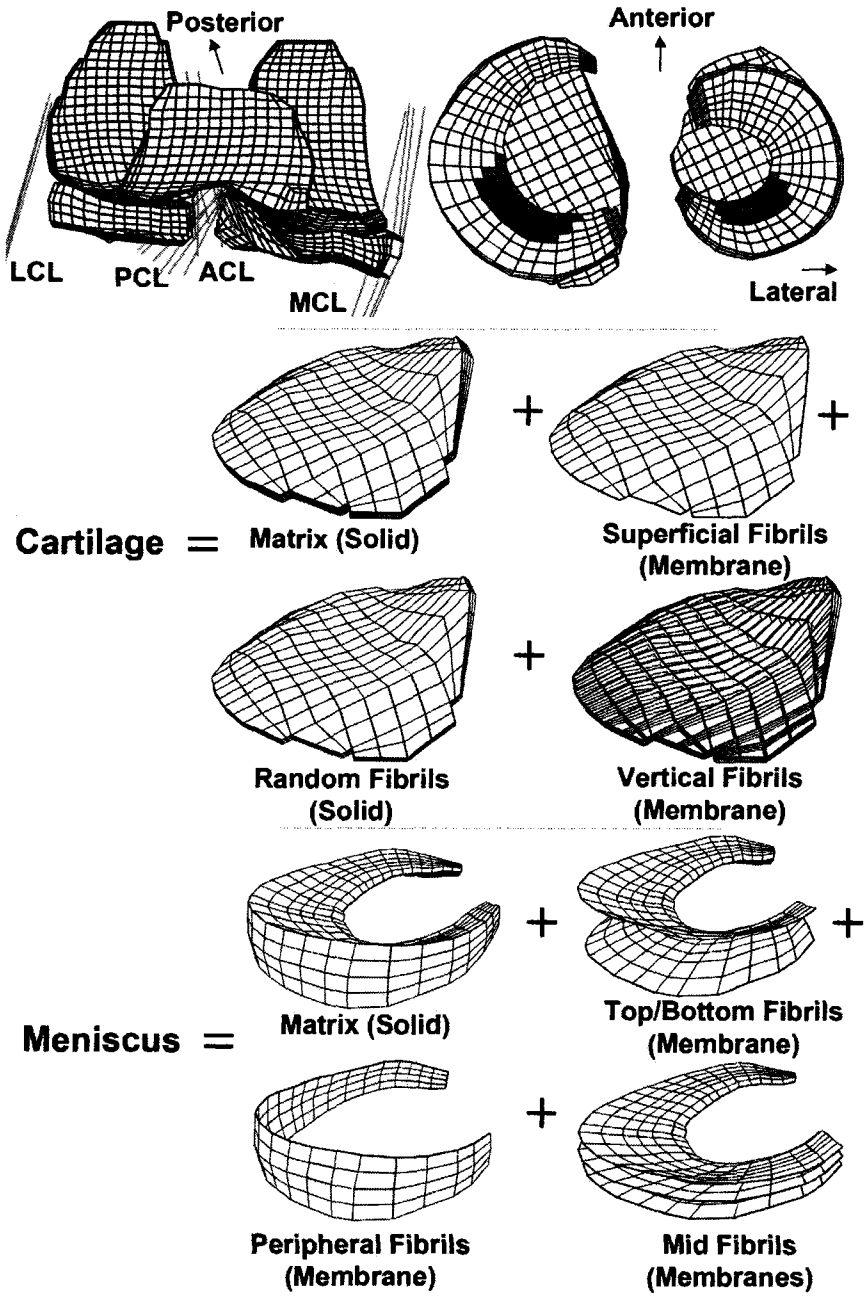

Figure 5. 1 Finite element mesh; Top left: anterior view of the knee joint with tibial and femoral cartilage layers, menisci and major ligaments. Top right: top view of menisci (shaded areas in red are removed one at a time to simulate either lateral or medial meniscectomy, horns are shaded in blue) and tibial articular cartilage. Middle and bottom: cartilage and meniscus showing distinct elements representing solid matrix along with collagen fibrils networks at different zones. Other cartilage layers and meniscus not shown here have similar structures. Random fibrils in cartilage are distributed on the two upper layers of cartilage.

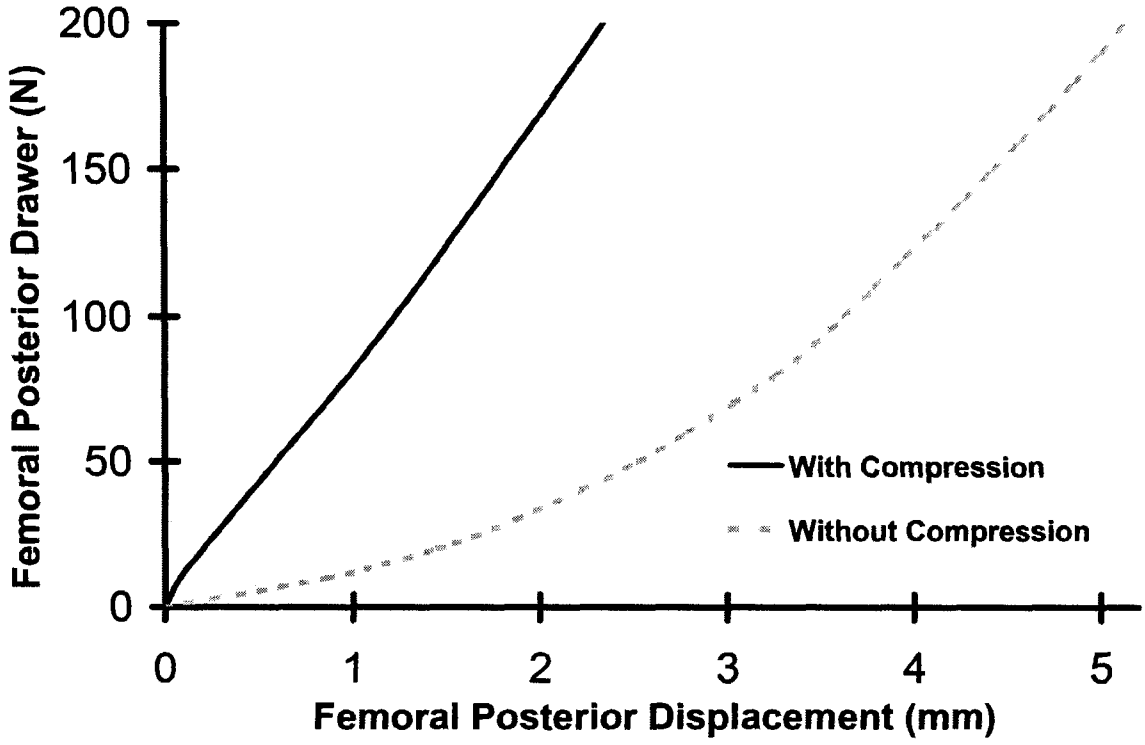

Figure 5. 2 Femoral posterior displacement relative to the tibia under femoral posterior drawer with and without a 1500 N preload compression. For the case of drawer with compression preload, the reference position is taken from the joint position after application of compression.

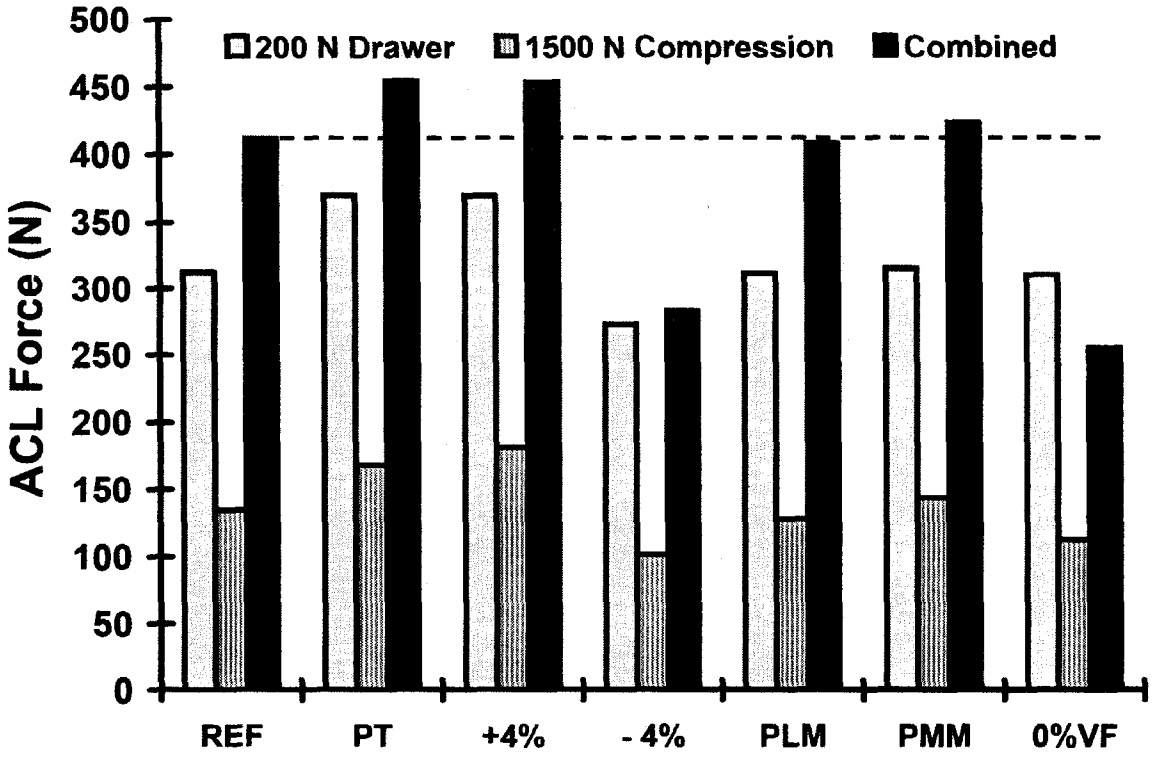

Figure 5. 3 Total ACL force under a femoral posterior drawer of 200 N and a compression of 1500 N, acting alone or combined. REF: reference intact case; PT: patellar tendon material properties are used for the ACL; +4%: ACL prestrain is increased by 4% strain in each bundle; -4%: ACL prestrain is decreased by 4% strain in each bundle; PLM: partial lateral menisectomy (see Figure 5.1); PMM: partial medial menisectomy (see Figure 5.1); 0%VF: vertical fibrils are absent everywhere in femoral and tibial cartilage.

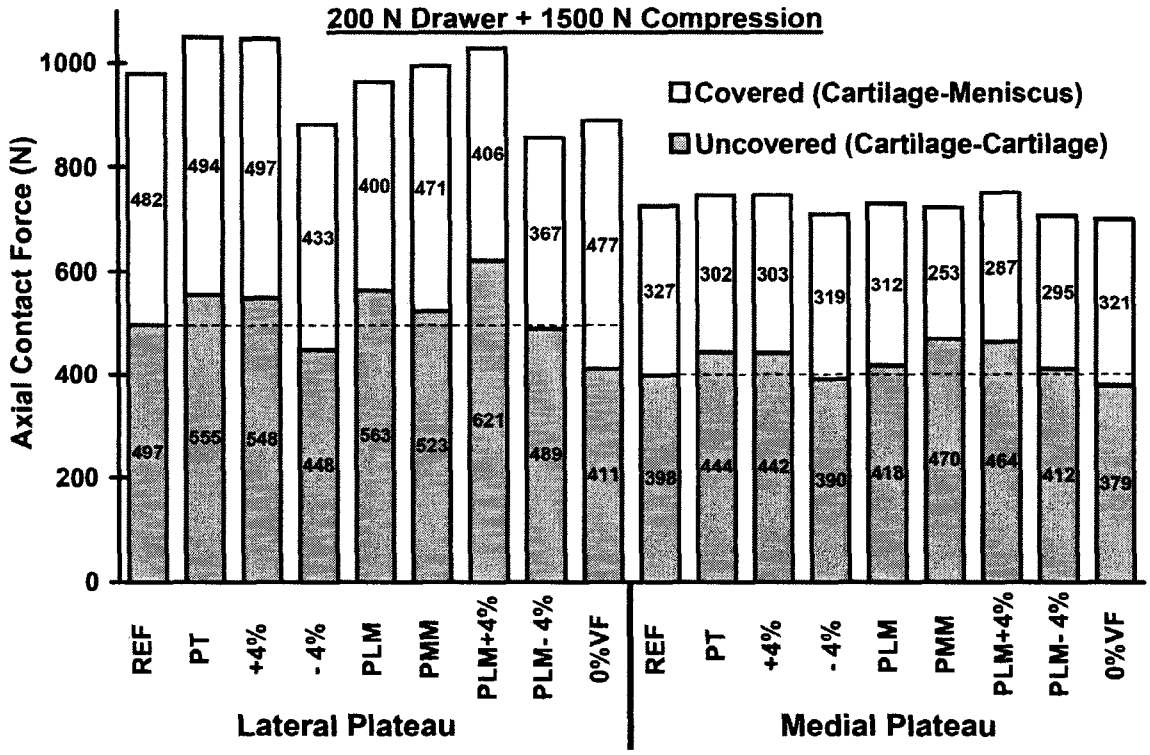

Figure 5. 4 Predicted total axial contact force transferred via covered (meniscotibial) and uncovered (tibiofemoral) areas for different cases under 200 N drawer with 1500 N compression preload. REF: reference intact case; PT: patellar tendon material properties are used for the ACL; +4%: ACL prestrain is increased by 4% strain in each bundle (tenser case); -4%: ACL prestrain is decreased by 4% strain in each bundle (slacker case); PLM: partial lateral menisectomy (see Figure 5.1); PMM: partial medial menisectomy (see Figure 5.1); PLM+4%: partial lateral meniscectomy with a 4% strain increase in ACL prestrain. PLM-4%: partial lateral meniscectomy with a 4% strain decrease in ACL prestrain; 0%VF: vertical fibrils are absent everywhere in femoral and tibial cartilage.

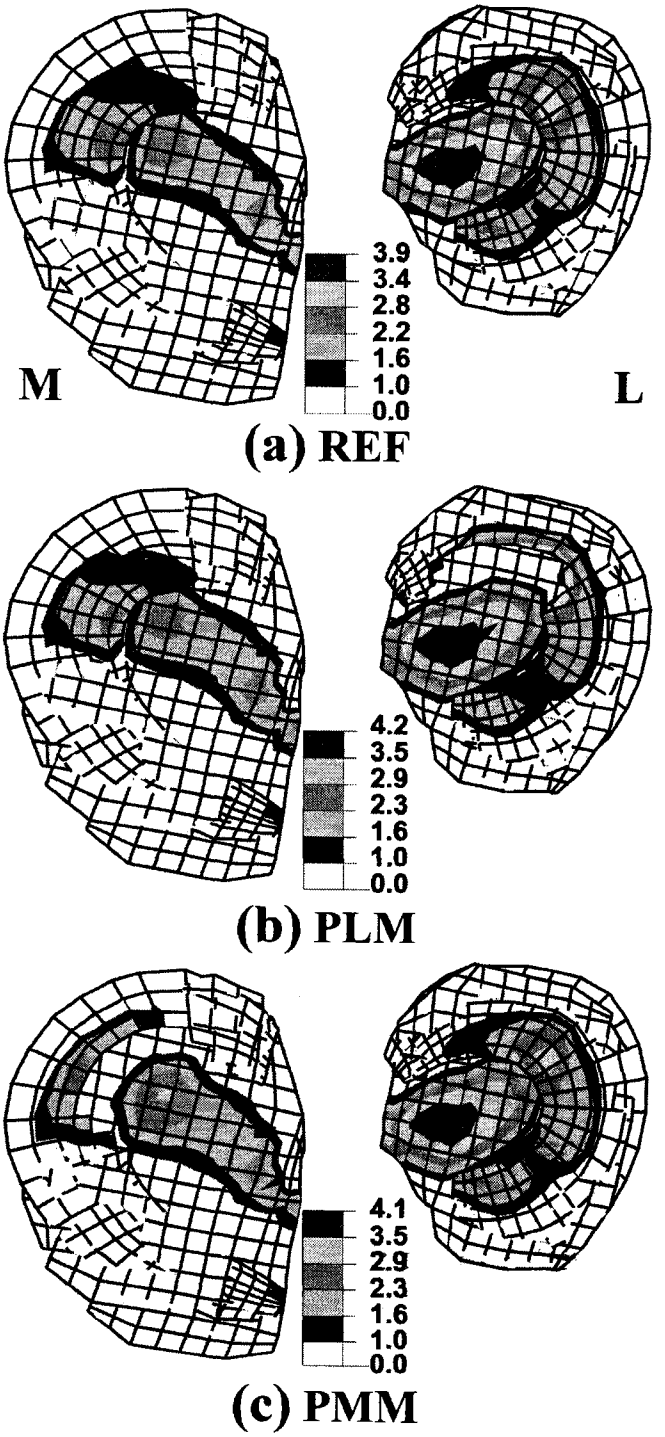

Figure 5. 5 Contact stress distribution on tibial plateaus under 200 N drawer and 1500 N compression preload (medial plateau on the left). (a) REF: reference intact; (b) PLM: partially lateral meniscectomy; (c) PMM: partially medial meniscectomy. Overlying meniscus surface is also shown.

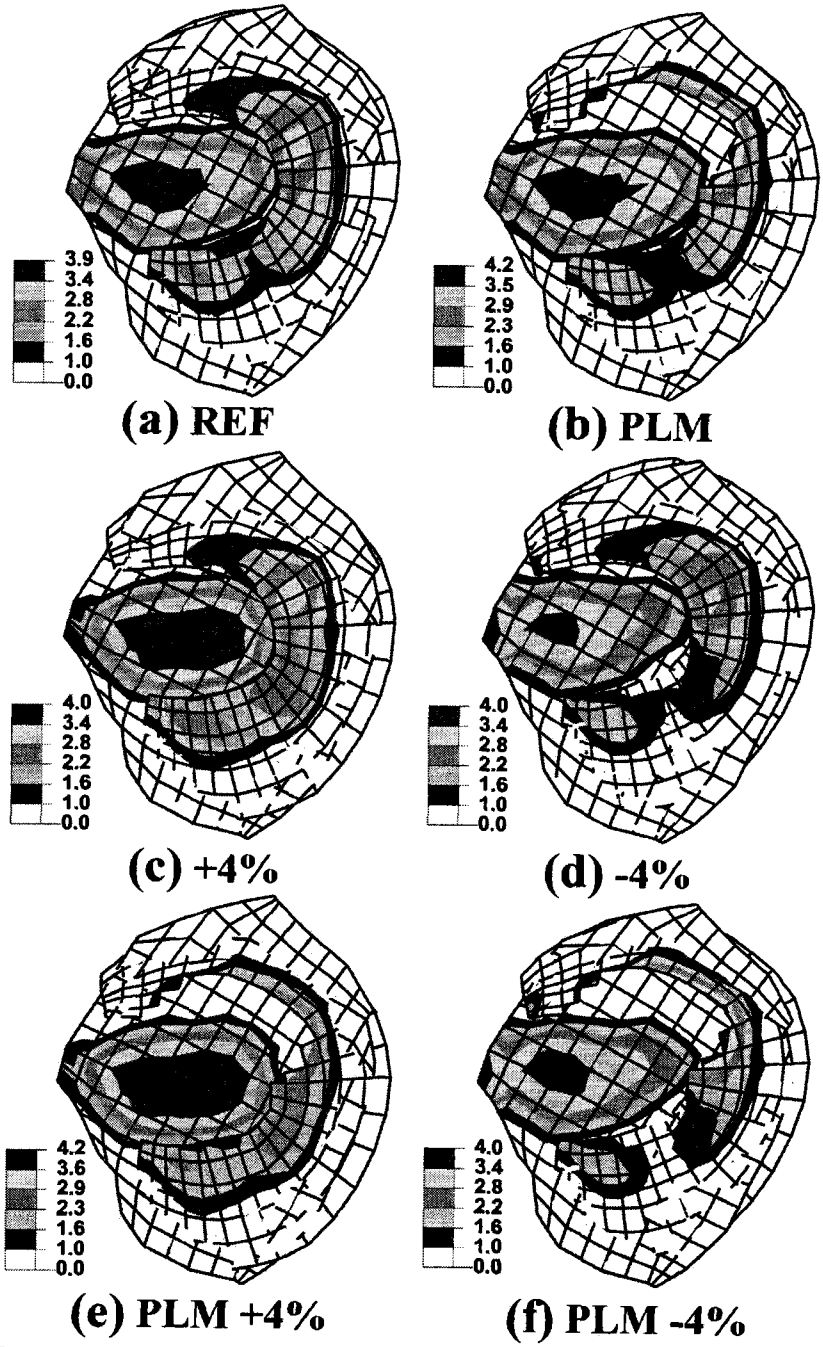

Figure 5. 6 Contact stress distribution on lateral tibial plateau under 200 N drawer and 1500 N compression preload. (a) REF: reference intact; (b) PLM: partially lateral meniscectomy; (c) +4%: plus 4% strain in ACL prestrain (tenser case); (d) -4%: minus 4% strain in ACL prestrain (slacker case); (e) PLM +4%: combined partially lateral meniscectomy with 4% strain increase in ACL prestrain; (f) PLM -4%: combined partially lateral meniscectomy with 4% decrease in ACL prestrain. See Figure 5.1 for resected area in partial lateral meniscectomy.

Chapter six

Discussion and conclusion

6.1 Overview

Despite the highly nonlinear, nonhomogeneous and anisotropic nature of articular cartilage, earlier theoretical models of the entire knee joint have considered it as a linear, homogeneous and isotropic material. Presence of collagen fibrils reinforcing nonfibrillar matrix has made it a challenge bearing in mind that these fibrils change orientation and content along the depth of cartilage. In this study, for the first time, tibial and femoral cartilages of the knee joint were simulated with distinct elements for nonfibrillar solid matrix (proteoglycans) and collagen fibrils. A composition-based fibril-reinforced finite element model of cartilage and meniscus was developed in which volume contents and orientation of collagen fibrils were explicitly accounted. The four major ligaments, i.e. ACL, PCL, MCL and LCL, were also taken into account and so the most detailed model, to our knowledge, of the human tibiofemoral joint was developed. This novel model was then used as an appropriate computational tool to investigate the effect on joint response of isolated or concurrent ACL reconstruction and unilateral partial meniscectomy.

To pave the way for developing the 3-D model of the entire knee joint, we initially developed an axisymmetric poroelastic fibril-reinforced model of cartilage in which membrane elements were used to represent collagen fibrils. Using membrane elements, the collagen fibril volume fraction in the tissue and the strain-dependent material properties reported in the literature were explicitly considered in the formulation. This approach, as compared to earlier ones (L. P. Li et al., 2001; L. P. Li et al., 1999), appears more meaningful in not lumping various fibril properties (such as volume fraction and nonlinear stress-strain curve) into one stiffness term which risks losing its physical interpretation and significance. This model with independent

variations in the volume fraction and material properties of collagen fibrils allowed for the development of a realistic cartilage model in which orientation and volume content of collagen fibrils change along the depth.

Subsequently, in an axisymmetric poroelastic model of cartilage, we introduced the three fibrillar networks at superficial, transitional and vertical zones based on the layerwise composite structure of cartilage. Collagen fibrils change their orientations from horizontal at superficial zone to random at transitional zone and finally to vertical in deep zone. An average of 2.5 mm thickness of cartilage of knee joint was assumed and extensive refinement along the depth allowed to appropriately assign 12, 19 and 69% of the thickness to respectively superficial, transitional and vertical zones. Membrane elements were used for horizontal superficial and vertical deep fibrils with appropriate formulation and volume content for each. Brick elements with tension-only stiffness were used for transitional zone to consider random distribution of fibrils in this region. Therefore, at each increment and iteration of solution, continuum elements that take the principal strain directions as the material principal axes can simulate reorientation of fibrils in tension. It was shown that deep vertical fibrils, and to a lesser extent, horizontal superficial fibrils play an important role in mechanics of articular cartilage by increasing the stiffness of the tissue and protecting the solid matrix against large distortions.

Subsequently, and due to important role of deep vertical collagen fibrils followed by horizontal superficial fibrils revealed by our previous study on an axisymmetric model of cartilage, the mesh of our existing validated 3-D model of the human knee joint (Bendjaballah et al., 1995; Mesfar & Shirazi-Adl, 2006a, 2006b) was modified for this study via an extensive refinement at articular cartilage and menisci regions. These refinements allowed for the incorporation of fibrils networks at different regions, based on the ultrastructural anatomy of cartilage and meniscus, along with depth-dependent variation in cartilage solid matrix properties. While the cartilage thickness changes from

a region to another, 15%, 22.5% and 62.5% of tissue thickness at each region was considered as superficial, transitional and vertical zones of collagen fibrils. The mechanical importance of deep vertical fibrils followed by horizontal superficial fibrils was confirmed in the entire knee joint under compression up to 2000N.

In the last phase of the current study, the 3-D novel and detailed model of the entire knee joint was used to study perturbations commonly occurring in sports activities. The effect of pre-load compression on biomechanics of intact knee joint under drawer loading was investigated, a configuration that occurs in many activities such as walking, running and stairs ascent/descent. In addition, the effect of isolated or concurrent ACL reconstruction/perturbations and unilateral partial meniscectomy was investigated under 200 N anterior drawer and 1500 N compression acting alone or combined. The extensive refinement in the meniscus allowed us both to consider its detailed ultrastructure of collagen fibrils with different arrangements at exterior surfaces and in the bulk regions and to properly simulate partial meniscectomy at the posterior region of meniscus simply by removing the elements at that region.

Definitions of material properties for memebrane and brick elements representing collagen fibrils in axisymmetric models of cartilage and 3-D model of cartilage and menisci were implemeneted via subroutines UMAT and ORIENT. General explanations of these subroutines are provided in the appendix.

6.2 Critical Evaluation of the Model

In our 3-D knee model, neglecting the patellofemoral joint, a passive tibiofemoral joint is considered to study biomechanics of the joint. Recently in our group, several studies were done on active response of the entire knee joint by considering quadriceps and hamstrings muscles (each simulated by three distinct fascicles) along with the patellar tendon to investigate biomechanics of the knee joint from full extension to 90° flexion (Mesfar, 2006; Mesfar & Shirazi-Adl, 2005, 2006a,

2006b, 2008a, 2008b). Future studies could extend the model to incorporate active components as well.

Some passive tissues like the capsule surrounding the knee joint are absent in our model. While the capsules are not expected to be one of the supporting structures in pure compression, they should play a minor role as secondary restraint to anterior-posterior loading and become even more important when ACL, which is the primary restraint to anterior translation of the tibia relative to the femur, is partially or totally impaired. The subchondral bone was taken rigid due to its much greater stiffness compared to joint soft tissues (Mente & Lewis, 1994); an assumption that would negligibly influence predictions (Donahue et al., 2002).

Alterations in split-line directions from a region to another on the femoral articular surface (Below et al., 2002) that influence tensile properties in split-line directions (Akizuki et al., 1986; Kempson et al., 1973; Roth & Mow, 1980; S. L. Woo et al., 1976) were not considered in our model studies. While changes in thickness (Kincaid & Van Sickle, 1981; Kiviranta et al., 1987) of tibial and femoral cartilage layers are present in our model, we have considered the classic 3-zone layerwise pattern (tangential, transitional and radial) for collagen fibrils everywhere in the cartilage from loaded to unloaded as well as central to peripheral areas. The fibrils structure has been shown (Xia et al., 2003) to change from this pattern when approaching the peripheral zones in humeral cartilage of young beagles. We have, however, not considered such alterations in fibrils networks when approaching the cartilage peripheral zone. The current model, nevertheless, is capable of simulating such complex alterations throughout knee joint cartilage when and if more precise data become available. It is also important to be prudent as the arrangement of collagen fibrils in tibial plateau of articular cartilage has been indicated to vary among different species (Kaab, Gwynn et al., 1998).

The axisymmetric models developed in the current study investigated transient, post-transient and equilibrium response of the cartilage under coupled pore fluid flow and stress analysis (also called soils or consolidation analysis) in ABAQUS. It should be noted that the choice of time step is important in a consolidation analysis. Due to the coupling of spatial and temporal scales, it follows that no useful information is provided by solutions generated with time steps smaller than a mesh and material-dependent characteristic time as time steps much smaller than this characteristic time cause spurious oscillatory results and avoid convergence to a solution. This issue is described in earlier studies (Murad & Loula, 1994; Vermeer & Verruijt, 1981) who propose the limit $\Delta T \geq \frac{\gamma_w}{6Ek}(\Delta h)^2$ where Δh is the distance between nodes of the finite element mesh, E is the elastic modulus of the soil skeleton, k is the soil permeability, and γ_w is the specific weight of the pore fluid. As the permeability of cartilage is very low, we extensively refined the mesh of our axisymmetric models to meet the above criterion in order to estimate the tissue response at transient periods under physiological loading rates. In the 3-D model of the knee joint, however, the mesh refinement more than that used in this study seemed unpractical. We, therefore, abandoned poroelastic analysis and opted for an equivalent elastic solution to investigate the transient behavior of the joint.

An equivalent elastic solution with a Poisson's ratio of 0.5 (i.e. an incompressible material) was used (Ateshian et al., 2007) for the short-time response analysis of the knee joint. The accuracy of equivalent solution as compared to a poroelastic biphasic solution was also evaluated and confirmed by our own axisymmetric model. When the loading rate is high, the water in the tissue is temporarily trapped and cannot exude due to extremely low permeabilities of cartilage and meniscus. The inherent incompressibility of water saturated inside pores of the tissue endows the whole tissue of cartilage and meniscus the ability of bearing high loads with almost no change in their volume. In daily activities like walking, running, stair ascending/descending, loads are applied in a fraction of seconds and so transient behavior of these activities are of great

interest. However, in activities with a constant load and long duration, like long standing, one may be more interested in post-transient behavior of the knee joint, when water starts to exude from cartilages and menisci. The post-transient behavior of the knee joint cannot hence be accurately predicted with this model. Due to the lower permeability of menisci compared to cartilage, the transfer of compression as time progresses is expected to increase at the covered areas (via menisci) in contrast to uncovered ones (cartilage-cartilage). This is due to greater loss of water in the latter zones and the crucial role of water in supporting compression. Therefore, the load-bearing role of menisci is expected to increase with time (Armstrong & Mow, 1982; Athanasiou et al., 1991; Proctor et al., 1989).

In both axisymmetric and 3-D models of cartilage and menisci, we assumed that collagen fibrils and nonfibrillar solid matrix are fully bonded together with no slip or debonding in between and hence subject to identical normal strain along the fibrils. Any microscopic slips level between the fibrillar and nonfibrillar structures were neglected in our study. The effect of any such microscopic debonding could influence the results at the micro-structural level and can be investigated only when relevant data become available.

In our axisymmetric cartilage models, we did not take into account the effect of swelling pressure, which is balanced with pretension in collagen fibrils networks. However, the swelling pressure is of order of 0.15 MPa (Buschmann & Grodzinsky, 1995; Williams & Comper, 1990) and has relatively small effects on the results bearing in mind that the pore pressure calculated in our models reached, for example, up to ~6 MPa under 20% strain in indentation configuration.

Transient characteristics of the joint and inertia were also neglected in this study. Moreover, 2000 N load applied in this study exceeding three-times body weight, although more than those applied in other earlier studies, is in the lower range of loads

expected during strenuous activities. Due to convergence problems, higher loads commonly occur in activities such as running and jumping were not however considered. Convergence difficulties were exacerbated likely due to the contact between highly compliant tissues with large relative displacements as well as material instabilities at large strain magnitudes.

The knee joint was studied only at full extension position. The anterior cruciate ligament is known to be most active near/at full exntension and thus our study on the effect of precompressive force on the strains and forces generated in ACL was performed at this stage only at full extension. Future extension of this work should consider other joint flexion angles as well.

The geometry used in the current study for the mesh of tibiofemoral knee joint was reconstructed based on the right knee of a 27-year-old female human knee joint (Bendjaballah et al., 1995). Changes in the geometry as well as material properties considered in the currently used model of the knee joint are expected to occur from a subject to another.

In its recent version, ABAQUS offers the useful surface-to-surface contact algorithm in which more accurate results are obtained by considering pair of surfaces in contact rather than traditional node-to-surface algorithm. Surface-to-surface approach enforces contact conditions in an average sense over the slave surface, rather than at discrete points and tends to provide more accurate stresses. We have used the surface-to-surface contact algorithm in our studies of the entire knee joint.

In Abaqus several contact pressure-overclosure relationships can be used to define the contact model. The "hard" contact relationship minimizes the penetration of the slave surface into the master surface at the constraint locations and gives more accurate results than others. We have used hard contact relationship in our axisymmetric

models of cartilage. In our studies of the entire knee joint, however, we opted to use "softened" contact relationship to reach application of higher loads. The "softened" contact relationship is also sometimes (such as our case) useful for numerical reasons because they can make it easier to resolve the contact condition (ABAQUS documentation).

The "softened" contact relationships are specified in terms of overclosure (or clearance) versus contact pressure. The pressure-overclosure relationship can be prescribed by using a linear law, a tabular piecewise-linear law, or an exponential law. In the current study, a tabular piecewise-linear law was used. To define a piecewise-linear pressure-overclosure relationship in tabular form, as shown in Fig 6.1, data pairs (p_i, h_i) of pressure versus overclosure (where overclosure corresponds to negative clearance) are specified. The data are specified as an increasing function of pressure and overclosure. In this relationship the surfaces transmit contact pressure when the overclosure between them, measured in the contact (normal) direction, is greater than h_1, where h_1 is the overclosure at zero pressure. For overclosures greater than the pressure-overclosure relationship is extrapolated based on the last slope computed from the user-specified data (ABAQUS documentation). The softened contact relationship used in our studies of the entire knee joint is given is Table 6.1. The difference between results obtained in the current study by hard and soft contact relationships is less than 3%.

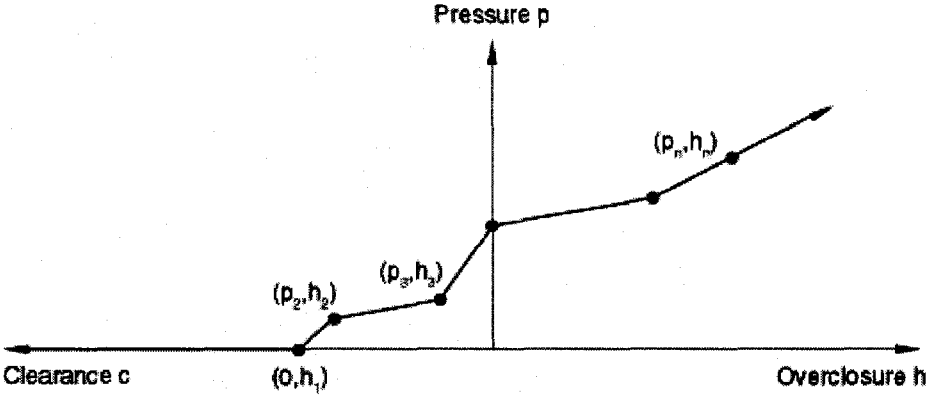

Figure 6. 1 "Softened" pressure-overclosure relationship defined in tabular form (ABAQUS documentation).

Table 6. 1 Pressure-overclosure relationship of contact used in the current study

Pressure (p_i) (MPa)	Overclosure (h_i) (mm)
0.0	-0.004
0.0125	0.004
12.	1.0
200	2.0

Parametric studies of ±4% strain change in ACL prestrain (Shirazi & Shirazi-Adl, 2008a) was done to simulate changes that may occur after ACL injury and/or reconstruction surgery. A decrease of 4% (-4%) in ACL prestrain appears to somewhat simulate a case with partial ACL damage. Replacement of a ruptured ACL by a patellar tendon graft with higher stiffness, which is also a common case in ACL reconstruction, is another factor that was simulated and investigated as well. Total removal of ACL that represents complete ACL rupture was not however investigated in this work due primarily to substantial convergence complications. On the other hand, partial unilateral meniscectomy was evaluated by removing the elements at the posterior region of meniscus. The effect of size of meniscectomy and its location was not considered.

6.3 Comparison with Experimental Measurements

The earlier fibril-reinforced model developed by our group (L. P. Li et al., 1999; Soulhat et al., 1999) has been validated by experimental tests of bovine samples (Fortin et al., 2000; Jurvelin et al., 1997). We successfully compared transient and equilibrium lateral/axial deformations of our axisymmetric models (Shirazi & Shirazi-Adl, 2005, 2008b) to those of earlier studies (Jurvelin et al., 1997; L. P. Li et al., 2000; L. P. Li et al., 1999). We have also observed zonal differences in lateral expansion in our axisymmetric model (Shirazi & Shirazi-Adl, 2008b) in agreement with experiments (Jurvelin et al., 1997). This is due to the known zonal differences in the fibrillar collagen architecture and proteoglycan concentration (Jurvelin et al., 1997). Chevron deformation

pattern of vertical fibrils at transient time that was further accentuated with the time (at post-transient period) in our axisymmetric model (Shirazi & Shirazi-Adl, 2008b) was also in agreement with reported observations on post-transient micro-deformation of cartilage in creep (Kaab, Ito et al., 1998; Notzli & Clark, 1997; Thambyah & Broom, 2006). Our results on the effect of strain and loading rate (Shirazi & Shirazi-Adl, 2008b) is also corroborated with experimental measurements (L. P. Li et al., 2003; Oloyede et al., 1992) reporting a progressive increase in tissue stiffness at low and medium strain rates while nearly no change at high strain rates.

The overall response of the current tibiofemoral knee joint with incompressible articular cartilage (Shirazi et al., 2008) is almost identical to the earlier validated model developed in our group (Bendjaballah et al., 1995). For example, the nonlinear axial deflection of the joint reached 0.83 and 1 mm under 1000 and 1500 N compression, which is similar to results predicted by the earlier compressible model. This axial displacement is, in addition, in agreement with measurements reported (Kurosawa et al., 1980; Walker & Erkman, 1975).

Total tibial contact area predicted in this study was in general agreement with measurements. The initial, unloaded, predicted contact area of 355 mm^2 compares well with 330 mm^2 averaged for measurements in 4 specimens (Walker & Hajek, 1972). Total contact area at different load levels from 200 N to 2000 N is also in good agreement with several measurements as shown in Table 1 of the third publication of this study (Shirazi et al., 2008).

Our model predicted a maximum contact pressure of 3.42 MPa under 1500 N compressive load which falls within the measurements reported in between 2.3 to 4 MPa (Fukubayashi & Kurosawa, 1980; Inaba et al., 1990; Walker & Erkman, 1975). The mean contact pressure is also in the range of reported values as shown in Table 1 (Shirazi et al., 2008).

The mean anterior tibial laxities of 2.8 mm to 6.7 mm are reported under 100 N anterior tibial force at full extension (Markolf et al., 1981; Rudy et al., 2000) that compare with our posterior femoral laxity of 3.6 mm under 100 N posterior femoral force. We observed a posterior translation of the femur relative to the tibia under compression which is due to the posterior slope of the tibia (Torzilli et al., 1994) and agrees with observation of anterior tibial displacement relative to the femur (Markolf et al., 1981; Torzilli et al., 1994). The relative magnitude and variation of femoral primary translation under drawer force with compression are also in agreement with measurements (Hsieh & Walker, 1976; G. Li et al., 1998; Markolf et al., 1981; Torzilli et al., 1994).

The predicted force of 170 N in ACL is in good agreement with measured values of 75-162 N reported under ~100 N drawer at full extension (Markolf et al., 1995; Takai et al., 1993). Compression preload further increases ACL force under drawer from ~1.6 times, in agreement with 150% in measurements (Markolf et al., 1995), to more than two-fold that of applied drawer force. Prediction of the marked increase in ACL force in presence of compression preload corroborates earlier findings (Fleming et al., 2001; G. Li et al., 1998; Torzilli et al., 1994) but contradicts others suggesting the notion that compression preload in drawer protects the ACL from damage (Markolf et al., 1990).

It is be emphasized that many factors such as difference in species, age and sex of cadavers used for tests as well as measurement devices/methods and loading rates could greatly influence the results of an investigation whether experimental or numerical. The predictions in the current study should be therefore compared with experimental results in the light of such dependence.

6.4 Clinical and Biomechanical Implications

6.4.1 Collagen Role/Damage in Cartilage

Cartilage and knee models developed during this study (Shirazi & Shirazi-Adl, 2005, 2008a, 2008b; Shirazi et al., 2008) are based on a physiological description of the tissue and are thus promising in improvement of our understanding of the cartilage and knee pathomechanics. We represented collagen fibrils networks of cartilage (Shirazi & Shirazi-Adl, 2005), for the first time, accounting for two of its key characteristics, i.e. collagen volume fraction and mechanical properties. By individual adjustment of these key factors, the model allows for the simulation of alterations in the fibril network structure of the tissue towards modeling damage processes or repair attempts. It was shown that the transient response of the tissue under a displacement-control loading significantly increases as the volume fraction of collagen fibrils increases whereas the equilibrium load remains nearly the same. On the contrary, however, when the size of a specimen increases from a radius of 1.4 mm often used in mechanical tests of cartilage to 11.2 mm thus approaching that of tibial plateaus the effect of collagen fibrils remains pronounced for longer periods even at the post-transient period.

By representing layer-wise collagen fibrils structure of cartilage along the depth in our axisymmetric model (Shirazi & Shirazi-Adl, 2008b), we were able to demonstrate the relative mechanical importance of each fibril zone. It was shown how damages to vertical collagen fibril network or their firm anchorage to the bone, associated with bone bruises for example, would weaken the transient stiffness and place the tissue at higher risk of failure, particularly at the deep zone. The vertical fibrils network substantially increased the transient stiffness of the cartilage; the ratio of transient to equilibrium force (i.e., dynamic to static stiffness) increased by approximately threefold (from ~18 to 51) when the volume fraction of vertical fibrils increased from 0% to 9%. The vertical fibrils also protected the solid matrix from excessive strains (Figures 3 and 4 (Shirazi & Shirazi-Adl, 2008b)) and, hence, damage and rupture; the transient maximum principal

strain diminished from 51.3% to 22.8% in presence of 9% vertical fibril content and that despite a concurrent near threefold increase in the applied force. The importance of vertical fibrils was dramatically compromised at slower strain rates while in contrast almost no difference in response was predicted as the strain rate increased 100 times from 40% s^{-1} expected in physiological activities to 4000% s^{-1} (Figure 6 (Shirazi & Shirazi-Adl, 2008b)). The results of this study, therefore, stress the important role of vertical fibrils in cartilage mechanics under physiological loading rates expected in walking, running, and jumping. The much slower rates that have often been considered in earlier measurement and model studies cannot, hence, be expected to adequately identify the mechanical influence of vertical collagen fibrils. The vertical fibrils and their roles are of prime importance bearing in mind the nature of loading/unloading cycles (i.e., high loading rates, short durations, high strain/stress magnitudes)

Our axisymmetric model studies (Shirazi & Shirazi-Adl, 2008b) served as a foundation to extensively improve an existing 3-D model of the entire knee joint towards a novel one (Shirazi et al., 2008) that considered, for the first time, the anisotropic nature of tibial and femoral cartilage layers in addition to menisci. We were subsequently able to evaluate role and relative importance of vertical and superficial fibrils in a more realistic model at transient time during which collagen fibrils had already shown to play significant roles in our poroelastic axisymmetric model. This 3-D knee joint model study highlights the primary role of vertical fibrils network in stiffening articular cartilage while protecting it from excessive strains and distortions. Despite a moderate (~10%) softening effect on overall response in axial displacement of the knee joint, removal of deep vertical fibrils substantially increased the maximum cartilage tensile/shear strains especially at subchondral junction where large strains already existed. Under 1800 N compression, the principal tensile strain in solid matrix of cartilage substantially increased everywhere when vertical fibrils were totally removed (Figure 6 (Shirazi et al., 2008)); the maximum tensile strain in cartilage matrix increased significantly from 37.8% to 101.7%. Unlike the peak compressive strains, the maximum shear and tensile

strains at deeper cartilage layers and in vertical fibrils themselves occur away from the loaded areas. The foregoing mechanical role of vertical fibrils further accentuate under larger compression loads expected for example in running, high impacts and more strenuous activities.

The importance of the integrity of cartilage anchorage at the subchondral bone junction in augmenting the tissue stability and load-bearing (Keinan-Adamsky et al., 2005) as well as in initiation of joint failure and osteoarthritis (Atkinson & Haut, 1995; Vener et al., 1992) has been recognized. Local damages at the subchondral junction could potentially precede degenerative changes in overlying cartilage (Atkinson & Haut, 1995; Keinan-Adamsky et al., 2005; Meachim & Bentley, 1978; Radin & Rose, 1986). Apart from bone bruises at the base (Henderson & La Valette, 2005; Tandogan et al., 2004), surface cartilage defects have also been reported (Hollander et al., 1995; Vande Berg et al., 2002). In this study, the effect of two distinct localized damages in tibial cartilage at loaded areas (~2 cm^2 in lateral plateau) were investigated; the tissue was either detached at the subchondral junction or weakened at the surface by removing the superficial fibrils. This model of detachment at the base did not intend to simulate the subchondral failures in which case the associated compromise in the underlying bone, not simulated in the current model study, would further increase distortions in overlying articular cartilage. The base split was computed to have much greater effect in increasing maximum tensile strain in cartilage matrix of the affected plateau. Any treatment modality attempting to repair or regenerate cartilage defects involving partial or full thickness osteochondral grafts should account for the crucial role of collagen fibrils networks and the demanding mechanical environment of the tissue.

6.4.2 ACL Damage/Reconstruction and Partial Meniscectomy

Injuries or alterations to the ACL and menisci would influence overall joint response as well as mechanical role of remaining components with the likelihood to exacerbate the joint condition causing recurrent injuries and further damages. Existing

ACL reconstruction techniques use different ligament pretension/prestrain levels and replacement materials such as bone-patellar-tendon-bone and hamstrings grafts with much stiffer material properties (Butler et al., 1986). The graft material and pretension have been recognized as primary variables that could influence the outcome of reconstruction attempts. Meniscal tears are also commonly observed along with ACL ruptures (Indelicato & Bittar, 1985) as the risk of meniscus failure increases in ACL deficient knees (Noyes et al., 1980). Due to the dramatic adverse effect of total meniscectomy on load distribution and development of joint osteoarthritis, partial meniscectomies are performed with the resection of the torn tissues. Concurrent ACL and meniscus ruptures are treated by ACL reconstruction and partial meniscectomy. Incidence of osteoarthritis in mid- and long-term outcome studies of ACL reconstruction (van der Hart et al., 2008) and partial meniscectomy (Rangger et al., 1995) has nevertheless persisted.

Axial compressive and anterior-posterior shear forces, commonly occurring in activities such as walking, running, jumping and stairs ascent/descent, are due both directly to gravity, external and inertia loads and indirectly to activation of muscles crossing the knee joint. As the final phase of this study we used our detailed 3-D model of the entire knee joint (Shirazi et al., 2008) to investigate the effects of partial medial and lateral meniscectomies, alterations in ACL prestrain and material properties, combined ACL-reconstruction and lateral meniscectomy on the response of the entire tibiofemoral joint as compared to the reference intact case (Shirazi & Shirazi-Adl, 2008a). To do so, the joint response in both intact and altered conditions under single as well as combined drawer and compression forces was investigated. Attention was focused on the effect of various loads and joint perturbations on the cartilage strains/stresses, contact loads and ACL forces.

Perturbations in prestrains/material properties of the ACL expected following reconstruction influenced the redistribution of contact forces on covered and uncovered

areas. Replacement of a ruptured ACL by a patellar tendon graft with higher stiffness had similar mechanical effect on the joint response as an increase of ~4% in ACL prestrain, a finding in agreement with our earlier studies of the knee joint under quadriceps activation (Mesfar & Shirazi-Adl, 2006a). On the contrary, a decrease of 4% in ACL prestrain appears to somewhat simulate a case with partial ACL damage. In this case with slacker ACL, the contact pressure pattern on the lateral plateau demonstrates an unloaded region of cartilage underneath meniscus. This unloading phenomenon would likely increase had a complete ACL rupture been simulated in this study. Such alterations in joint load redistribution (i.e., contact forces and pressure) following ACL reconstruction or ACL rupture could hence contribute to the development of OA (van der Hart et al., 2008).

While under loads considered in this study partial meniscectomy did not noticeably influence ACL forces, it did however substantially alter contact stress distribution on the articular cartilage. Partial meniscectomy shifted the transfer of applied compression away from the resected meniscus onto the nearby cartilage while completely unloading previously covered femoral/tibial cartilage areas that otherwise would articulate with the meniscus. In addition, the peak pressure on nearby uncovered cartilage increased by ~5%. When partial lateral meniscectomy is combined with a 4% increase in ACL prestrain (a tenser ACL), contact load/pressure further increased on the nearby cartilage at uncovered areas. A concurrent 4% decrease in ACL (slacker ACL), however, diminished the load via lateral meniscus to its minimum among all cases considered in this study and created an additional unloaded area on the cartilage covered by the lateral meniscus. Absence of the ACL in ACL deficient joints, not simulated in this work, would further influence the above alterations in pattern of stress distribution away from that expected in intact reference case. Such changes in contact stresses on the joint cartilage that are expected to further accentuate under larger loads than those considered in this work adversely affect the cartilage function and health likely leading in long-term to OA (Rangger et al., 1995; van der Hart et al., 2008).

6.5 Summary and Concluding Remarks

The fibril-reinforced composite model of the articular cartilage has been successful in describing the experimentally observed temporal response characteristics of the articular cartilage in confined and unconfined testing configurations (L. P. Li et al., 2000, 2003; L. P. Li et al., 1999; Shirazi & Shirazi-Adl, 2005; Soulhat et al., 1999). We have also observed zonal differences in lateral expansion in our axisymmetric model (Shirazi & Shirazi-Adl, 2008b) in agreement with experiments (Jurvelin et al., 1997). The ever-important mechanical role of collagen fibrils in tension and its interaction with the pore fluid flow have been found responsible for the strain and strain rate dependencies of the cartilage tissue (L. P. Li et al., 2003; Shirazi & Shirazi-Adl, 2008b). The fibril networks while under tension, in turn, confine the bulk and apply compression on the matrix thus influencing the stress field in the tissue as a whole as compared with that in homogeneous orthotropic models. The prediction of tensile stresses in fibril networks and of compressive stresses in the matrix appears desirable in employing each component to resist stresses for which it is best structured.

In earlier model studies of the articular cartilage in our group (L. P. Li et al., 2000; L. P. Li et al., 1999), the fibril networks in the radial direction were represented by uniaxial spring elements with nonlinear properties in tension and no resistance in compression. These studies, however, did not explicitly account for the important physical properties of the tissue, such as the volume fraction and nonlinear stress-strain curves of the fibril networks at different locations and directions. Moreover, the radial fibrils were modified to also account for the circumferential fibrils by using equivalent strain energies in a disc under a uniform state of stress. In the current study, however, membrane elements are used to directly represent fibril networks in both axisymmetric and 3-D model studies (Shirazi & Shirazi-Adl, 2005). The formulation of the membrane element also explicitly accounts for the tissue collagen fibrils properties, such as volume fraction and stress-strain curve. This approach appears more meaningful in not lumping various fibril properties into one stiffness term which risks losing its physical

interpretation and, hence, significance. By separate variations in the collagen volume fraction and in the collagen mechanical properties, the individual role of each physical parameter can be considered and identified.

Introducing membrane element to represent collagen fibrils set the foundation for considering change in orientation and content of collagen fibrils along the depth of cartilage (Shirazi & Shirazi-Adl, 2008b). Doing so, role and relative importance of fibrils at each zone was demonstrated. The vertical fibril network substantially increased the transient stiffness of the cartilage; the ratio of transient to equilibrium force (i.e., dynamic to static stiffness) increased by approximately threefold (from ~18 to 51) when the volume fraction of vertical fibrils increased from 0% to 9%. The vertical fibrils also protected the solid matrix from excessive strains and, hence, damage and rupture. The transient maximum principal strain diminished from 51.3% to 22.8% in presence of 9% vertical fibril content and that despite a concurrent near threefold increase in the applied force. For nearly the same relative change, vertical fibrils had greater influence on cartilage mechanics than had the superficial and transitional fibril networks. It was also shown that vertical fibrils play a significant role at physiological loading rates or higher. Therefore, much slower rates that have often been considered in earlier measurements and model studies cannot capture the mechanical role of vertical fibrils.

The chevron deformation pattern of vertical fibrils observed in creep further accentuated with the time, in agreement with reported observations on post-transient microdeformation of cartilage in creep (Thambyah & Broom, 2006). In general, the results of this study corroborated with earlier experimental investigations. This axisymmetric model study paved the way to step into the more realistic geometry of our existing entire knee joint (Bendjaballah et al., 1995; Mesfar & Shirazi-Adl, 2006a).

Our 3-D model of entire knee joint into which depth-dependent orientation of collagen fibrils of cartilage and meniscus were incorporated also confirmed the

significant role of cartilage deep vertical fibrils in protecting the solid matrix against large tensile and shear strains, in particular at the subchondral junction (Shirazi et al., 2008). Similar to our axisymmetric studies, it was shown that vertical fibrils at the deep zone play more important roles in protecting solid matrix of cartilage than fibrils at horizontal and transitional zone. This model allowed us to investigate the relative importance of collagen fibrils network at superficial and vertical zones on the strain and load/stress distribution in cartilages and menisci as well as forces in the ligaments. Despite a moderate (~10%) softening effect on overall response in axial displacement, removal of deep vertical fibrils substantially increased the maximum cartilage tensile/shear strains especially at subchondral junction where large strains already existed.

Unlike the peak compressive strains, the maximum shear and tensile strains at deeper cartilage layers and in vertical fibrils themselves occur away from the loaded areas. The prediction of crimped fibrils underneath the loaded areas is corroborated by experimental studies. The results of this study were generally in good agreement with experimental measurements. The model was validated by comparing axial deflection, cartilage mean and maximum contact stresses/areas and the contribution percentage of meniscus and cartilage in bearing loads under up to 2000 N compression with those of earlier measurements. Some other cases such as local split between subchondral bone and cartilage as well as disruption in superficial fibrils were also investigated. The base split was computed to have much greater effect in increasing maximum tensile strain in cartilage matrix of the affected plateau. Cartilage and knee models developed during this study were based on a physiological description of the tissue and are thus promising in improvement of our understanding of the cartilage and knee pathomechanics.

Extensive refinement and detailed representation of collagen fibrils in cartilages and menisci made the 3-D model of the entire knee joint an appropriate computational tool to study the effect of isolated or concurrent ACL injury/reconstruction and

unilateral partial meniscectomy on the knee joint under single as well as combined drawer and compression forces. The predictions in this study were generally in good agreement with experimental measurements. The mean anterior tibial laxities reported under up to 134 N anterior tibial force at full extension compare with our predictions. The computed force in ACL was also in good agreement with measured values reported under ~100 N drawer at full extension. Compression preload further increased ACL force under drawer from ~1.6 times, in agreement with 150% in measurements, to more than two-fold that of applied drawer force.

Large ACL force was computed under femoral posterior drawer that further increased by 30% with compression preload, which advocate rehabilitation and training strategies that avoid large axial compression preloads at near full extension on the joint subject to drawer forces. While under loads considered in this study partial meniscectomy did not noticeably influence ACL forces, it did however substantially alter contact stress distribution on the articular cartilage. Partial meniscectomy shifted the transfer of applied compression away from the resected meniscus onto the nearby cartilage while completely unloading previously covered femoral/tibial cartilage areas that otherwise would articulate with the meniscus. An additional unloaded area on the cartilage covered by the lateral meniscus was caused when the situation was worsened by a concurrent decrease in ACL prestrain. Such changes in contact stresses on the joint cartilage that are expected to further accentuate under larger loads than those considered in this work adversely affect the cartilage function and health likely leading in long-term to OA.

6.6 Future Studies

6.6.1 Cartilage Modeling

Although our existing model of cartilage takes into account the change in orientation and content of collagen fibrils arrangement and depth-dependent material properties in solid matrix and water, a mechanobiological feedback algorithm reacting to

mechanical loads is however absent that can be incorporated into our existing model. To do so, experimental studies should be done to initially calibrate the theoretical model by adjusting the important parameters and then testing the model by comparing with another experimental configuration. The solid matrix can also take into account the swelling pressure balanced out by strained collagen network at initial configuration to develop even more realistic models of cartilage. Cartilage nutrition can also be added to the model by considering important factors i.e. concentration of glucose, oxygen and lactic acid (Soukane et al., 2007) while accounting for the coupling between these species via the pH level in the tissue and the nonlinear concentration-consumption (for glucose and oxygen) and concentration-production (for lactate) relations.

6.6.2 Entire Knee Joint Modeling

With detailed representation of cartilage in the current novel model of the knee joint, effect of loading configurations such as varus-valgus and internal-external rotations acting alone or combined with compression on cartilage biomechanics, not simulated in the current study, can be evaluated.

Muscles can also be incorporated into the current model of the knee joint to simulate more accurately the daily activities of the knee joint and rehabilitation treatments such as open kinetic chain extension exercises. The muscle activities input can come from Magnetic resonance imaging (Besier et al., 2005).

The current study investigates only instantaneous (short-term) response of the entire knee joint at full extension. Presence of water is simulated by using an equivalent elastic solution. To study effect of cyclic loading/unloading and creep where water exudes out from cartilages and menisci, a poroelastic solution must be sought. For example, long-standing is an important daily activity and needs more investigation.

The current quasi-static model does not take into account the inertia loads/effects on the biomechanics of the knee joint. The inertia loads are expected to be important in sports related activities. For example, ACL injury commonly occurs during single limb landing or stopping from a run (Shin et al., 2007).

A decrease of 4% in ACL prestrain, investigated in the current study, appears to somewhat simulate a case with partial ACL damage. The current novel model of the knee joint developed in this study is an appropriate computational tool to study the effect of ACL absence (complete injury), not simulated in this study, on cartilage and meniscus biomechanics. The ACL absence can also be combined with partial meniscectomy under combined load.

References

Ahmed, A. M., and Burke, D. L. (1983). In-vitro measurement of static pressure distribution in synovial joints--Part I: Tibial surface of the knee. *J Biomech Eng, 105*(3), 216-225.

Ahmed, A. M., Hyder, A., Burke, D. L., and Chan, K. H. (1987). In-vitro ligament tension pattern in the flexed knee in passive loading. *J Orthop Res, 5*(2), 217-230.

Akizuki, S., Mow, V. C., Muller, F., Pita, J. C., Howell, D. S., and Manicourt, D. H. (1986). Tensile properties of human knee joint cartilage: I. Influence of ionic conditions, weight bearing, and fibrillation on the tensile modulus. *J Orthop Res, 4*(4), 379-392.

Allen, C. R., Wong, E. K., Livesay, G. A., Sakane, M., Fu, F. H., and Woo, S. L. (2000). Importance of the medial meniscus in the anterior cruciate ligament-deficient knee. *J Orthop Res, 18*(1), 109-115.

Armstrong, C. G., Lai, W. M., and Mow, V. C. (1984). An analysis of the unconfined compression of articular cartilage. *J Biomech Eng, 106*(2), 165-173.

Armstrong, C. G., and Mow, V. C. (1982). Variations in the intrinsic mechanical properties of human articular cartilage with age, degeneration, and water content. *J Bone Joint Surg Am, 64*(1), 88-94.

Aspden, R. M., Yarker, Y. E., and Hukins, D. W. (1985). Collagen orientations in the meniscus of the knee joint. *J Anat, 140 (Pt 3)*, 371-380.

Ateshian, G. A., Ellis, B. J., and Weiss, J. A. (2007). Equivalence between short-time biphasic and incompressible elastic material responses. *J Biomech Eng, 129*(3), 405-412.

Athanasiou, K. A., Agarwal, A., and Dzida, F. J. (1994). Comparative study of the intrinsic mechanical properties of the human acetabular and femoral head cartilage. *J Orthop Res, 12*(3), 340-349.

Athanasiou, K. A., Rosenwasser, M. P., Buckwalter, J. A., Malinin, T. I., and Mow, V. C. (1991). Interspecies comparisons of in situ intrinsic mechanical properties of distal femoral cartilage. *J Orthop Res, 9*(3), 330-340.

Atkinson, P. J., and Haut, R. C. (1995). Subfracture insult to the human cadaver patellofemoral joint produces occult injury. *J Orthop Res, 13*(6), 936-944.

Below, S., Arnoczky, S. P., Dodds, J., Kooima, C., and Walter, N. (2002). The split-line pattern of the distal femur: A consideration in the orientation of autologous cartilage grafts. *Arthroscopy, 18*(6), 613-617.

Bendjaballah, M. Z., Shirazi-Adl, A., and Zukor, D. J. (1995). Biomechanics of the human knee joint in compression: reconstruction, mesh generation and finite element analysis. *The Knee, 2*(2), 69-79.

Bendjaballah, M. Z., Shirazi-Adl, A., and Zukor, D. J. (1997). Finite element analysis of human knee joint in varus-valgus. *Clin Biomech (Bristol, Avon), 12*(3), 139-148.

Bendjaballah, M. Z., Shirazi-Adl, A., and Zukor, D. J. (1998). Biomechanical response of the passive human knee joint under anterior-posterior forces. *Clin Biomech (Bristol, Avon), 13*(8), 625-633.

Benninghoff, A. (1925). Form und Bau der Gelenkknorpel in ihren Beziehungen zur Funktion. *Zeitschrift für Zellforschung, 2*, 783-862.

Besier, T. F., Gold, G. E., Beaupre, G. S., and Delp, S. L. (2005). A modeling framework to estimate patellofemoral joint cartilage stress in vivo. *Med Sci Sports Exerc, 37*(11), 1924-1930.

Blankevoort, L., Kuiper, J. H., Huiskes, R., and Grootenboer, H. J. (1991). Articular contact in a three-dimensional model of the knee. *J Biomech, 24*(11), 1019-1031.

Broom, N. D., and Marra, D. L. (1986). Ultrastructural evidence for fibril-to-fibril associations in articular cartilage and their functional implication. *J Anat, 146*, 185-200.

Broom, N. D., and Poole, C. A. (1982). A functional-morphological study of the tidemark region of articular cartilage maintained in a non-viable physiological condition. *J Anat, 135*(Pt 1), 65-82.

Brown, C. H., Jr., and Carson, E. W. (1999). Revision anterior cruciate ligament surgery. *Clin Sports Med, 18*(1), 109-171.

Brown, T. D., and Shaw, D. T. (1984). In vitro contact stress distribution on the femoral condyles. *J Orthop Res, 2*(2), 190-199.

Brown, T. D., and Singerman, R. J. (1986). Experimental determination of the linear biphasic constitutive coefficients of human fetal proximal femoral chondroepiphysis. *J Biomech, 19*(8), 597-605.

Buckwalter, J. A., and Mankin, H. J. (1998). Articular cartilage: degeneration and osteoarthritis, repair, regeneration, and transplantation. *Instr Course Lect, 47*, 487-504.

Buschmann, M. D., and Grodzinsky, A. J. (1995). A molecular model of proteoglycan-associated electrostatic forces in cartilage mechanics. *J Biomech Eng, 117*(2), 179-192.

Buschmann, M. D., Soulhat, J., Shirazi-Adl, A., Jurvelin, J. S., and Hunziker, E. B. (1998). Confined compression of articular cartilage: linearity in ramp and sinusoidal tests and the importance of interdigitation and incomplete confinement. *J Biomech, 31*(2), 171-178.

Butler, D. L., Kay, M. D., and Stouffer, D. C. (1986). Comparison of material properties in fascicle-bone units from human patellar tendon and knee ligaments. *J Biomech, 19*(6), 425-432.

Butler, D. L., Noyes, F. R., and Grood, E. S. (1980). Ligamentous restraints to anterior-posterior drawer in the human knee. A biomechanical study. *J Bone Joint Surg Am, 62*(2), 259-270.

Chahine, N. O., Wang, C. C., Hung, C. T., and Ateshian, G. A. (2004). Anisotropic strain-dependent material properties of bovine articular cartilage in the transitional range from tension to compression. *J Biomech, 37*(8), 1251-1261.

Chandrashekar, N., Hashemi, J., Slauterbeck, J., and Beynnon, B. D. (2008). Low-load behaviour of the patellar tendon graft and its relevance to the biomechanics of the reconstructed knee. *Clin Biomech (Bristol, Avon), 23*(7), 918-925.

Charlebois, M., McKee, M. D., and Buschmann, M. D. (2004). Nonlinear tensile properties of bovine articular cartilage and their variation with age and depth. *J Biomech Eng, 126*(2), 129-137.

Clarke, I. C. (1974). Articular cartilage: a review and scanning electron microscope study. II. The territorial fibrillar architecture. *J Anat, 118*(Pt 2), 261-280.

Cohen, B., Lai, W. M., Chorney, G. S., Dick, H. M., and Mow, V. C. (1992). *Unconfined compression of transversely-isotropic biphasic tissues.* vol. 22. 187-190, Anaheim, CA, USA.

Crowninshield, R., Pope, M. H., and Johnson, R. J. (1976). An analytical model of the knee. *J Biomech, 9*(6), 397-405.

Davis, M. A., Ettinger, W. H., Neuhaus, J. M., and Mallon, K. P. (1991). Knee osteoarthritis and physical functioning: evidence from the NHANES I Epidemiologic Followup Study. *J Rheumatol, 18*(4), 591-598.

Donahue, T. L., Hull, M. L., Rashid, M. M., and Jacobs, C. R. (2002). A finite element model of the human knee joint for the study of tibio-femoral contact. *J Biomech Eng, 124*(3), 273-280.

Favenesi, J. A., Shaffer, J. C., and Mow, V. C. (1983). *Biphasic mechanical properties of knee meniscus.* Paper presented at the Trans Orthop Res Soc. vol. 8. 57.

Fithian, D. C., Kelly, M. A., and Mow, V. C. (1990). Material properties and structure-function relationships in the menisci. *Clin Orthop Relat Res*(252), 19-31.

Fleming, B. C., Renstrom, P. A., Beynnon, B. D., Engstrom, B., Peura, G. D., Badger, G. J., and Johnson, R. J. (2001). The effect of weightbearing and external loading on anterior cruciate ligament strain. *J Biomech, 34*(2), 163-170.

Fortin, M., Soulhat, J., Shirazi-Adl, A., Hunziker, E. B., and Buschmann, M. D. (2000). Unconfined compression of articular cartilage: nonlinear behavior and comparison with a fibril-reinforced biphasic model. *J Biomech Eng, 122*(2), 189-195.

Frank, E. H., and Grodzinsky, A. J. (1987). Cartilage electromechanics--II. A continuum model of cartilage electrokinetics and correlation with experiments. *J Biomech, 20*(6), 629-639.

Froimson, M. I., Ratcliffe, A., Gardner, T. R., and Mow, V. C. (1997). Differences in patellofemoral joint cartilage material properties and their significance to the etiology of cartilage surface fibrillation. *Osteoarthritis Cartilage, 5*(6), 377-386.

Froimson, M. I., Ratcliffe, A., and Mow, V. C. (1989). *Patellar cartilage mechanical properties vary with site and biochemical composition.* Paper presented at the Trans. Orthop. Res. Soc. vol. 14. 150.

Fujie, H., Livesay, G. A., Woo, S. L., Kashiwaguchi, S., and Blomstrom, G. (1995). The use of a universal force-moment sensor to determine in-situ forces in ligaments: a new methodology. *J Biomech Eng, 117*(1), 1-7.

Fukubayashi, T., and Kurosawa, H. (1980). The contact area and pressure distribution pattern of the knee. A study of normal and osteoarthrotic knee joints. *Acta Orthop Scand, 51*(6), 871-879.

Fukubayashi, T., Torzilli, P. A., Sherman, M. F., and Warren, R. F. (1982). An in vitro biomechanical evaluation of anterior-posterior motion of the knee. Tibial displacement, rotation, and torque. *J Bone Joint Surg Am, 64*(2), 258-264.

Glaser, C., and Putz, R. (2002). Functional anatomy of articular cartilage under compressive loading Quantitative aspects of global, local and zonal reactions of the collagenous network with respect to the surface integrity. *Osteoarthritis Cartilage, 10*(2), 83-99.

Gollehon, D. L., Torzilli, P. A., and Warren, R. F. (1987). The role of the posterolateral and cruciate ligaments in the stability of the human knee. A biomechanical study. *J Bone Joint Surg Am, 69*(2), 233-242.

Gore, D. M., Higginson, G. R., and Minns, R. J. (1983). Compliance of articular cartilage and its variation through the thickness. *Phys Med Biol, 28*(3), 233-247.

Grood, E. S., and Hefzy, M. S. (1982). An analytical technique for modeling knee joint stiffness--Part I: Ligamentous forces. *J Biomech Eng, 104*(4), 330-337.

Guccione, A. A., Felson, D. T., Anderson, J. J., Anthony, J. M., Zhang, Y., Wilson, P. W., Kelly-Hayes, M., Wolf, P. A., Kreger, B. E., et al. (1994). The effects of specific medical conditions on the functional limitations of elders in the Framingham Study. *Am J Public Health, 84*(3), 351-358.

Haut, R. C., and Little, R. W. (1972). A constitutive equation for collagen fibers. *J Biomech, 5*(5), 423-430.

Hayes, W. C., Keer, L. M., Herrmann, G., and Mockros, L. F. (1972). A mathematical analysis for indentation tests of articular cartilage. *J Biomech, 5*(5), 541-551.

Hayes, W. C., and Mockros, L. F. (1971). Viscoelastic properties of human articular cartilage. *J Appl Physiol, 31*(4), 562-568.

Health Canada. *Arthritis in Canada: An ongoing Challenge*: Ministry of Public Work and Government Services Canada.

Henderson, I. J., and La Valette, D. P. (2005). Subchondral bone overgrowth in the presence of full-thickness cartilage defects in the knee. *Knee, 12*(6), 435-440.

Hill, C. L., Seo, G. S., Gale, D., Totterman, S., Gale, M. E., and Felson, D. T. (2005). Cruciate ligament integrity in osteoarthritis of the knee. *Arthritis Rheum, 52*(3), 794-799.

Hodge, W. A., Fijan, R. S., Carlson, K. L., Burgess, R. G., Harris, W. H., and Mann, R. W. (1986). Contact pressures in the human hip joint measured in vivo. *Proc Natl Acad Sci U S A, 83*(9), 2879-2883.

Hollander, A. P., Pidoux, I., Reiner, A., Rorabeck, C., Bourne, R., and Poole, A. R. (1995). Damage to type II collagen in aging and osteoarthritis starts at the articular surface, originates around chondrocytes, and extends into the cartilage with progressive degeneration. *J Clin Invest, 96*(6), 2859-2869.

Hsieh, H. H., and Walker, P. S. (1976). Stabilizing mechanisms of the loaded and unloaded knee joint. *J Bone Joint Surg Am, 58*(1), 87-93.

Huang, A., Hull, M. L., and Howell, S. M. (2003). The level of compressive load affects conclusions from statistical analyses to determine whether a lateral meniscal

autograft restores tibial contact pressure to normal: a study in human cadaveric knees. *J Orthop Res, 21*(3), 459-464.

Huang, C. Y., Stankiewicz, A., Ateshian, G. A., and Mow, V. C. (2005). Anisotropy, inhomogeneity, and tension-compression nonlinearity of human glenohumeral cartilage in finite deformation. *J Biomech, 38*(4), 799-809.

Inaba, H. I., Arai, M. A., and Watanabe, W. W. (1990). Influence of the varus-valgus instability on the contact of the femoro-tibial joint. *Proc Inst Mech Eng [H], 204*(1), 61-64.

Indelicato, P. A., and Bittar, E. S. (1985). A perspective of lesions associated with ACL insufficiency of the knee. A review of 100 cases. *Clin Orthop Relat Res*(198), 77-80.

Johnson, G. R., Dowson, D., and Wright, V. (1977). The elastic behaviour of articular cartilage under a sinusoidally varying compressive stress. *International Journal of Mechanical Sciences, 19*(5), 301-308.

Joshi, M. D., Suh, J. K., Marui, T., and Woo, S. L. (1995). Interspecies variation of compressive biomechanical properties of the meniscus. *J Biomed Mater Res, 29*(7), 823-828.

Julkunen, P., Kiviranta, P., Wilson, W., Jurvelin, J. S., and Korhonen, R. K. (2007). Characterization of articular cartilage by combining microscopic analysis with a fibril-reinforced finite-element model. *J Biomech, 40*(8), 1862-1870.

Jurvelin, J. S., Buschmann, M. D., and Hunziker, E. B. (1997). Optical and mechanical determination of Poisson's ratio of adult bovine humeral articular cartilage. *J Biomech, 30*(3), 235-241.

Kaab, M. J., Gwynn, I. A., and Notzli, H. P. (1998). Collagen fibre arrangement in the tibial plateau articular cartilage of man and other mammalian species. *J Anat, 193 (Pt 1)*, 23-34.

Kaab, M. J., Ito, K., Clark, J. M., and Notzli, H. P. (1998). Deformation of articular cartilage collagen structure under static and cyclic loading. *J Orthop Res, 16*(6), 743-751.

Kanamori, A., Sakane, M., Zeminski, J., Rudy, T. W., and Woo, S. L. (2000). In-situ force in the medial and lateral structures of intact and ACL-deficient knees. *J Orthop Sci, 5*(6), 567-571.

Keinan-Adamsky, K., Shinar, H., and Navon, G. (2005). The effect of detachment of the articular cartilage from its calcified zone on the cartilage microstructure, assessed by 2H-spectroscopic double quantum filtered MRI. *J Orthop Res, 23*(1), 109-117.

Kempson, G. E., Freeman, M. A., and Swanson, S. A. (1968). Tensile properties of articular cartilage. *Nature, 220*(172), 1127-1128.

Kempson, G. E., Muir, H., Pollard, C., and Tuke, M. (1973). The tensile properties of the cartilage of human femoral condyles related to the content of collagen and glycosaminoglycans. *Biochim Biophys Acta, 297*(2), 456-472.

Kincaid, S. A., and Van Sickle, D. C. (1981). Regional histochemical and thickness variations of adult canine articular cartilage. *Am J Vet Res, 42*(3), 428-432.

Kiviranta, I., Tammi, M., Jurvelin, J., and Helminen, H. J. (1987). Topographical variation of glycosaminoglycan content and cartilage thickness in canine knee (stifle) joint cartilage. Application of the microspectrophotometric method. *J Anat, 150*, 265-276.

Krause, W. R., Pope, M. H., Johnson, R. J., and Wilder, D. G. (1976). Mechanical changes in the knee after meniscectomy. *J Bone Joint Surg Am, 58*(5), 599-604.

Kurosawa, H., Fukubayashi, T., and Nakajima, H. (1980). Load-bearing mode of the knee joint: physical behavior of the knee joint with or without menisci. *Clin Orthop Relat Res*(149), 283-290.

Lane, J. M., and Weiss, C. (1975). Review of articular cartilage collagen research. *Arthritis Rheum, 18*(6), 553-562.

Lawrence, R. C., Felson, D. T., Helmick, C. G., Arnold, L. M., Choi, H., Deyo, R. A., Gabriel, S., Hirsch, R., Hochberg, M. C., et al. (2008). Estimates of the prevalence of arthritis and other rheumatic conditions in the United States. Part II. *Arthritis Rheum, 58*(1), 26-35.

Levy, I. M., Torzilli, P. A., and Warren, R. F. (1982). The effect of medial meniscectomy on anterior-posterior motion of the knee. *J Bone Joint Surg Am, 64*(6), 883-888.

Li, G., Rudy, T. W., Allen, C., Sakane, M., and Woo, S. L. (1998). Effect of combined axial compressive and anterior tibial loads on in situ forces in the anterior cruciate ligament: a porcine study. *J Orthop Res, 16*(1), 122-127.

Li, L. P., Buschmann, M. D., and Shirazi-Adl, A. (2000). A fibril reinforced nonhomogeneous poroelastic model for articular cartilage: inhomogeneous response in unconfined compression. *J Biomech, 33*(12), 1533-1541.

Li, L. P., Buschmann, M. D., and Shirazi-Adl, A. (2001). The asymmetry of transient response in compression versus release for cartilage in unconfined compression. *J Biomech Eng, 123*(5), 519-522.

Li, L. P., Buschmann, M. D., and Shirazi-Adl, A. (2003). Strain-rate dependent stiffness of articular cartilage in unconfined compression. *J Biomech Eng, 125*(2), 161-168.

Li, L. P., Soulhat, J., Buschmann, M. D., and Shirazi-Adl, A. (1999). Nonlinear analysis of cartilage in unconfined ramp compression using a fibril reinforced poroelastic model. *Clin Biomech, 14*(9), 673-682.

Lipshitz, H., Etheredge, R., 3rd, and Glimcher, M. J. (1976). Changes in the hexosamine content and swelling ratio of articular cartilage as functions of depth from the surface. *J Bone Joint Surg Am, 58*(8), 1149-1153.

Lyyra-Laitinen, T., Niinimaki, M., Toyras, J., Lindgren, R., Kiviranta, I., and Jurvelin, J. S. (1999). Optimization of the arthroscopic indentation instrument for the measurement of thin cartilage stiffness. *Phys Med Biol, 44*(10), 2511-2524.

Maquet, P. G., Van de Berg, A. J., and Simonet, J. C. (1975). Femorotibial weight-bearing areas. Experimental determination. *J Bone Joint Surg Am, 57*(6), 766-771.

Markolf, K. L., Bargar, W. L., Shoemaker, S. C., and Amstutz, H. C. (1981). The role of joint load in knee stability. *J Bone Joint Surg Am, 63*(4), 570-585.

Markolf, K. L., Burchfield, D. M., Shapiro, M. M., Shepard, M. F., Finerman, G. A., and Slauterbeck, J. L. (1995). Combined knee loading states that generate high anterior cruciate ligament forces. *J Orthop Res, 13*(6), 930-935.

Markolf, K. L., Gorek, J. F., Kabo, J. M., and Shapiro, M. S. (1990). Direct measurement of resultant forces in the anterior cruciate ligament. An in vitro study performed with a new experimental technique. *J Bone Joint Surg Am, 72*(4), 557-567.

Markolf, K. L., Mensch, J. S., and Amstutz, H. C. (1976). Stiffness and laxity of the knee--the contributions of the supporting structures. A quantitative in vitro study. *J Bone Joint Surg Am, 58*(5), 583-594.

Markolf, K. L., Willems, M. J., Jackson, S. R., and Finerman, G. A. (1998). In situ calibration of miniature sensors implanted into the anterior cruciate ligament part I: strain measurements. *J Orthop Res, 16*(4), 455-463.

Maroudas, A. (1968). Physicochemical properties of cartilage in the light of ion exchange theory. *Biophys J, 8*(5), 575-595.

McNicholas, M. J., Rowley, D. I., McGurty, D., Adalberth, T., Abdon, P., Lindstrand, A., and Lohmander, L. S. (2000). Total meniscectomy in adolescence. A thirty-year follow-up. *J Bone Joint Surg Br, 82*(2), 217-221.

Meachim, G., and Bentley, G. (1978). Horizontal splitting in patellar articular cartilage. *Arthritis Rheum, 21*(6), 669-674.

Mente, P. L., and Lewis, J. L. (1994). Elastic modulus of calcified cartilage is an order of magnitude less than that of subchondral bone. *J Orthop Res, 12*(5), 637-647.

Mesfar, W. (2006). *Biomecanique du genou humain en flexion sous les activites musculaires: Modelisation par la methode des elements finis.* Unpublished Dissertation, Ecole Polytechnique.

Mesfar, W., and Shirazi-Adl, A. (2005). Biomechanics of the knee joint in flexion under various quadriceps forces. *Knee, 12*(6), 424-434.

Mesfar, W., and Shirazi-Adl, A. (2006a). Biomechanics of changes in ACL and PCL material properties or prestrains in flexion under muscle force-implications in

ligament reconstruction. *Comput Methods Biomech Biomed Engin, 9*(4), 201-209.

Mesfar, W., and Shirazi-Adl, A. (2006b). Knee joint mechanics under quadriceps--hamstrings muscle forces are influenced by tibial restraint. *Clin Biomech (Bristol, Avon), 21*(8), 841-848.

Mesfar, W., and Shirazi-Adl, A. (2008a). Computational biomechanics of knee joint in open kinetic chain extension exercises. *Comput Methods Biomech Biomed Engin, 11*(1), 55-61.

Mesfar, W., and Shirazi-Adl, A. (2008b). Knee joint biomechanics in open-kinetic-chain flexion exercises. *Clin Biomech (Bristol, Avon), 23*(4), 477-482.

Michaud, C. M., McKenna, M. T., Begg, S., Tomijima, N., Majmudar, M., Bulzacchelli, M. T., Ebrahim, S., Ezzati, M., Salomon, J. A., et al. (2006). The burden of disease and injury in the United States 1996. *Popul Health Metr, 4*, 11.

Minns, R. J., and Steven, F. S. (1977). The collagen fibril organization in human articular cartilage. *J Anat, 123*(Pt 2), 437-457.

Miyasaka, K., Daniel, D., and Stone, M. (1991). The incidence of knee ligament injuries in the general population. *Am J Knee Surg, 4*, 43-48.

Moglo, K. E., and Shirazi-Adl, A. (2003). On the coupling between anterior and posterior cruciate ligaments, and knee joint response under anterior femoral drawer in flexion: a finite element study. *Clin Biomech (Bristol, Avon), 18*(8), 751-759.

Moglo, K. E., and Shirazi-Adl, A. (2005). Cruciate coupling and screw-home mechanism in passive knee joint during extension--flexion. *J Biomech, 38*(5), 1075-1083.

Morgan, F. R. (1960). Mechanical properties of collagen and leather fibres. *American Leather Chemists Association Journal, 55*(1), 4-23.

Mow, V. C., Kuei, S. C., Lai, W. M., and Armstrong, C. G. (1980). Biphasic creep and stress relaxation of articular cartilage in compression? Theory and experiments. *J Biomech Eng, 102*(1), 73-84.

Mow, V. C., Ratcliffe, A., and Woo, S. L. Y. (1991). *Biomechanics of Diarthrodial Joints*. New York: Springer-Verlag.

Muir, H. (1983). Proteoglycans as organizers of the intercellular matrix. *Biochem Soc Trans, 11*(6), 613-622.

Muir, H., Bullough, P., and Maroudas, A. (1970). The distribution of collagen in human articular cartilage with some of its physiological implications. *J Bone Joint Surg Br, 52*(3), 554-563.

Murad, M. A., and Loula, A. F. D. (1994). On stability and convergence of finite element approximations of Biot's consolidation problem. *International Journal for Numerical Methods in Engineering, 37*(4), 645-667.

Neuman, P., Englund, M., Kostogiannis, I., Friden, T., Roos, H., and Dahlberg, L. E. (2008). Prevalence of Tibiofemoral Osteoarthritis 15 Years After Nonoperative Treatment of Anterior Cruciate Ligament Injury: A Prospective Cohort Study. *Am J Sports Med.*

Notzli, H., and Clark, J. (1997). Deformation of loaded articular cartilage prepared for scanning electron microscopy with rapid freezing and freeze-substitution fixation. *J Orthop Res, 15*(1), 76-86.

Noyes, F. R., Bassett, R. W., Grood, E. S., and Butler, D. L. (1980). Arthroscopy in acute traumatic hemarthrosis of the knee. Incidence of anterior cruciate tears and other injuries. *J Bone Joint Surg Am, 62*(5), 687-695.

Oliveria, S. A., Felson, D. T., Reed, J. I., Cirillo, P. A., and Walker, A. M. (1995). Incidence of symptomatic hand, hip, and knee osteoarthritis among patients in a health maintenance organization. *Arthritis Rheum, 38*(8), 1134-1141.

Oloyede, A., Flachsmann, R., and Broom, N. D. (1992). The dramatic influence of loading velocity on the compressive response of articular cartilage. *Connect Tissue Res, 27*(4), 211-224.

Parsons, J. R., and Black, J. (1977). The viscoelastic shear behavior of normal rabbit articular cartilage. *J Biomech, 10*(1), 21-29.

Pena, E., Calvo, B., Martinez, M. A., Palanca, D., and Doblare, M. (2005). Finite element analysis of the effect of meniscal tears and meniscectomies on human knee biomechanics. *Clin Biomech (Bristol, Avon), 20*(5), 498-507.

Petersen, W., and Tillmann, B. (1998). Collagenous fibril texture of the human knee joint menisci. *Anat Embryol (Berl), 197*(4), 317-324.

Proctor, C. S., Schmidt, M. B., Whipple, R. R., Kelly, M. A., and Mow, V. C. (1989). Material properties of the normal medial bovine meniscus. *J Orthop Res, 7*(6), 771-782.

Radin, E. L., and Rose, R. M. (1986). Role of subchondral bone in the initiation and progression of cartilage damage. *Clin Orthop Relat Res*(213), 34-40.

Rangger, C., Klestil, T., Gloetzer, W., Kemmler, G., and Benedetto, K. P. (1995). Osteoarthritis after arthroscopic partial meniscectomy. *Am J Sports Med, 23*(2), 240-244.

Ratcliffe, A., Fryer, P. R., and Hardingham, T. E. (1984). The distribution of aggregating proteoglycans in articular cartilage: comparison of quantitative immunoelectron microscopy with radioimmunoassay and biochemical analysis. *J Histochem Cytochem, 32*(2), 193-201.

Redler, I., Mow, V. C., Zimny, M. L., and Mansell, J. (1975). The ultrastructure and biomechanical significance of the tidemark of articular cartilage. *Clin Orthop Relat Res*(112), 357-362.

Roos, H., Lauren, M., Adalberth, T., Roos, E. M., Jonsson, K., and Lohmander, L. S. (1998). Knee osteoarthritis after meniscectomy: prevalence of radiographic changes after twenty-one years, compared with matched controls. *Arthritis Rheum, 41*(4), 687-693.

Roth, V., and Mow, V. C. (1980). The intrinsic tensile behavior of the matrix of bovine articular cartilage and its variation with age. *J Bone Joint Surg Am, 62*(7), 1102-1117.

Rudy, T. W., Sakane, M., Debski, R. E., and Woo, S. L. (2000). The effect of the point of application of anterior tibial loads on human knee kinematics. *J Biomech, 33*(9), 1147-1152.

Sakane, M., Fox, R. J., Woo, S. L., Livesay, G. A., Li, G., and Fu, F. H. (1997). In situ forces in the anterior cruciate ligament and its bundles in response to anterior tibial loads. *J Orthop Res, 15*(2), 285-293.

Sakane, M., Livesay, G. A., Fox, R. J., Rudy, T. W., Runco, T. J., and Woo, S. L. (1999). Relative contribution of the ACL, MCL, and bony contact to the anterior stability of the knee. *Knee Surg Sports Traumatol Arthrosc, 7*(2), 93-97.

Schinagl, R. M., Gurskis, D., Chen, A. C., and Sah, R. L. (1997). Depth-dependent confined compression modulus of full-thickness bovine articular cartilage. *J Orthop Res, 15*(4), 499-506.

Seedhom, B. B., Dowson, D., and Wright, V. (1973, 13-15 September). *The load-bearing function of the menisci: a preliminary study.* Paper presented at the Proceedngs of Internationl Congress on the Knee Joint. vol. 37-42, Rotterdam.

Seedhom, B. B., and Hargreaves, D. J. (1979). Transmission of the load in the knee joint with special reference to the role of the menisci. II. Experimental results, discussion and conclusions. *Engineering in Medicine, 8*(4), 220-228.

Setton, L. A., Tohyama, H., and Mow, V. C. (1998). Swelling and curling behaviors of articular cartilage. *J Biomech Eng, 120*(3), 355-361.

Shin, C. S., Chaudhari, A. M., and Andriacchi, T. P. (2007). The influence of deceleration forces on ACL strain during single-leg landing: a simulation study. *J Biomech, 40*(5), 1145-1152.

Shirazi, R., and Shirazi-Adl, A. (2005). Analysis of articular cartilage as a composite using nonlinear membrane elements for collagen fibrils. *Med Eng Phys, 27*(10), 827-835.

Shirazi, R., and Shirazi-Adl, A. (2008a). Analysis of partial meniscectomy and ACL reconstruction in knee joint biomechanics under combined loading. *Submitted to J Orthop Res.*

Shirazi, R., and Shirazi-Adl, A. (2008b). Deep vertical collagen fibrils play a significant role in mechanics of articular cartilage. *J Orthop Res, 26*(5), 608-615.

Shirazi, R., Shirazi-Adl, A., and Hurtig, M. (2008). Role of cartilage collagen fibrils networks in knee joint biomechanics under compression. *Accepted for Publication in J Biomech.*

Shoemaker, S. C., and Markolf, K. L. (1985). Effects of joint load on the stiffness and laxity of ligament-deficient knees. An in vitro study of the anterior cruciate and medial collateral ligaments. *J Bone Joint Surg Am, 67*(1), 136-146.

Shrive, N. G., O'Connor, J. J., and Goodfellow, J. W. (1978). Load-bearing in the knee joint. *Clin Orthop Relat Res*(131), 279-287.

Skaggs, D. L., Warden, W. H., and Mow, V. C. (1994). Radial tie fibers influence the tensile properties of the bovine medial meniscus. *J Orthop Res, 12*(2), 176-185.

Slemenda, C., Heilman, D. K., Brandt, K. D., Katz, B. P., Mazzuca, S. A., Braunstein, E. M., and Byrd, D. (1998). Reduced quadriceps strength relative to body weight: a risk factor for knee osteoarthritis in women? *Arthritis Rheum, 41*(11), 1951-1959.

Soltz, M. A., and Ateshian, G. A. (1998). Experimental verification and theoretical prediction of cartilage interstitial fluid pressurization at an impermeable contact interface in confined compression. *J Biomech, 31*(10), 927-934.

Soukane, D. M., Shirazi-Adl, A., and Urban, J. P. (2007). Computation of coupled diffusion of oxygen, glucose and lactic acid in an intervertebral disc. *J Biomech, 40*(12), 2645-2654.

Soulhat, J., Buschmann, M. D., and Shirazi-Adl, A. (1999). A fibril-network-reinforced biphasic model of cartilage in unconfined compression. *J Biomech Eng, 121*(3), 340-347.

Sweigart, M. A., Zhu, C. F., Burt, D. M., DeHoll, P. D., Agrawal, C. M., Clanton, T. O., and Athanasiou, K. A. (2004). Intraspecies and interspecies comparison of the compressive properties of the medial meniscus. *Ann Biomed Eng, 32*(11), 1569-1579.

Takai, S., Woo, S. L., Livesay, G. A., Adams, D. J., and Fu, F. H. (1993). Determination of the in situ loads on the human anterior cruciate ligament. *J Orthop Res, 11*(5), 686-695.

Tandogan, R. N., Taser, O., Kayaalp, A., Taskiran, E., Pinar, H., Alparslan, B., and Alturfan, A. (2004). Analysis of meniscal and chondral lesions accompanying anterior cruciate ligament tears: relationship with age, time from injury, and level of sport. *Knee Surg Sports Traumatol Arthrosc, 12*(4), 262-270.

Thambyah, A., and Broom, N. (2006). Micro-anatomical response of cartilage-on-bone to compression: mechanisms of deformation within and beyond the directly loaded matrix. *J Anat, 209*(5), 611-622.

Tissakht, M., and Ahmed, A. M. (1995). Tensile stress-strain characteristics of the human meniscal material. *J Biomech, 28*(4), 411-422.

Torzilli, P. A., Deng, X., and Warren, R. F. (1994). The effect of joint-compressive load and quadriceps muscle force on knee motion in the intact and anterior cruciate ligament-sectioned knee. *Am J Sports Med, 22*(1), 105-112.

van der Hart, C. P., van den Bekerom, M. P., and Patt, T. W. (2008). The occurrence of osteoarthritis at a minimum of ten years after reconstruction of the anterior cruciate ligament. *J Orthop Surg, 3*, 24.

Vande Berg, B. C., Lecouvet, F. E., and Malghem, J. (2002). Frequency and topography of lesions of the femoro-tibial cartilage at spiral CT arthrography of the knee: a study in patients with normal knee radiographs and without history of trauma. *Skeletal Radiol, 31*(11), 643-649.

Veltri, D. M., Deng, X. H., Torzilli, P. A., Warren, R. F., and Maynard, M. J. (1995). The role of the cruciate and posterolateral ligaments in stability of the knee. A biomechanical study. *Am J Sports Med, 23*(4), 436-443.

Vener, M. J., Thompson, R. C., Jr., Lewis, J. L., and Oegema, T. R., Jr. (1992). Subchondral damage after acute transarticular loading: an in vitro model of joint injury. *J Orthop Res, 10*(6), 759-765.

Vermeer, P. A., and Verruijt, A. (1981). ACCURACY CONDITION FOR CONSOLIDATION BY FINITE ELEMENTS. *International Journal for Numerical and Analytical Methods in Geomechanics, 5*(1), 1-14.

von Porat, A., Roos, E. M., and Roos, H. (2004). High prevalence of osteoarthritis 14 years after an anterior cruciate ligament tear in male soccer players: a study of radiographic and patient relevant outcomes. *Ann Rheum Dis, 63*(3), 269-273.

Walker, P. S., and Erkman, M. J. (1975). The role of the menisci in force transmission across the knee. *Clin Orthop Relat Res*(109), 184-192.

Walker, P. S., and Hajek, J. V. (1972). The load-bearing area in the knee joint. *J Biomech, 5*(6), 581-589.

Williams, R. P., and Comper, W. D. (1990). Osmotic flow caused by polyelectrolytes. *Biophys Chem, 36*(3), 223-234.

Wilson, W., van Donkelaar, C. C., van Rietbergen, B., and Huiskes, R. (2005). A fibril-reinforced poroviscoelastic swelling model for articular cartilage. *J Biomech, 38*(6), 1195-1204.

Wilson, W., van Donkelaar, C. C., van Rietbergen, B., Ito, K., and Huiskes, R. (2004). Stresses in the local collagen network of articular cartilage: a poroviscoelastic fibril-reinforced finite element study. *J Biomech, 37*(3), 357-366.

Wismans, J., Veldpaus, F., Janssen, J., Huson, A., and Struben, P. (1980). A three-dimensional mathematical model of the knee-joint. *J Biomech, 13*(8), 677-685.

Woo, S. L., Akeson, W. H., and Jemmott, G. F. (1976). Measurements of nonhomogeneous, directional mechanical properties of articular cartilage in tension. *J Biomech, 9*(12), 785-791.

Woo, S. L. Y., Fox, R. J., Sakane, M., Livesay, G. A., Rudy, T. W., and Fu, F. H. (1998). Biomechanics of the ACL: Measurements of in situ force in the ACL and knee kinematics. *The Knee, 5*(4), 267-288.

Xia, Y., Moody, J. B., Alhadlaq, H., and Hu, J. (2003). Imaging the physical and morphological properties of a multi-zone young articular cartilage at microscopic resolution. *J Magn Reson Imaging, 17*(3), 365-374.

Zhu, W., Mow, V. C., Koob, T. J., and Eyre, D. R. (1993). Viscoelastic shear properties of articular cartilage and the effects of glycosidase treatments. *J Orthop Res, 11*(6), 771-781.

Appendix A

A.1 User-Defined Materials and Validations

User subroutine UMAT is used to define a material's mechanical behavior. The code must be written in FORTRAN and will be called at all material calculation points of elements for which the material definition includes a user-defined material behavior. It updates the stresses to their values at the end of the increment for which it is called and must provide the material Jacobian matrix, $\frac{\partial \Delta \sigma}{\partial \Delta \varepsilon}$, for the mechanical constitutive model.

The use of this subroutine generally requires considerable expertise and the implementation of any realistic constitutive model requires extensive development and testing. All the user-defined materials were thoroughly validated by different methods. Initially, testings on single-element models with prescribed traction loading were perfomed to evaluate validity of the codes. In addition, material properties in the code were modified to represent different built-in materials available in ABAQUS and the results between the two approaches were compared.

A.2 User-Defined Material Orientations and Validations

User subroutine ORIENT is used to provide an orientation for defining local material directions, which can be used for definition of material properties, for example, anisotropic materials. An array (3×3) containing the direction cosines of the preferred orientation in terms of the default basis directions must be defined in the subroutine. For shell and membrane elements only the first and second directions are used. This subroutine will be called at the start of the analysis at each location (material point) for which local directions are defined with a user-subroutine-defined orientation. The material directions can be visualized in Abaqus/CAE by selecting Plot→Material Orientations in the Visualization module. Therefore, the user-defined orientations in each element can be directly validated.

In the current study of the entire knee joint, the subroutine ORIENT is used to define local material directions in membrane elements used to represent deep vertical fibrils in cartilage and fibrils with dominant circumferential direction in the bulk of the menisci between peripheral surfaces. These local directions were subsequently served for material properties in the User subroutine UMAT.

A.3 UMAT and ORIENT Codes

Due to their excessive lengths, the codes written in subroutines UMAT and ORIENT for different axisymmetric and 3-D models of cartilage and meniscus are not provided in the thesis.

A.4 Additional Relevant Results for Case Study I.

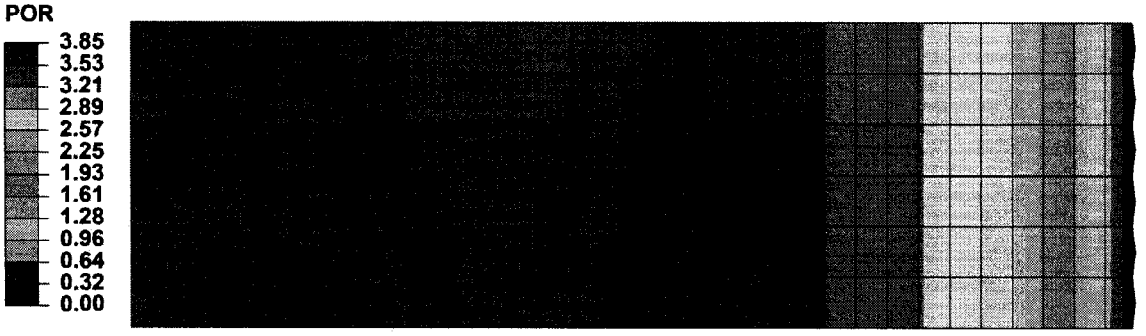

Figure A. 1 Contour of pore pressure at the transient time (t=0.5s) in the unconfined configuration test for the reference case in study I. The numbers are in MPa.

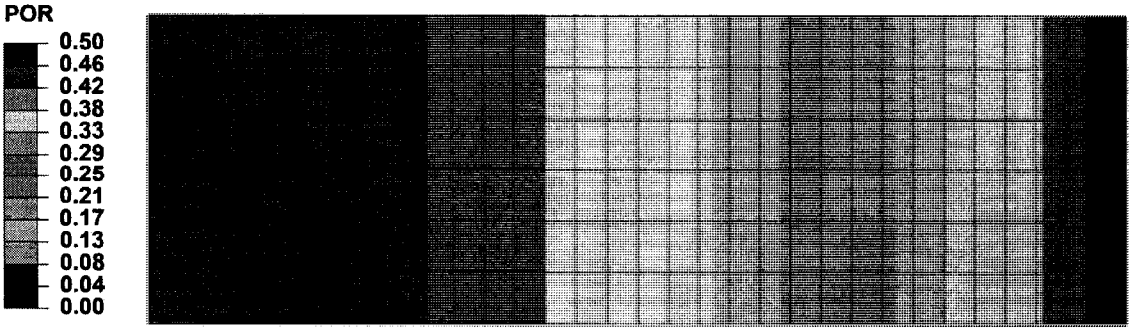

Figure A. 2 Contour of pore pressure at the post-transient time (t=50s) in the unconfined configuration test for the reference case in study I. The numbers are in MPa.

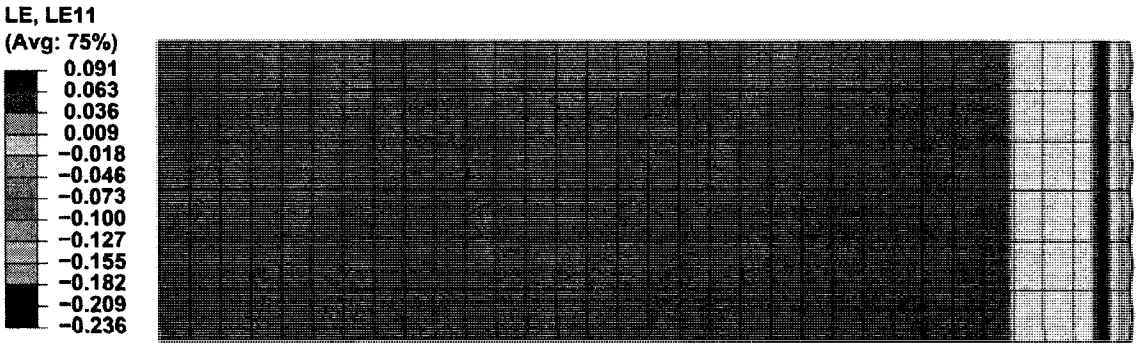

Figure A. 3 Contour of radial strain at the transient time (t=0.5s) in the unconfined configuration test for the reference case in study I.

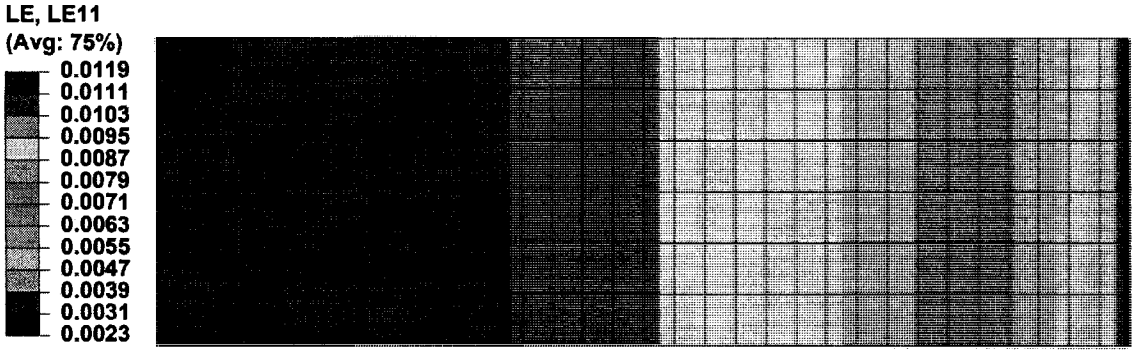

Figure A. 4 Contour of radial strain at the post-transient time (t=50s) in the unconfined configuration test for the reference case in study I.

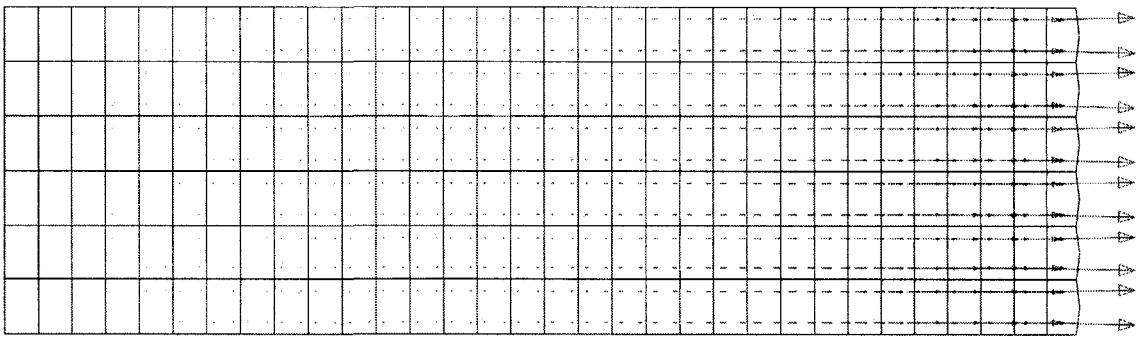

Figure A. 5 Fluid velocity direction and its relative magnitude at transient time for the smallest specimen in the case study on size of specimen in study I. The water direction is toward the edge every where.

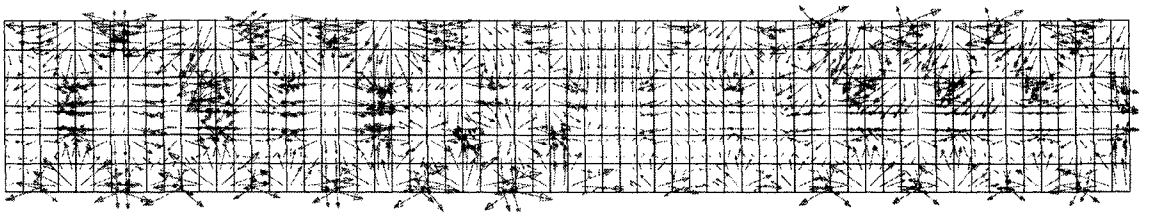

Figure A. 6 Fluid velocity direction and its relative magnitude at transient time for the largest specimen in the case study on size of specimen in study I. Only the inner quarter of the sample is shown so the water direction is visible in this region. The water direction is toward the center in some locations that causes substantial delay for the pore pressure at the center to reach its maximum in the larger specimens when compared to the smaller ones (the Mandel-Cryer effect).